PAGE-101

REPORT DOCUMENTATION PAGE	1. REPORT NO. NSF/RA-790487	2.	3. Recipient's Accession No. PB80-212525

Title and Subtitle
Direct Simple Shear Behavior of Fine Grained Soils Subjected to Repeated Loads, Interim Report

5. Report Date: December 1979
6.

7. Author(s): C. H. L. Floess, T. F. Zimmie

9. Performing Organization Name and Address:
Rensselaer Polytechnic Institute
Civil Engineering Department
Troy, NY 12181

8. Performing Organization Rept. No.
10. Project/Task/Work Unit No.
11. Contract(C) or Grant(G) No.
(C)
(G) PFR7818743

12. Sponsoring Organization Name and Address:
Engineering and Applied Science (EAS)
National Science Foundation
1800 G Street, N.W.
Washington, D.C. 20550

13. Type of Report & Period Covered: Interim
14.

15. Supplementary Notes
This is a progress report of "Simple Shear Behavior of Fine Grained Soils Subjected to Earthquake and Other Repeated Loading," (PB298123).

16. Abstract (Limit: 200 words)

Consolidated constant volume static and cyclic loading tests were performed using the Norwegian Geotechnical Institute (NGI) direct simple shear device. Emphasis was placed on high strain level repetitive loading, such as that caused by earthquakes and storm waves. Cyclic loading tests were performed using a square wave pulse shape with complete stress reversal on Gulf of Alaska and Blue Concord clays. Lateral stresses acting on soil samples were measured by means of calibrated, wire-reinforced rubber membranes. The membranes provided a convenient method of experimentally determining the coefficient of lateral stress at rest, K_o. The measured value of K_o for Gulf of Alaska clay was 0.54. Lateral stress measurements also provided sufficient information to determine Mohr's circle of stress for an infinitesimal element of soil at the center of the sample. It was determined that the coefficient of lateral stress increases with greater shear strain, and that the horizontal plane of the sample is approximately the plane of maximum shear stress, not the plane of maximum obliquity. Cyclic loading failure does not occur if the cyclic shear stress is small. For both clays, the critical level of repeated loading is approximately 25 percent of the peak static undrained shear strength. For lightly overconsolidated Concord Blue clay, the critical level of repeated loading is about 15 percent.

17. Document Analysis a. Descriptors

Earthquakes
Stress analysis
Shear tests
Cyclic loads
Measurement
Clay soils
Calibrating

b. Identifiers/Open-Ended Terms
Mohr's circle analysis
Concord Blue Clay
Gulf of Alaska Clay
Shear devices
Earthquake Hazards Mitigation

c. COSATI Field/Group

18. Availability Statement: NTIS

19. Security Class (This Report)
20. Security Class (This Page)
21. No. of Pages
22. Price

DIRECT SIMPLE SHEAR BEHAVIOR OF FINE GRAINED SOILS SUBJECTED TO REPEATED LOADS

by

Carsten H.L. Floess
PRINCIPAL INVESTIGATOR
Thomas F. Zimmie

NSF Grant No. PFR-7818743

INTERIM REPORT

DIRECT SIMPLE SHEAR BEHAVIOR OF FINE GRAINED SOILS SUBJECTED TO REPEATED LOADS

To: William Hakala, Program Manager
National Science Foundation

FROM: Thomas F. Zimmie, Associate Professor
Civil Engineering Department
Rensselaer Polytechnic Institute
Troy, New York

The report attached is a progress report on NSF Grant No. PFR-7818743 titled "Simple Shear Behavior of FIne Grained Soils Subjected to Earthquake and Other Repeated Loading", under the direction of Thomas F. Zimmie.

The report was done by Carsten H.L. Floess under the supervision of Professor Thomas F. Zimmie. Mr. Floess also used the report as his Doctoral Thesis in partial fulfillment of the requirements for the degree of Doctor of Philosophy at Rensselaer Polytechnic Institute.

DIRECT SIMPLE SHEAR BEHAVIOR OF FINE GRAINED SOILS SUBJECTED TO REPEATED LOADS

by

Carsten H.L. Floess

Sponsored by the National Science Foundation,
Directorate for Engineering and Applied Science,
Division of Problem-Focused Research (PFR),
Earthquake Hazards Mitigation Program
Grant No. PFR-7818743

Interim Report

Principal Investigator
Thomas F. Zimmie
Associate Professor of Civil Engineering

Rensselaer Polytechnic Institute
Troy, New York

December 1979

TABLE OF CONTENTS

TABLE OF CONTENTS

(CONTINUED)

LIST OF TABLES

LIST OF TABLES
(CONTINUED)

PAGE

LIST OF FIGURES

LIST OF FIGURES

(CONTINUED)

PAGE

LIST OF FIGURES

(CONTINUED)

LIST OF FIGURES (CONTINUED)

LIST OF FIGURES (CONTINUED)

PAGE

LIST OF FIGURES

(CONTINUED)

LIST OF FIGURES

(CONTINUED) PAGE

ACKNOWLEDGEMENT

The author would like to express his sincere appreciation and thanks to Dr. Thomas F. Zimmie for the guidance and encouragement he provided throughout this study.

The author also wishes to express his gratitude to Dr. Jay Leonard, Dr. Ricardo Dobry, and Dr. Dimitri Athanasiou-Grivas for their critical review of this report and for their valuable comments.

Thanks are due to Dr. Dwight Sangrey, Cornell University, for providing soil samples and many helpful comments; and to the United States Geological Survey for providing the offshore marine samples. Special thanks are extended to Betty Alix, Bonnie Hoag, and Rita Vooris for their patience and diligence in preparing the typed manuscript.

Funds for this project were provided by grants from the National Science Foundation, Grant No. PFR76-14220 (formerly ENV76-14220) and Grant No. PFR78-18743, sponsored by the Earthquake Engineering Program for the Directorate for Applied Science and Research Applications (ASRA) (formerly RANN).

ABSTRACT

This report contains the results of a laboratory investigation on the behavior of fine grained soils subjected to repeated loads. Consolidated constant volume static (monotonic) and cyclic loading tests were performed using the NGI direct simple shear device. Emphasis was placed on high strain level repetitive loading, such as that caused by earthquakes and storm waves. All cyclic loading tests were performed using a square wave pulse shape, with complete stress reversal.

Two soils were studied: an offshore marine clay from the Gulf of Alaska and Concord Blue clay. Because the in situ structure of cohesive soils is an important parameter in determining their behavior, only natural undisturbed samples were tested.

Data for the Gulf of Alaska clay include lateral stress measurements. The lateral stresses acting on the soil samples were measured by means of calibrated wire reinforced rubber membranes. Prior to this study, the lateral stresses acting on direct simple shear soil samples have seldom been measured. The additional information provided by the lateral stress measurements adds considerably to the knowledge of the stress conditions existing in the soil sample.

The calibrated wire reinforced rubber membrane provides a convenient method to determine, experimentally, the coefficient of lateral stress at rest, K_o. For the Gulf of Alaska clay, the measured value of K_o equals 0.54, which agrees well with empirical data. The lateral stress measurements also provide sufficient information to determine Mohr's circle of

stress for an infinitesimal element of soil at the center of the sample. On the basis of Mohr's circle analysis, information can be obtained about the state of stress within the soil sample during shear. For example, it was found (for both the static and cyclic loading tests) that: 1. the coefficient of lateral stress, $K = \bar{\sigma}_h/\bar{\sigma}_v$, increases with increasing shear strain; 2. the horizontal plane of the sample is approximately the plane of maximum shear stress, not the plane of maximum obliquity.

For direct simple shear tests, it is conventionally assumed that the horizontal plane of the sample is the plane of maximum obliquity, and the mobilized angle of internal friction is computed from the equation: $\phi = \tan^{-1}(\tau_h/\bar{\sigma}_v)$. Alternatively, if lateral stresses are measured, the mobilized friction angle can be computed from Mohr's circle: $\phi_m = \sin^{-1}(q/\bar{p})$. For the static tests performed on the Gulf of Alaska clay, it was found that ϕ_m is greater than ϕ, and at large shear strains, the difference between the two is approximately 7°.

Cyclic loading failure does not occur if the cyclic shear stress is small. For both the Gulf of Alaska clay and normally consolidated Concord Blue clay, the critical level of repeated loading is approximately 25 percent of the peak static undrained shear strength. For lightly overconsolidated Concord Blue clay (OCR = 2) the critical level of repeated loading is approximately 15 percent.

Testing errors inherent to the NGI direct simple shear device were evaluated. It was found that two testing errors are significant: 1. false (vertical) deformation in the NGI device; 2. secondary consolidation (creep) in the soil sample. Methods to correct for these testing errors are presented.

Also included in this report are a literature review, a discussion of the stress conditions existing in direct simple shear samples, and a description of equipment and testing procedures.

PART 1

INTRODUCTION

Understanding the cyclic loading behavior of soils has become increasingly more important for the modern geotechnical engineer. Typical examples of cyclic loading include: earthquake shaking, wind and wave action, vehicular traffic, pile driving, fluctuating live loads, and machine vibrations.

Early research studies had indicated that the effects of cyclic loading were less severe for fine grained silts and clays than they were for sands and other coarse grained soils (66). As a result, research and publications have been concerned, for the most part, with the cyclic loading behavior of these coarse grained soils rather than the fine grained silts and clays. Recently, however, there has been a renewed interest in the cyclic loading behavior of fine grained soils. This interest has been stimulated largely by various construction projects, such as the Alaska pipeline, offshore oil platforms, and a proposed offshore nuclear power plant in New Jersey.

Numerous specific topics could be the focus of a research effort concerned with the response of fine grained soils to cyclic loading. Compared with work on sands, relatively little has been done. The overall purpose of this research project was to investigate, experimentally, the cyclic loading behavior of fine grained soils under controlled laboratory conditions. Emphasis was placed on high strain

level cyclic loading, such as that caused by earthquakes and storm waves.

All laboratory tests were performed using the Norwegian Geotechnical Institute (NGI) direct simple shear device. This device has been modified for cyclic loading capabilities. The NGI direct simple shear device has been used by a number of researchers and practitioners for cyclic loading studies (114), and it is an excellent device in spite of some limitations (18,79).

Two soils were studied: Concord Blue clay (19) and a Gulf of Alaska clay (14,35). Consolidated, constant volume (CCV) static (monotonic) and cyclic tests were performed on undisturbed samples of these two soils. All cyclic loading tests were performed using a square wave pulse shape, with complete stress reversal.

Specific objectives of this research included:

1. Setup and evaluation of the NGI direct simple shear apparatus. This was the initial phase of the research project. Detailed procedures were developed for sample trimming and testing. Testing errors inherent to the NGI direct simple shear apparatus were also evaluated, and methods to correct for these errors are presented.

2. Investigation of the static and cyclic loading behavior of an offshore clay from the Gulf of Alaska. Petroleum related activities in the Gulf of Alaska may stimulate major marine construction in this area. Since it is likely that a number of offshore structures will be situated on soft marine clays, it is important to determine the static and cyclic loading behavior of these soils.

3. Measurement of the horizontal (lateral) stresses acting on the soil samples during consolidation and shear. The horizontal stresses were measured by means of calibrated wire reinforced rubber membranes. The horizontal stress measurements that were made during consolidation were used to determine the coefficient of lateral stress at rest, K_o. The horizontal stress measurements that were made during shear were used to gain additional information about the state of stress within the soil sample. The test results were analyzed on the basis of this extra information.

4. Determination of the critical level of repeated loading (CLRL) for the soils tested. The critical level of repeated loading, as defined by Sangrey (92,93), was determined for both the Concord Blue clay and the Gulf of Alaska clay. The concept of non-failure equilibrium (92,93) was verified for a large number of loading cycles.

PART 2

LITERATURE REVIEW

2.1 Previous Studies of the Cyclic Loading Behavior of Fine Grained Soils

Early research studies indicated that clay soils were less prone to strength loss from cyclic loading than sands were (66). Consequently, most studies of the cyclic loading behavior of soils have dealt with sands (15,23,24,26,33,57,96,99,111). However, in this section, the cyclic loading behavior of fine grained soils is emphasized.

Research projects dealing with the cyclic loading behavior of fine grained soils have focused on various specific topics: cyclic loading strength (67,69,72,74,92); cyclic stress-strain relationships, including moduli and damping parameters (4,5,37,38,39,40,45,100); anisotropy (89); static shear strength and static stress-strain behavior following cyclic loading (102,107,108,109); and long term effects, such as changes in strength and volume (12,30,73). Various practical applications have also been investigated: response of level ground to earthquake shaking (47,48), earthquake and wave loadings on offshore soils and structures (3,20,22,28,29,42,43), pile driving (21,51,91), traffic loading (13,63,64,98), slope stability (6,54,70), and cyclic loading of frozen soils (105,112).

Early studies of the cyclic loading behavior of clay soils were connected with pavement design (63). The cyclic loads caused by traffic

were usually simulated by applying repeated compressive loads on undrained triaxial samples. It was generally found that if the cyclic stresses were less than a threshold value, equilibrium conditions resulted, and failure did not occur in the sample. Lashine (64), for example, found that cyclic stresses less than 75 to 80 percent of the static undrained shear strength did not cause failure* for the silty clay that was tested. Other researchers have found similar results (13,93). These results for one-directional cyclic loading of clay soils indicated that the cyclic strength was only slightly less than the static undrained shear strength.

For earthquake related laboratory research, soil samples were subjected to reversing, two-directional cyclic stresses or strains. The effect of this type of loading was found to be more severe than it was for one-directional cyclic loading. Seed and Chan (97), for example, found that the cyclic strength of a Vicksburg silty clay subjected to reversing, two-directional loading was only 30 percent of its cyclic strength for one-directional loading**.

Various theoretical and empirical models have been proposed to describe the cyclic loading behavior of soils. For example, Sangrey (92,93), in his work with fine grained soils, has developed a qual-

*Failure was defined by Lashine (64) as the point at which the strain rate begins to accelerate. Typically, failure is defined in terms of a cyclic strain amplitude (67).
**Cyclic strength was defined by Seed and Chan (97) as the cyclic loading stress level required to induce failure in a given number of loading cycles.

itative model to describe cyclic loading behavior. This model may be briefly summarized as follows: When saturated soil is subjected to an undrained load-unload cycle, there will be a residual pore pressure and a residual distortional strain after the cycle is completed. With additional loading cycles, the residual pore pressures and strains will increase until the soil either fails or attains a state of non-failure equilibrium. For each soil, there is a critical level of repeated loading separating these two types of behavior.

A general analytical model describing the anisotropic, elasto-plastic, path dependent, stress-strain-strength behavior of saturated clays under undrained loading conditions has been developed by Prevost (78,80). This model is based on plasticity theory, and it uses the concepts of isotropic and kinematic hardening. With this model, the stress-strain behavior of clays can be determined for complex loading paths.

Other models of the cyclic loading behavior of soils that have been developed are based on plasticity theory (76), endochronic theory (56), elastic and viscoelastic models (34), and rheologic models (55).

2.2 Laboratory Testing Techniques and Equipment Used for Cyclic Loading Studies of Soil

The solution of many problems in geotechnical engineering requires a knowledge of soil moduli, damping parameters, soil strength, or other data. Some of this data is measured best in the laboratory under controlled conditions.

There are various laboratory testing devices available today that are used to determine the strength and stress-strain relationship of soils. These devices are usually designed to simulate field conditions in the laboratory. Conceptually, it may appear relatively simple to build such a device, but in practice, it is extremely difficult to do so. It may, in fact, be impossible to construct a completely satisfactory testing apparatus (65).

The triaxial device has been frequently used for cyclic loading studies of soil (13,65,93), and it is the most widely used testing apparatus for determing the liquefaction characteristics of cohesionless soil (114). In a typical cyclic loading triaxial test, the cylindrical sample is first consolidated under an isotropic state of stress. An axial load or strain is then cycled between two limits under undrained conditions. If care is taken in the preparation and performance of cyclic loading triaxial tests, then the results of these tests have been found to be quite repeatable, even when using several different triaxial devices (103).

As with any laboratory testing apparatus, the triaxial device has its limitations. In general, the stresses and strains in the sample are nonuniform (77). Stress concentrations occur near the ends of the sample, although this effect can be lessened by using lubricated end plates (52). Experimental details, such as piston friction, membrane leakage, and air diffusion, must also be considered (9,94). For cyclic testing, the extension and compression phases of the test may produce

different results. For example, hysteresis loops may be asymmetric in strain controlled tests, and necking tends to occur in stress controlled tests. The principal stresses also change directions by 90° during cyclic tests with stress reversal. In spite of these difficulties, cyclic loading triaxial tests can produce valid results (65, 95).

Direct simple shear devices have also been frequently used for cyclic loading studies of soil (2,27,36,73). The direct simple shear device simulates earthquake loading conditions better than the triaxial device (95).

The Swedish Geotechnical Institute (SGI) direct simple shear device, which was first built in 1936, is described by Kjellman (53). In this device, a cylindrical sample is confined by a rubber membrane and a series of sliding metal rings. The Norwegian Geotechnical Institute direct simple shear apparatus, which was developed in 1961, is basically and adaptation of the SGI device. The NGI apparatus also tests cylindrical samples, but they are confined by a wire reinforced rubber membrane. This device is described by Bjerrum and Landva (10). The Cambridge simple shear apparatus is described by Roscoe (86). The Cambridge device has a rectangular sample, which is enclosed by hinged rigid walls. Later models of the Cambridge apparatus employ special load cells in the rigid walls; these load cells are used to measure the normal and shear stresses acting on the sample (87).

A number of practical problems exist with the direct simple shear apparatus. The most serious problem is the lack of complementary shear stresses on the sides of the sample (see Figure 5.1). As with most laboratory testing devices, the sample size is small, and no soil element is far away from the sample boundaries and their resulting stress concentrations. These problems make the interpretation of direct simple shear tests difficult.

Numerous investigators have analyzed the stress conditions produced in direct simple shear device samples (18,68,79,101,115). The findings of these theoretical and experimental studies are discussed further in Part 5 of this report.

The direct simple shear device is not perfect, but the device has been useful for studying the static and cyclic loading behavior of soils. The results of direct simple shear tests have been found to be consistent with the results of triaxial tests and shake table tests (17,27,75,95). Therefore, while there are some uncertainties with regard to the stress distributions produced in the soil sample by direct simple shear devices, these devices clearly produce reasonable test results.

Cyclic torsional simple shear devices have been developed to overcome some of the difficulties encountered with the direct simple shear device (114). However, these devices do not produce uniform shear strains within the soil sample. When the cylindrical sample is sub-

jected to a torque, the shear strain varies linearly with distance along the radius of the sample. In an effort to overcome this difficulty, the hollow cylinder torsional shear apparatus was developed (49,116).

Hollow cylinder torsional simple shear devices also have their limitations (114,115). Wright, et al (115), have developed criteria for selecting a sample size and configuration that will leave the central zone of the sample free of end effects. Although the stress distributions in torsional hollow cylinder samples may be more uniform than they are in direct simple shear samples, difficulties arise in sample preparation for undisturbed soils. For some soils it may be impossible to make hollow cylinder samples.

Shake table tests have been used to determine the cyclic loading behavior of soils (17,25,81). The large sample size used in these tests decreases the stress concentrations that are caused by end effects. Data from shake table tests correlate well with data from direct simple shear and torsional shear tests (17). The main difficulties with this test are the large sample size and the effects of membrane compliance (95).

Resonant column devices have been used to determine soil moduli and damping data (4,5,104). The resonant column test is based on the theory of wave propagation in prismatic rods, and it is used primarily for small strain applications. The resonant column test is described by Richart, et al (85).

Model tests have been used for cyclic loading studies of soil. Kovacs, et al (54), used this approach in their study of the seismic behavior of clay banks. Rowe, et al (88), used model tests to study the behavior of offshore gravity platforms during storms. Richart (84) described some model tests of footings subjected to cyclic loads. Model tests clearly have their merits and many potential applications in geotechnical engineering.

In summary, there are various laboratory testing devices available that can be used for cyclic loading studies of soil. All laboratory testing devices have their limitations, and the test results must be interpreted accordingly. Triaxial devices and direct simple shear devices are the laboratory equipment most commonly used for cyclic loading studies of soil.

PART 3

DESCRIPTION OF THE NGI DIRECT SIMPLE SHEAR DEVICE AND RELATED EQUIPMENT

3.1 Introduction

The Norwegian Geotechnical Institute (NGI) direct simple shear apparatus, model number 4, was used for this investigation. This device was developed by NGI, and it is manufactured commercially by Geonor. It is similar to the machine described by Bjerrum and Landva (10).

The NGI direct simple shear apparatus was designed to produce uniform shear strains throughout the soil sample. The cross sectional area of the cylindrical sample is kept constant by a wire reinforced rubber membrane, which constrains the sample in the radial direction. The sample is sheared by displacing its top horizontally relative to its bottom. The sample assembly also keeps the upper and lower ends of the sample parallel at all times.

Sands, silts, stiff clays, soft clays, and quick clays can be tested under drained or constant volume conditions. Additionally, either stress controlled or strain controlled testing modes can be performed.

In the following sections, the NGI direct simple shear device and its associated equipment are described. First, the standard NGI direct simple shear device and the soil trimming apparatus are

described. This is followed by a description of the wire reinforced rubber membranes. Modifications that were made to the NGI direct simple shear device, including modifications for cyclic loading capabilities, are described next. Part 3 concludes with a discussion of calibration procedures, including several examples of calibration curves. Testing errors that are inherent to the NGI direct simple shear device are also discussed, and methods to correct for these errors are proposed.

3.2 The Standard NGI Direct Simple Shear Device

The NGI direct simple shear device consists of the sample assembly, the vertical loading unit, and the horizontal loading unit. The sample assembly is shown in Figure 3.1; the complete apparatus is shown in Figure 3.2. A photograph of the device is shown in Figure 3.3.

The sample assembly consists of the pedestal, the upper cap*, the lower cap*, and the wire reinforced rubber membrane. The upper and lower caps have recesses for porous stones**. Either conventional porous stones or porous stones furnished with 1 mm long needles can be used. The needles inhibit slippage between the sample and the stones. The caps are also equipped with drainage tubes, which can be connected to an external water supply. Alternatively, a plastic cylinder can be placed around the sample; the cylinder is then filled with water to keep the sample submerged. O-rings are used to provide a watertight seal between the wire reinforced rubber membrane and

*Geonor refers to the upper and lower caps as the upper and lower filter holders.
** Geonor refers to the porous stones as filter plates.

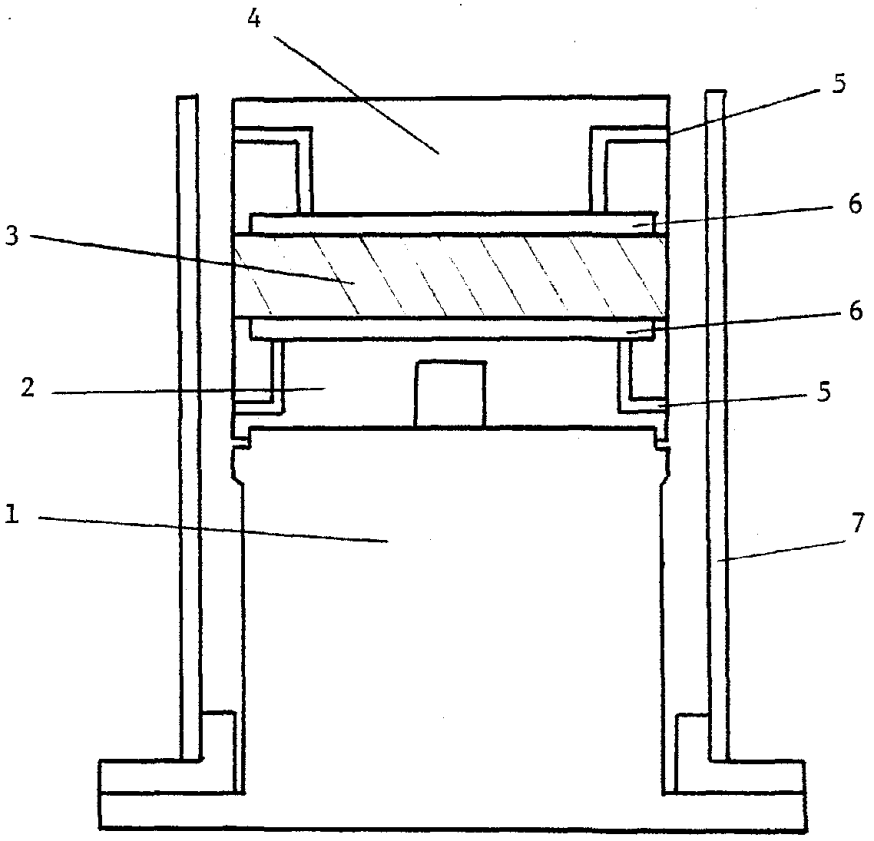

1. PEDESTAL
2. LOWER CAP
3. SAMPLE
4. UPPER CAP
5. DRAINAGE TUBE
6. POROUS STONE
7. PLASTIC CYLINDER

FIGURE 3.1. THE SAMPLE ASSEMBLY FOR THE NGI DIRECT SIMPLE SHEAR DEVICE

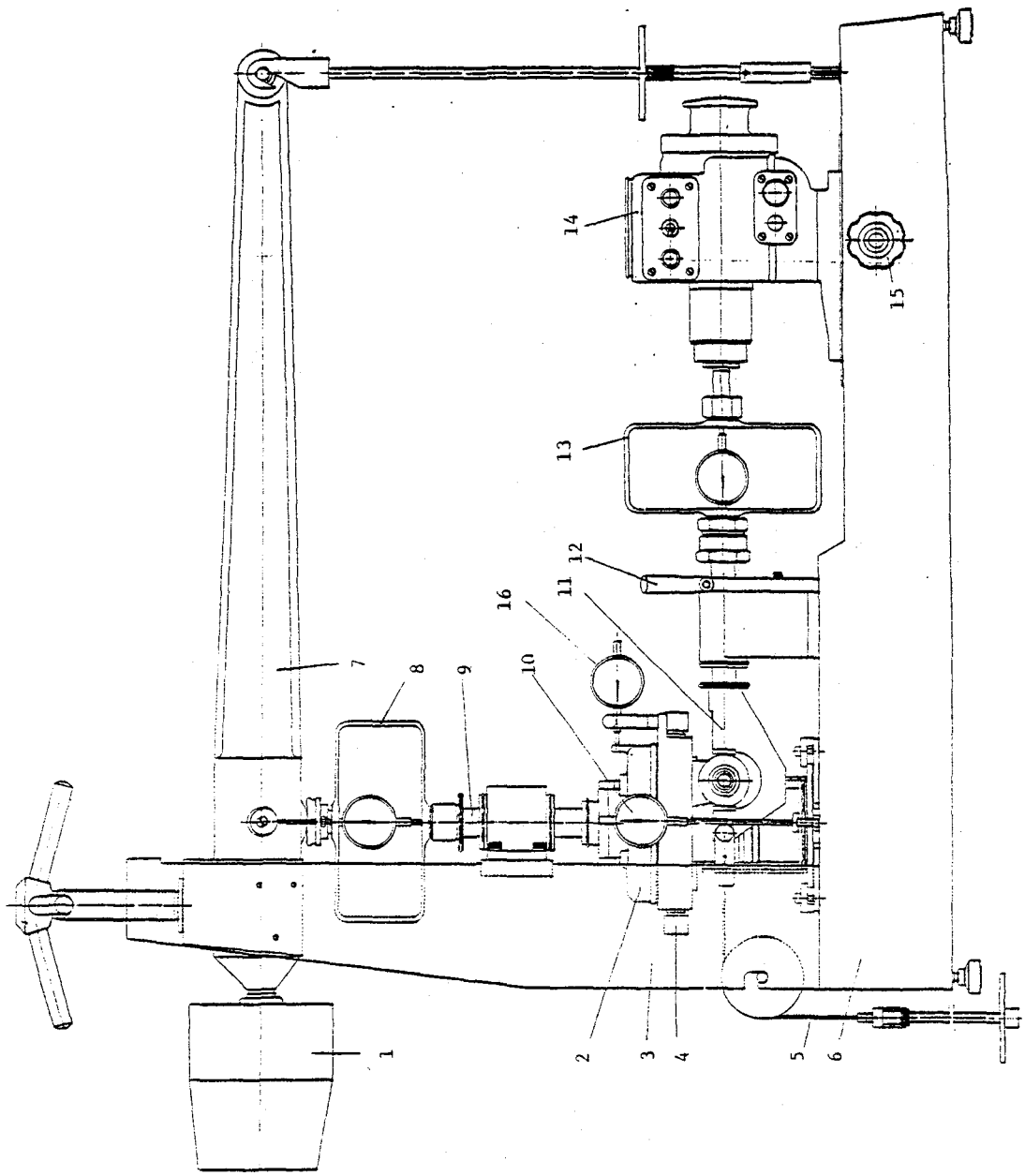

FIGURE 3.2. THE NGI DIRECT SIMPLE SHEAR DEVICE (ADOPTED FROM REFERENCE 31)

1. Counterweight
2. Sliding Shear Box
3. Tower
4. Lugs
5. Hanger
6. Base
7. Lever Arm
8. Proving Ring Load Gauge
9. Piston
10. Vertical Dial Gauge
11. Connection Fork
12. Locking Clamp
13. Proving Ring Load Gauge
14. Electric Motor and Gear Box
15. Adjusting Mechanism
16. Horizontal Dial Gauge

FIGURE 3.2. (CONTINUED)

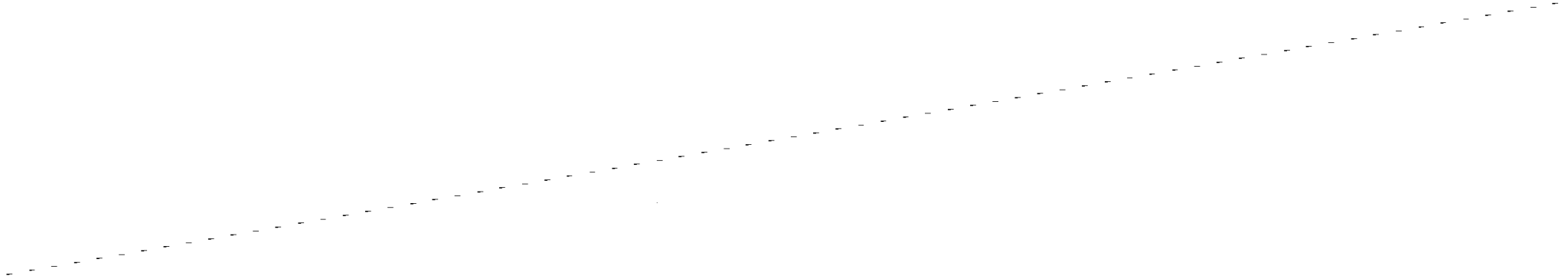

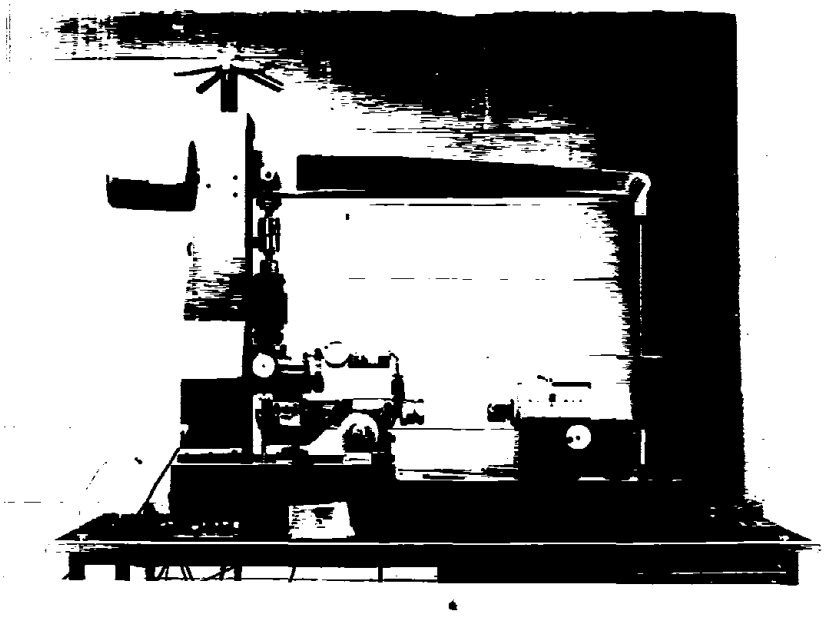

FIGURE 3.3. A PHOTOGRAPH OF THE NGI DIRECT SIMPLE SHEAR DEVICE

the caps. The sample assembly unit is available for both the standard 50.0 cm^2 sample cross section and the smaller 17.81 cm^2 sample cross section.

The vertical loading unit consists of the base, the tower, the 10:1 lever arm, the proving ring load gauge, the piston, the sliding shear box, the vertical dial gauge, and the adjusting mechanism. A counterweight balances the weight of the lever arm, the proving ring load gauge, the piston, and the sliding shear box.

The horizontal loading unit for strain controlled testing includes the electric motor and gear box, the proving ring load gauge, the horizontal piston, the locking clamp, the connection fork, the sliding shear box, and the horizontal dial gauge.

The gear box has a stepless speed adjustment, with speeds ranging from 10 to 300 minutes per mm of horizontal travel. The total available travel is 4.5 cm. The direction of movement is controlled by a switch, and the power shuts off automatically when either end position is reached.

The horizontal loading unit for stress controlled testing consists of the horizontal piston, the locking clamp, the connection fork, the sliding shear box, the dial gauge, the axle with two mounted pulleys, and the hanger. The hanger is attached to the connection fork by two wires, which pass through holes in the table on which the shear apparatus is mounted. For stress controlled testing, the horizontal

proving ring load gauge is not needed, and it should be disconnected.

The connection between the upper cap of the sample assembly and the lower part of the sliding shear box is made by two adjustable lugs. The lugs are brought into contact with the cap by two allen-head screws. The sample is sheared by displacing the upper cap horizontally relative to the lower cap and the pedestal. For strain controlled tests, a constant rate of shear strain is applied to the sample by the gear box and electric motor. For stress controlled tests, the horizontal shear stress is applied by adding dead load increments to the hanger.

The applied vertical and horizontal loads are measured by the rectangular proving ring load gauges. Interchangeable proving rings with ranges of $\pm$ 50, 100, 200, 400 and 800 kg are available. Vertical and horizontal displacements are measured by the dial gauges.

During shear, undrained conditions are simulated by keeping the volume of the sample constant. Assuming that the sample cross sectional area does not change, constant volume is maintained by keeping the sample height constant. The change in vertical stress, needed to maintain a constant sample height, is equated to the change in pore water pressure that would have occurred during an undrained test.

The fine adjustments in the vertical load, needed to maintain constant volume conditions, are made by the adjusting mechanism. After consolidation, the lever arm is pinned to the adjusting mechanism. Once

pinned into position, the vertical load can be changed by controlled movements of the lever arm upwards or downwards. This is accomplished by rotating a worm gear connected to the adjusting knob.

3.3 The NGI Trimming Apparatus

The trimming apparatus and methods are, in principle, similar to those described by Landva (62). The trimming apparatus was designed for use with the soft, sensitive clays that are common in Norway. The basic design principles are that the sample should be completely and rigidly supported at all times, and that it should never be touched by hand.

The trimming apparatus consists of a base, and a set of three yokes. The base has two vertical columns on which the yokes can slide. The yokes can be positioned at any point on the columns by locking thumb screws. The base also has two pins by which it can be attached to the direct simple shear apparatus.

One yoke acts as a guide for the reinforced rubber membrane expander. The membrane expander consists of a cylindrical porous stone, which is pressed into the yoke. The wire reinforced section of the membrane is placed inside the cylindrical porous stone, and the unreinforced parts are folded over the ends. The yoke also contains a fitting to which a vacuum source can be attached. When vacuum is applied, the reinforced rubber membrane stretches; the membrane can then be mounted on the sample with a minimum of disturbance.

The second yoke guides the stainless steel cutting cylinder. It contains provisions for attaching the lower cap to the bottom of the sample. The third yoke acts as a guide for attaching the upper cap to the sample.

Proper use of the trimming apparatus ensures that the sample stands vertical and that the ends of the sample are horizontal and parallel. A photograph of the trimming apparatus is shown in Figure 3.4.

3.4 Wire Reinforced Rubber Membranes

The reinforced rubber membranes used in this investigation were manufactured by Geonor. The reinforcement is constantan wire with a diameter of 0.015 cm, a Young's Modulus of 1.55×10^6 kg/cm^2 (1.52×10^8 kN/m^2), and a tensile strength of 5,800 kg/cm^2 (5.69×10^5 kN/m^2). The wire is wound at 20 turns per centimeter of membrane height. The rubber material is natural latex. These membranes are available in two sizes, the standard 50 cm^2 size and the smaller 17.81 cm^2 size; both are shown in Figure 3.4.

The membranes must provide adequate lateral resistance to maintain the sample at a constant cross sectional area during consolidation and shear. The wire reinforcing will deform as the lateral stress increases, but this yields only a small error (31). The membranes must also allow the sample to strain vertically during consolidation and drained shear. Vertical strains are permitted by the spaces between

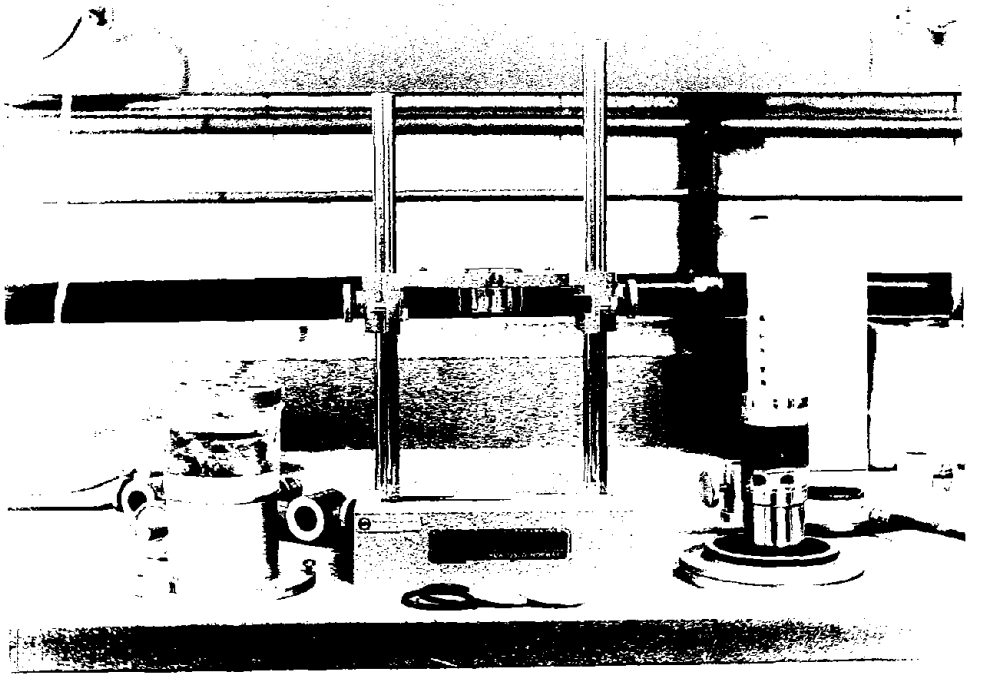

FIGURE 3.4. A PHOTOGRAPH OF THE NGI TRIMMING APPARATUS AND THE WIRE REINFORCED RUBBER MEMBRANES

the reinforcing wire windings. However, if the consolidation strains are very large, the wire windings will tend to overlap. This may present some difficulties in testing highly compressible soils.

Calibrated wire reinforced rubber membranes used for the measurement of lateral stress are also manufactured by Geonor. These membranes operate on a strain gauge principle; the average lateral stress acting on the sample is calculated from changes in the electrical resistance of the reinforcing wire. The entire length of the reinforcing wire windings is 3 cm, with the middle third of it acting as the strain gauge.

The active (strain gauge) reinforcing wire is made from constantan. This wire has the same physical properties that were given previously for the conventional membranes. The electrical resistance of the active wire is approximately 138 ohms, and the gauge factor is approximately 2.18. Calibrated membranes are available in both the 50 cm^2 size and the 17.81 cm^2 size.

Calibrated membranes are manufactured by Geonor with either butyl latex or neoprene as the rubber material. It was found in this investigation that the butyl latex does not form a watertight seal around the active reinforcing wire. During tests, water came into contact with the active wire, causing partial short circuits. This resulted in a decreased electrical resistance, and erroneous microstrain readings. The membranes made with neoprene did not have this leakage problem.

The electrical resistance of the active reinforcing wire is also very sensitive to temperature changes. Temperature variations result in resistance changes, which can be mistaken for changes in lateral stress. To compensate for temperature changes, the active membrane and a matching dummy membrane can be connected in a bridge arrangement. If both the temperature coefficient of resistivity and the gauge factor of the active and the dummy membranes are equal, resistance changes caused by temperature fluctuations will cancel. Under these conditions, microstrain readings will be unaffected by small temperature changes. The active and dummy membranes should be placed as close to each other as physically possible.

3.5 Modification for Cyclic Loading Capabilities

The NGI direct simple shear apparatus was modified by Geonor for cyclic loading capabilities. With the existing modifications, stress controlled tests with square wave loading can be performed.

The cyclic loading mechanism is illustrated in Figure 3.5. The hydraulic piston travels up and down at controlled frequencies. The weights shown are attached by wires to the connection fork. When the piston is in the down position, the left weights hang free; when the piston is up, it supports these weights. If exactly twice as much weight (including the weight of the hanger) hangs from the left side as from the right side, equal shear forces will alternately be transmitted in opposite directions to the sample. Thus, the mechanism

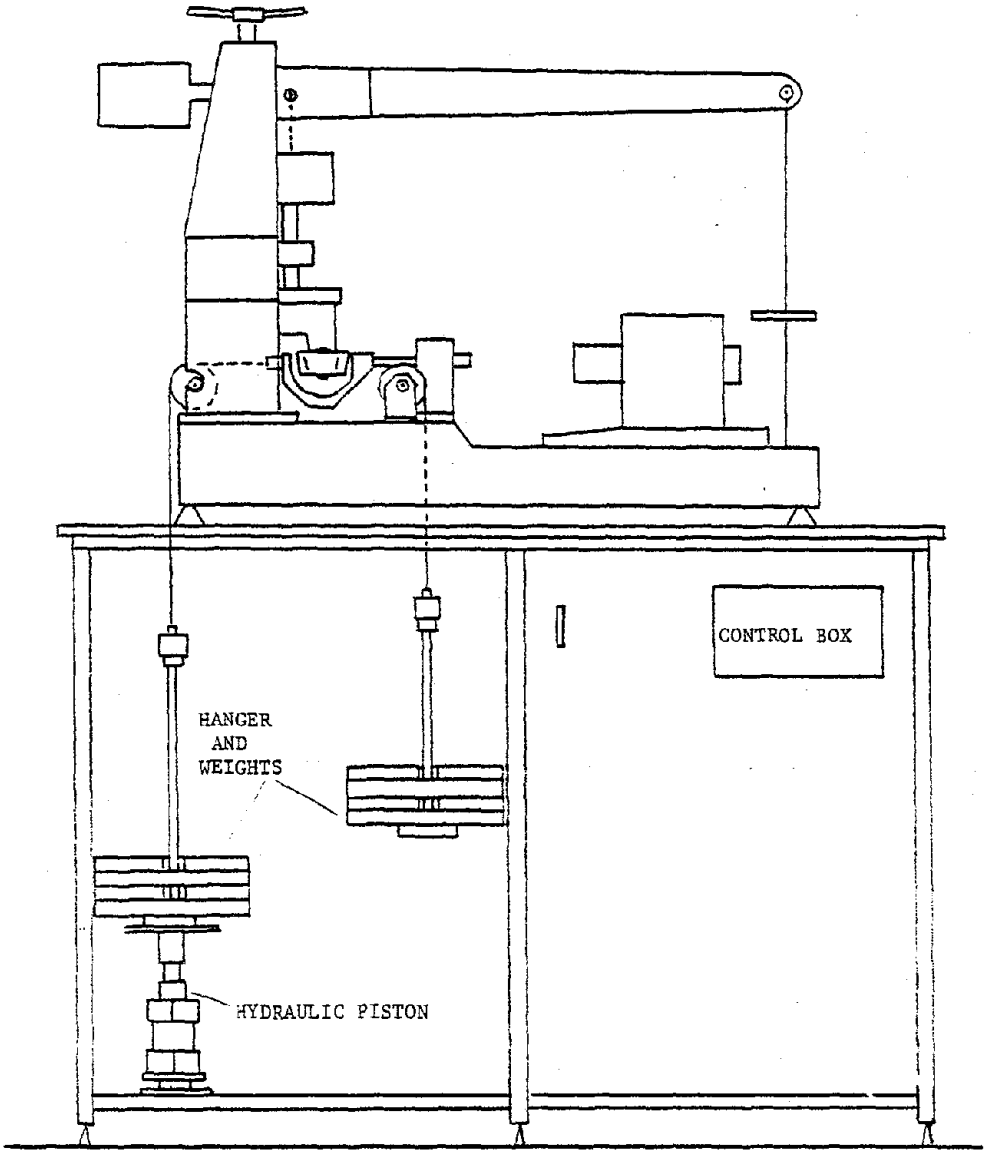

FIGURE 3.5. THE NGI DIRECT SIMPLE SHEAR DEVICE
WITH MODIFICATIONS FOR CYCLIC LOADING

shown induces a stress controlled square wave loading on the sample.

The control unit consists of a counter and a timer. The counter can be preset for a given number of cycles, and cycling will terminate after the desired number of cycles has been reached. The timer has a digital control for the cycling frequency. Half period frequencies from 1 to 99 seconds are possible. The timer controls a 4-way solenoid operated air valve, which actuates the piston motion.

3.6 Additional Modifications

To facilitate data acquisition, some additional modifications were made to the NGI direct simple shear apparatus.

The vertical load proving ring was replaced by a Schaevitz FTD-1U-200 load cell. This load cell has a capacity of 200 lb (890 N) in tension and compression. Its linearity is better than 0.2 percent, and its resolution is better than 0.1 percent.

A Hewlett-Packard 7DCDT-050 Linear Variable Differential Transformer (LVDT) was used to measure horizontal displacements. The range of this LVDT is $\pm$ 0.050 in. ($\pm$0.27 cm). The LVDT was connected in series with the horizontal dial gauge by an aluminum mounting block. Thus, horizontal displacements could be measured by either the LVDT or the dial gauge. Typically, the LVDT and the dial gauge were used together, thereby providing a convenient cross-check at all times.

The voltage outputs of the LVDT and the load cell were recorded by a Gould Brush 2400 four channel strip chart recorder. The electrical resistance changes in the calibrated reinforced rubber membranes were measured by a BLH 120C strain gauge indicator.

3.7 Equipment Calibration

3.7.1 Load Cell. The Schaevitz load cell was calibrated on the direct simple shear apparatus. Loads were applied to it through the lever arm, and the corresponding output voltages were measured. The voltage output was linear throughout (and beyond) the nominal range of the load cell.

3.7.2 LVDT. The Hewlett-Packard LVDT was also calibrated on the direct simple shear apparatus. Voltage outputs were recorded for horizontal displacements measured by the dial gauge. The voltage output was linear throughout (and beyond) the nominal range of the LVDT.

3.7.3 Friction. Friction in the vertical loading unit and the horizontal loading unit originates primarily in the ball bearing bushings. This friction can be measured by the 50 kg proving ring load gauge or by the Schaevitz load cell. It was found to be negligible.

3.7.4 Membrane Resistance to Shear. The resistance of the reinforced rubber membranes to shear can be determined by shearing them while they are filled with water. Using this procedure, Ladd and

Edgers (59) found that the resistance to shear increases with increasing shear strain and with decreasing normal stress. It was determined that the resistance to shear was less than 0.01 kg/cm^2 (0.98 kN/m^2) for a normal stress of 0.3 kg/cm^2 (29 kN/m^2). Similar results have been found by Geonor (31).

These results are valid only for the particular membranes tested. However, it seems reasonable that other membranes should behave similarly. Since the soil samples tested in this study were consolidated to stresses greater than 0.3 kg/cm^2 (29 kN/m^2), the membrane resistance was considered to be negligible.

3.7.5 False (Vertical) Deformation. The vertical deformation of soil samples is measured between two reference points, the top half of the sliding shear box and the base. Since the parts of the direct simple shear apparatus between these two points will also deform under the action of a vertical load, it is necessary to distinguish this deformation (false deformation) from the deformation of the sample itself. This is especially important for constant volume tests, because the vertical load is changed in order to keep the sample height (volume) constant. As the vertical load is changed, the false deformation also changes, and this must be taken into account.

The parts of the direct simple shear apparatus of interest for false deformation studies include the sliding shear box assembly, the caps, the porous stones, and the pedestal. The deformation of all these

parts can be measured by inserting a steel dummy sample between the caps. Loads are then applied through the lever arm, and the vertical deflection is measured by the dial gauge. The steel dummy sample also deforms under stress application, but the deformation of this steel cylinder can be determined from theoretical considerations. It was found to be negligible.

An effort was made to determine the false deformation under conditions similar to those in an actual test. Using the steel dummy sample, the sample assembly was prepared in the standard way. The consolidation loading sequence was also identical to that used for the actual tests. After the final consolidation load was applied, the vertical load was decreased in small increments; this procedure simulates the load decrease necessary to maintain constant volume conditions during shear for normally consolidated and lightly over-consolidated soil samples.

The false deformation measured by these calibration tests showed some variation, especially during the loading sequence. Average false deformation curves were obtained for each consolidation history used. An example is shown in Figure 3.6 for the 50 cm^2 size sample consolidated to 0.510 kg/cm^2 (50 kN/m^2).

To correct for false deformation during a constant volume test, the appropriate false deformation curve is entered at the final consolidation load. As the load is changed during the test, the vertical

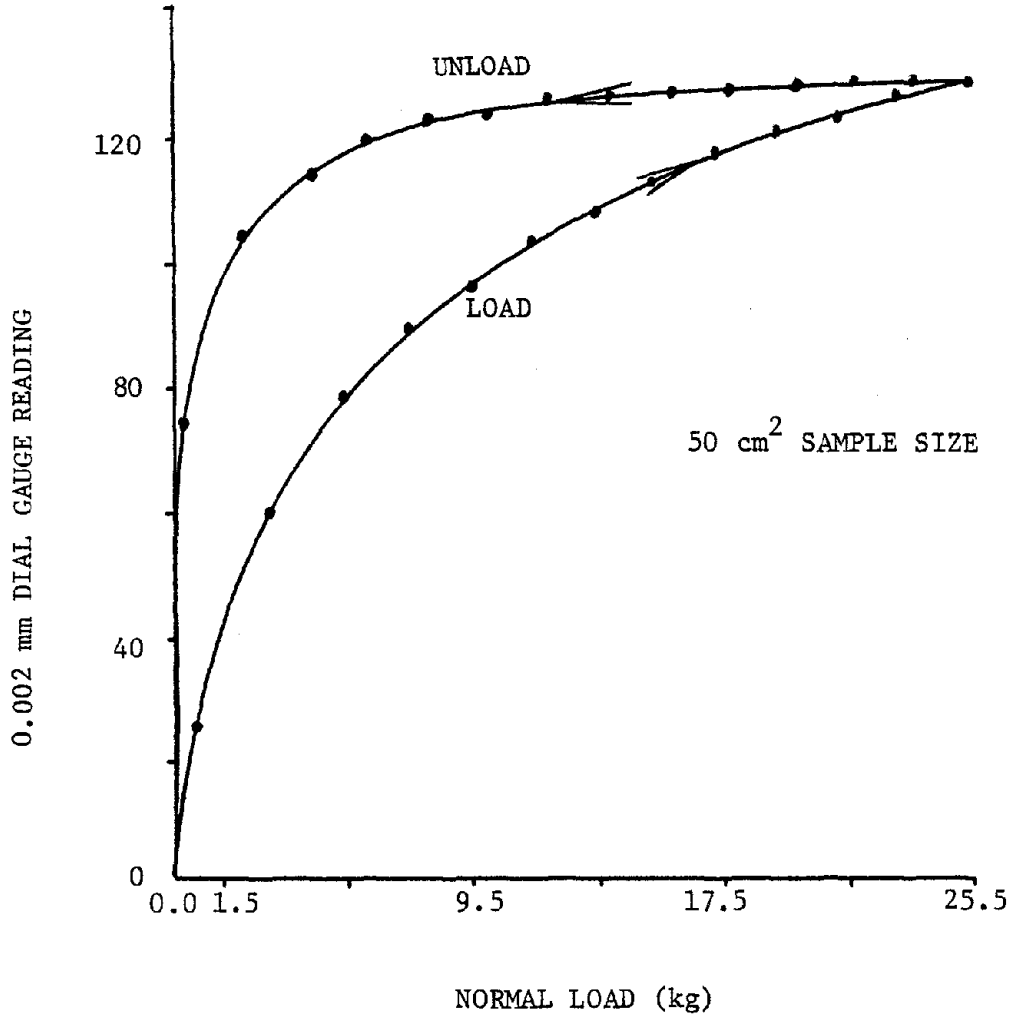

FIGURE 3.6. FALSE (VERTICAL) DEFORMATION IN THE NGI DIRECT SIMPLE SHEAR DEVICE

dial gauge reading is adjusted according to this curve. With the use of this procedure, the false deformation is accounted for, and the volume of the sample remains constant.

3.7.6 Calibrated Membranes. The calibrated wire reinforced rubber membranes (used for the measurement of lateral stress) were supplied with a calibration curve from Geonor, and they were also recalibrated in the laboratory. The membranes were calibrated by means of a calibration cylinder, which is manufactured by Geonor. Basically, this device is a plexiglass cylinder with a thin, expandable rubber membrane attached to the middle part of it.

The wire reinforced membrane to be calibrated is first placed on the calibration cylinder. A hydrostatic pressure* is then applied to the interior of the calibration cylinder, causing its membrane to expand and transmit a lateral stress to the wire reinforced membrane. The pressure in the cylinder is increased in small increments, and the corresponding microstrain readings, measured by a strain gauge indicator, are recorded. After the maximum lateral stress is reached, the pressure is decreased in small increments, and the corresponding microstrain readings are recorded.

A number of calibration tests should be performed for each membrane. A calibration curve can then be obtained by plotting average values of change in microstrain reading versus lateral stress. The slope of

*Air or water pressure may be used; however, air pressure is recommended (7). For this investigation, air pressure was used to calibrate the membranes. The air pressure supplied to the calibration cylinder was controlled by a pressure regulator, and it was measured by a mercury manometer.

this curve, in the form of change in microstrain per unit of stress, is the calibration factor for the membrane.

A typical example of a calibration curve is shown in Figure 3.7. It should be noted from this figure that:

1. There is a small bend in the initial part of the calibration curve. The reason for this bend is that the membrane in the calibration cylinder needs a certain pressure before it begins to expand. This threshold pressure was observed to be approximately 0.05 kg/cm^2 (5 kN/m^2).

2. Of primary importance is the calibration factor of the membrane. Except for the initial bend, the slope of the calibration curve is approximately constant. However, for increased accuracy, the slope of the curve in the stress range of interest can be used.

3.7.7 Secondary Consolidation or Creep. Although this section does not deal with the NGI direct simple shear apparatus per se, it is included here because of its relevance to constant volume testing.

Creep* in soils has been studied and described, among other ways, in terms of pore pressure buildup under undrained conditions. Holzer, Höeg, and Arulanandan (44) concluded that the increase in pore pressure with time under undrained conditions is caused by the arrest of secondary consolidation. The undrained creep rate (rate of pore pressure buildup)

*Creep is defined as the phenomenon, when soil is subjected to a sustained stress, of either continued strain under drained conditions or pore pressure buildup and strain under undrained conditions. A detailed discussion of creep is not included in this report.

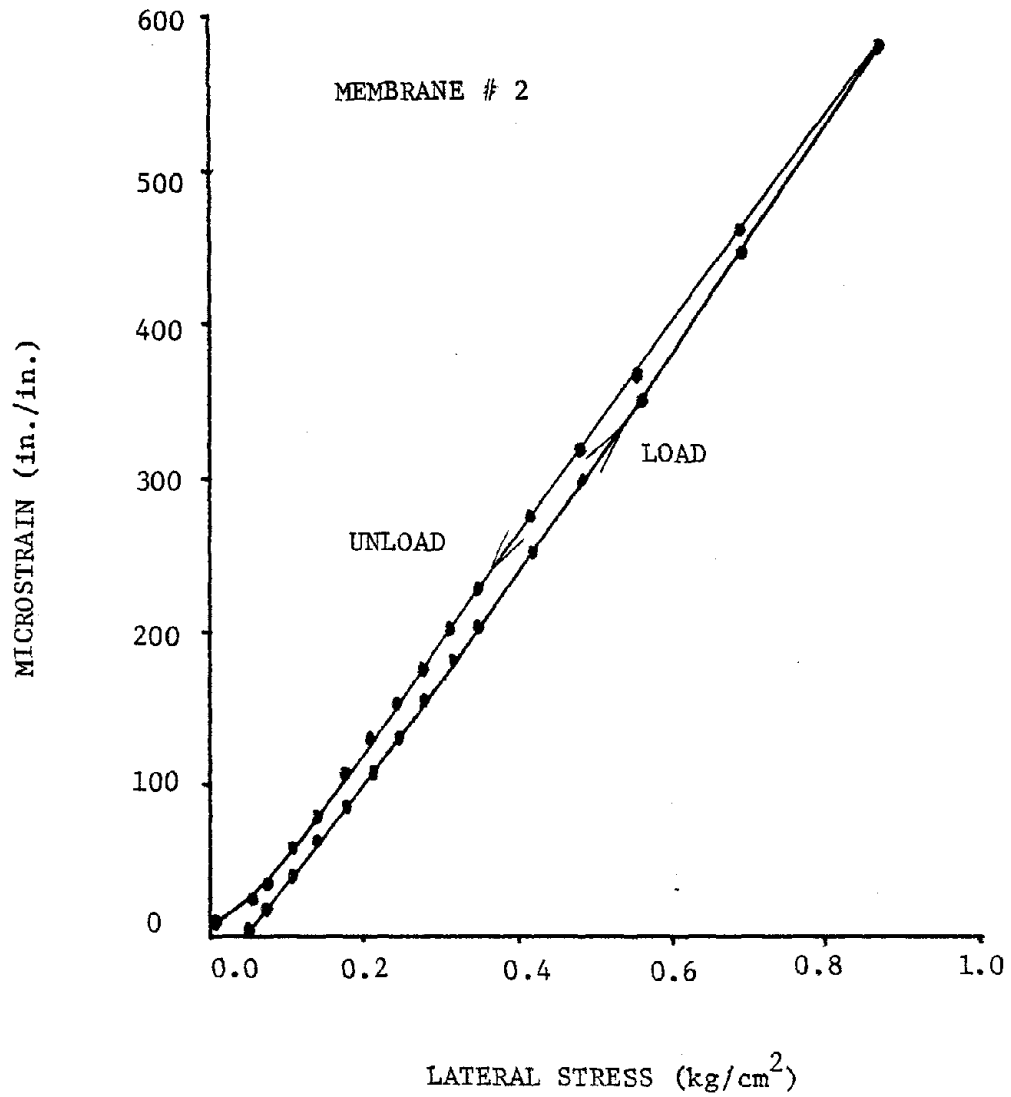

FIGURE 3.7. CALIBRATION OF A (STRAIN GAUGE EQUIPPED) WIRE REINFORCED RUBBER MEMBRANE

will be greater for a soil sample consolidated for only a few days in the laboratory than it will be for the same soil in situ, which has undergone secondary consolidation for a long period of time. For this reason, undrained creep can be considered to be a testing error (94).

As a typical example of secondary consolidation, data for a Gulf of Alaska clay sample (Test 1) is presented. For the final consolidation load increment, the vertical dial gauge reading versus log time curve is shown in Figure 3.8. For large values of time, the secondary consolidation portion of the curve can be represented by a straight line. A linear regression analysis of the data results in the equation:

$$DR = 297.34 + 33.74 \log t \qquad 3.1$$

where DR is the dial gauge reading, and t is time, in minutes.

Because of secondary consolidation, constant volume conditions cannot be maintained in a soil sample for any period of time unless the vertical stress is reduced. This reduction in vertical stress is equivalent to an increase in pore pressure with time during an undrained test. The change in pore pressure caused by creep should be distinguished from the change in pore pressure caused by shear. This can be done in the following ways:

1. Increase the consolidation time in the laboratory until the effect of secondary consolidation is negligible.

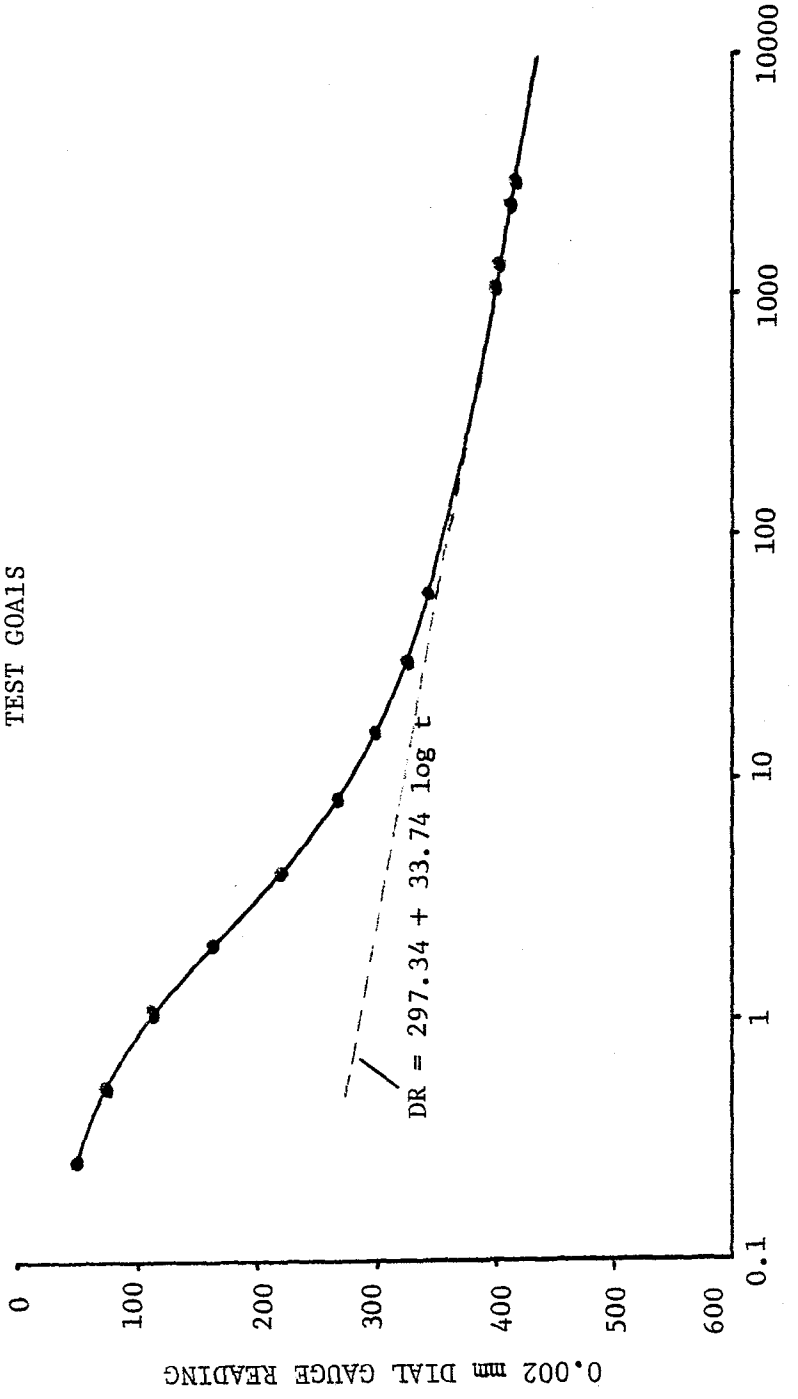

FIGURE 3.8. SECONDARY CONSOLIDATION IN THE NGI DIRECT SIMPLE SHEAR SAMPLE

2. Correct the sample height to account for secondary consolidation. Prior to shear, the dial gauge versus log time relation can be drawn, and the secondary consolidation portion of this curve can be extrapolated and fitted to a straight line. During shear, the sample height is adjusted at convenient time intervals according to this relation.

3. Perform a creep test by measuring the change in vertical stress needed to maintain a soil sample at constant volume. The equivalent pore pressures can then be used to correct the results of shear tests for creep. However, this procedure only corrects the pore pressures; the shear strains (which depend on the effective stress in the sample during the test) are not corrected.

Alternatively, the effect of secondary consolidation or creep can be ignored. This results in conservative laboratory results: higher pore pressures are developed in laboratory samples than in situ, and consequently, the laboratory samples are weaker.

PART 4

TESTING PROCEDURES

The soils investigated in this study were stored in an environmentally controlled room under high humidity conditions (98% relative humidity). The storage temperature was kept at 3C to simulate in situ conditions and to inhibit the generation of gases within the samples. The soils, Concord Blue clay and Gulf of Alaska clay, are described in Part 6. The block sample of Concord Blue clay was cut into smaller sections, which were sealed in wax and plastic. The Gulf of Alaska clay was sealed in its core tube.

The soil samples were trimmed and prepared for testing in an adjacent environmentally controlled room. This second room was also maintained under high humidity conditions to prevent sample drying during the trimming operation, but the temperature was kept at 20C.

The NGI trimming apparatus, supplied by Geonor, was used for all tests. Except for minor details, the trimming procedure is identical to the one described by Geonor (31). Because of the detailed procedure and the close mechanical tolerances of the trimming apparatus, it was found that sample trimming is not only a science, but also an art. The average trimming time was approximately one hour.

After sample trimming was completed, the sample was carefully moved from the environmentally controlled room to the NGI direct simple shear apparatus. Drainage hoses, leading to water supplies, were connected to the upper and lower caps of the sample. For the Gulf of Alaska clay, a salt water solution (obtained from a local aquarium supply store) was

used as the water supply. A quantity of water was circulated through the caps and the enclosed porous stones to flush out any air that may have been trapped there during the trimming process.

The sample was next clamped to the direct simple shear device. The sliding shear box was brought into contact with the top of the sample, and the lever arm was leveled. A small weight (10 grams) was placed at the end of the lever arm to insure contact between the sample and the shear box. For tests in which lateral stress measurements were taken, the calibrated membrane was connected to the strain gauge indicator. Because the calibrated membranes are very sensitive to temperature changes, which may be caused by handling the sample, the sample was allowed to sit for at least one hour before an initial microstrain reading was taken.

The sample was then consolidated. The consolidation loads were applied in increments, similar to the procedure used in the standard laboratory consolidation test. The time between each load increment was approximately twice the time needed for 100 percent primary consolidation. The final consolidation load was applied for a minimum of 24 hours before the sample was sheared.

All tests were run as constant volume tests. Since the sample has a constant cross sectional area, constant volume is maintained by keeping the sample height constant. The change in vertical stress necessary to maintain a constant sample height is equated to the excess pore pressure that would have developed in an undrained test (79). It

should be noted that drainage is allowed during shear, and no excess pore pressure develops in the sample if the rate of shear is sufficiently slow to permit drainage. Therefore, all measured stresses are effective stresses. Typically, static tests were performed in about seven hours. Cyclic tests were performed at frequencies of 0.5 and 0.1 Hz. These frequencies were selected to simulate earthquake and storm wave loading applications.

Following the completion of testing, the sample was removed from the shear apparatus. The final water content of the sample was measured at this time. The measured water content agreed well with the water content computed for the sample at the end of consolidation. For the Gulf of Alaska clay, for example, the measured and computed water contents agreed within an average of five percent.

The data obtained from each test was compiled from the strip chart recordings. The data was reduced and processed by computer. The test results are presented in Part 7 and discussed in Part 8.

PART 5

STRESS CONDITIONS IN THE NGI SAMPLE

5.1 Introduction

As is the case with every laboratory soil testing device, the NGI direct simple shear apparatus has some limitations. Numerous investigators have analyzed the stress conditions produced in the soil sample by direct simple shear devices. The findings of these theoretical and experimental studies are discussed in the following section.

The assumptions necessary for the interpretation of test results are discussed next. For the tests in which lateral stresses were measured, sufficient information is available to determine Mohr's circle of stress for a soil element at the center of the sample. On the basis of Mohr's circle, information can be obtained about the state of stress within the sample (for example, the magnitude and orientation of the principal stresses). Equations are presented for various parameters that can be determined from Mohr's circle.

5.2 Review of Theoretical and Experimental Studies of the Stress Conditions Produced in Direct Simple Shear Samples

Cyclic stresses induced on an in situ soil element can often be closely approximated by cyclic shear stresses acting on the horizontal planes of the soil element. If an initial shear stress exists on the horizontal planes prior to cyclic loading, then the cyclic shear stresses can be superimposed upon this static shear stress.

The cyclic direct simple shear apparatus was developed to reproduce these field conditions in the laboratory. The stress conditions imposed on a soil element in the field and on the boundaries of the NGI direct simple shear sample are compared in Figure 5.1. The lack of complementary shear stresses on the sides of the sample implies that the boundary stress conditions are not ideal, making the interpretation of direct simple shear tests rather difficult.

With regard to the SGI direct simple shear device, Kjellman (53) noted that, for equilibrium requirements, the normal stresses on the upper and lower surfaces of the sample must be unevenly distributed. The shear stresses on these surfaces are also unevenly distributed, since they must be zero close to the front and rear of the sample. It was concluded that the distribution of stresses in the sample is not perfect, but certainly better than it is in conventional direct shear devices.

Hvorslev and Kaufman (46) also examined the SGI direct simple shear device. It was found that neither the vertical normal stresses nor the horizontal shear stresses acting on the sample are distributed uniformly. The nonuniformity tends to increase with increasing deformation.

Roscoe (86) analyzed the stresses acting on a sample in the Cambridge simple shear device. The analysis was based on the theory of elasticity, assuming that the soil behaves as a linear elastic, isotropic material. It was concluded that shear loading induces changes in normal stress

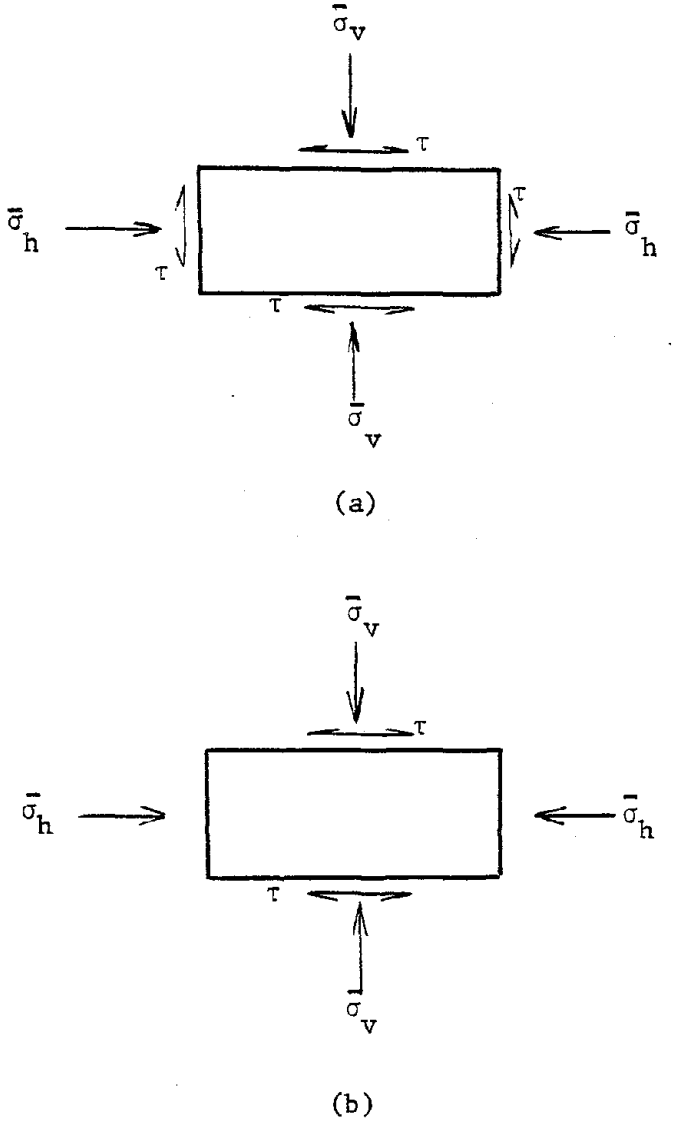

FIGURE 5.1. COMPARISON OF THE SHEAR STRESSES IMPOSED ON THE BOUNDARIES OF AN IN SITU SOIL ELEMENT AND ON THE BOUNDARIES OF THE NGI DIRECT SIMPLE SHEAR SAMPLE: (a) IN SITU; (b) NGI SAMPLE

($\bar{\sigma}_v$ and $\bar{\sigma}_h$) near the edges of the sample, but not at its center. The moment produced by the applied shear stress is exactly balanced by the moment produced by the nonuniform normal stress distributions acting on the sample boundaries.

Roscoe (86) also noted that the distribution of shear stresses on the upper and lower boundaries of the sample is nonuniform. The magnitude of the shear stress increases rapidly with distance from the ends of the sample and is quite uniform in the middle third of the upper and lower sample boundaries. The shear stress in the central portion of the sample is approximately 10 percent greater than the average applied shear stress.

Duncan and Dunlop (18) investigated the stress conditions existing within a sample tested in the Cambridge simple shear apparatus. The stress conditions were analyzed by the finite element method, assuming nonlinear and anisotropic stress-strain characteristics for the sample material. The stress distributions were found to be nonuniform. These stress nonuniformities result from the lack of complementary shear stresses on the sides of the sample. It was also determined that progressive failure occurs, with failure beginning near the ends of the sample. The size of these failure zones gradually increases, and with increasing shear strain, the failure zones eventually merge.

Duncan and Dunlop (18) pointed out that their analysis shows that the stress nonuniformities are most severe near the ends of the sample. They concluded that the stresses in the center of the sample are reasonably uniform and correspond closely to pure shear conditions. The assumption of a uniform stress condition provides a simple and useful means of comparing strength values measured in simple shear tests with those measured in other tests.

Lucks, et al (68), analyzed the stress conditions existing in a NGI direct simple shear sample. A three-dimensional finite element model was employed, assuming linear elastic, isotropic material parameters. It was found that stress concentrations are quite local. Approximately 70 percent of the sample has fairly uniform stress conditions, which are representative of the applied boundary stresses. It was also concluded that progressive yielding is only of minor importance.

Provost and Höeg (79) recently investigated the stress conditions occurring in simple shear test samples. The effects of partial boundary slippage at the interface between the soil sample and the caps of the Cambridge simple shear apparatus were determined, using an isotropic elastic analysis. Such slippage increases the nonuniformity of stress within the sample. For the case of no boundary slippage, it was found that an applied shear stress does not induce significant changes in normal stress in the central portion of the upper and lower faces of the sample. The shear stress in the central portion of these faces is approximately 10 percent greater than the average applied shear stress.

A finite element study of the NGI direct simple shear sample subjected to cyclic loading conditions was conducted by Shen, et al (101). It was found that the shear strain distribution in the soil sample is nonuniform and asymmetric. For the soils studied, the measured shear modulus was found to be in error by 5 to 15 percent. It was concluded that this magnitude of error may be viewed as acceptable for most geotechnical engineering work.

Wright, et al (115), studied the stress distributions in samples for the Cambridge simple shear device and the NGI direct simple shear device. Results were based on elasticity theory, using the Saint Venant solution (110) for a fixed end beam of square or circular cross section subjected to an end load. It was concluded, on the basis of this study and an experimental photoelastic study, that the stress distributions within the sample are totally nonuniform. However, the authors noted that their conclusions were based on elasticity theory, and that the boundary conditions in the Saint Venant problem are not exactly the same as they are in simple shear samples. It was argued that it is important to determine the character of the stress distributions, and to compute their order of magnitude, in order to interpret simple shear test results.

In a recent state of the art publication on the measurement of dynamic soil properties, Woods (114) concluded that despite the internal complexities and uncertainties associated with the simple shear

test, it has been a useful tool in studying cyclic shear phenomena. For practical purposes, the potential effects of stress nonuniformities may be minimal.

It should be noted that all laboratory soil testing devices have their advantages and disadvantages. Most devices test relatively small samples, thereby making boundary effects and end conditions, with their resulting stress concentrations, a major concern. Nevertheless, it is typically assumed that the stress conditions are uniform throughout the soil sample and are representative of the stresses imposed on the boundaries of the sample.

5.3 Assumed Stress Conditions in the NGI Direct Simple Shear Sample

On the basis of the previous discussion, it can be seen that there is some disagreement with regard to the state of stress within direct simple shear samples. Nevertheless, it will be assumed that the stress conditions existing in the central part of the NGI direct simple shear sample are reasonably uniform and representative of the stresses imposed on the sample boundaries.

Undrained conditions are simulated in the NGI direct simple shear device by maintaining the sample at constant volume. Prevost and Höeg (79) have noted that it will not be possible in general to conduct a constant volume direct simple shear test that is truly identical to an undrained direct simple shear test. In a constant volume test, incompressibility is satisfied only in an average sense for the entire

sample, while in an undrained test, incompressibility is satisfied everywhere within the sample.

Although some argument may exist, it will be assumed for this investigation that a constant volume test is equivalent to an undrained test. The change in vertical stress that is necessary to maintain a constant sample volume during shear is equated to the excess pore pressure that would have developed in an undrained test (10).

During constant volume shear, drainage is allowed, and no excess pore pressure develops in the sample if the rate of shear is sufficiently slow to permit drainage. For both the Gulf of Alaska clay and Concord Blue clay, the time needed for 100 percent primary consolidation in the soil sample is approximately 10 minutes*. Since the static tests were performed in about 7 hours, it seems likely that there is adequate time for complete drainage during these tests. It is questionable, though, whether there is adequate time for drainage during the cyclic loading tests, especially for tests of short duration (less than 10 minutes). Nevertheless, it will be assumed for this investigation that the sample is completely drained, and therefore, all measured stresses are effective stresses.

For tests in which lateral stresses were measured, the vertical normal stress, $\bar{\sigma}_v$; the horizontal normal stress, $\bar{\sigma}_h$; and the horizontal shear stress, τ_h, acting on the boundaries of the sample are known. The

*This value was determined from consolidation test data

three measured boundary stresses acting on the NGI direct simple shear sample are shown in Figure 5.2. The stresses assumed to be acting on an infinitesimal element at the center of the sample are also shown in this figure. The shear stresses acting on the sides of this element are assumed to be equal in magnitude to the measured (horizontal) shear stress.

From the three measured stresses, a Mohr's circle of stress can be drawn for the soil element at any time during the test, as shown in Figure 5.3. The variables indicated in the figure can be determined from the geometry of the Mohr's circle, as follows:

$$\bar{p} = \frac{\bar{\sigma}_v + \bar{\sigma}_h}{2} = \frac{\bar{\sigma}_1 + \bar{\sigma}_3}{2} \qquad 5.1$$

$$q = \left[\frac{(\bar{\sigma}_v - \bar{\sigma}_h)^2}{4} + \tau_h^2\right]^{1/2} = \frac{\bar{\sigma}_1 - \bar{\sigma}_3}{2} \qquad 5.2$$

where $\bar{p}$ and q define the effective stress point (61), which is the uppermost point of the Mohr's circle;

$$\phi_m = \sin^{-1}\left(\frac{q}{\bar{p}}\right) \qquad 5.3$$

where ϕ_m is the mobilized friction angle of the soil;

$$\theta_p = \tan^{-1}\left[\frac{\tau_h}{\frac{(\bar{\sigma}_v - \bar{\sigma}_h)}{2} + q}\right] \qquad 5.4$$

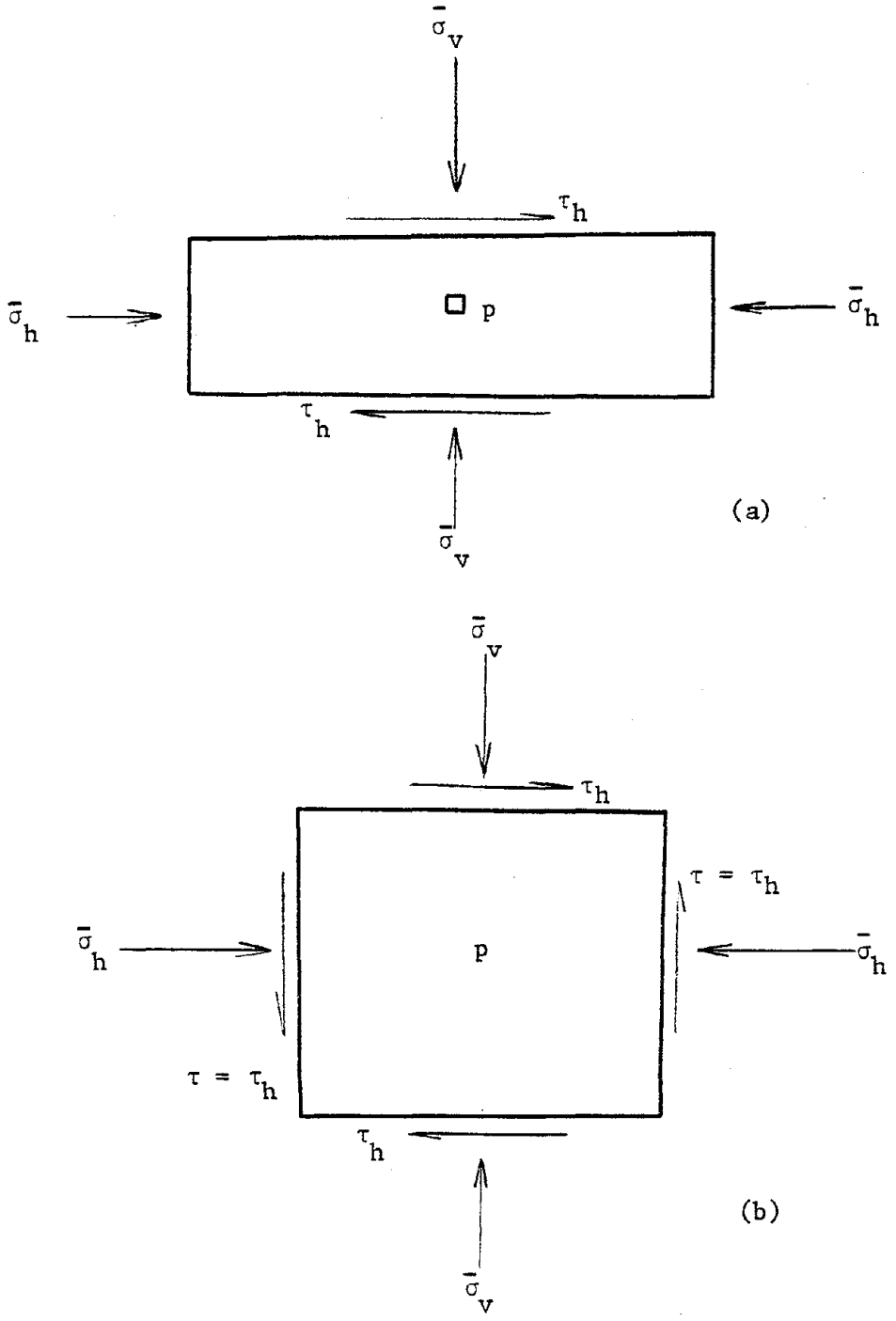

FIGURE 5.2. STRESSES IN THE NGI DIRECT SIMPLE SHEAR SAMPLE: (a) MEASURED BOUNDARY STRESSES; (b) STRESSES ACTING ON AN INFINITESIMAL ELEMENT AT THE CENTER OF THE SAMPLE

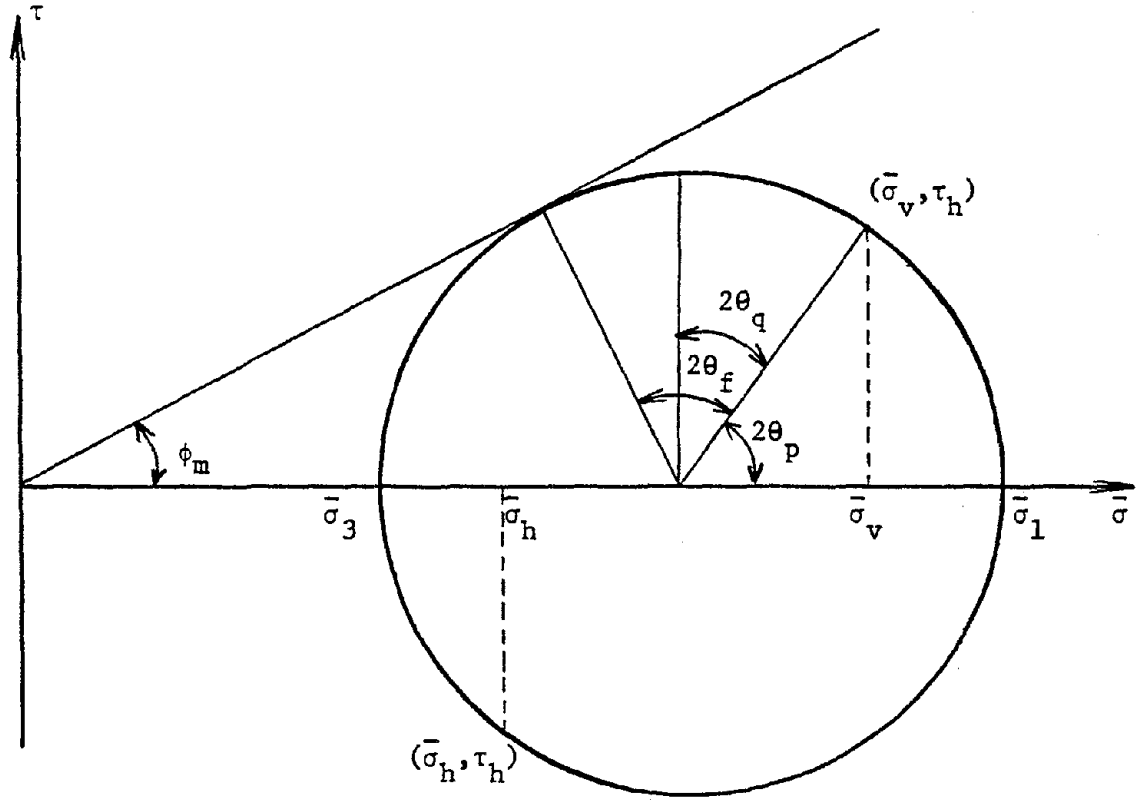

$$\bar{p} = \frac{\bar{\sigma}_v + \bar{\sigma}_h}{2} = \frac{\bar{\sigma}_1 + \bar{\sigma}_3}{2}$$

$$q = \left[\frac{(\bar{\sigma}_v - \bar{\sigma}_h)^2}{4} + \tau_h^2\right]^{1/2} = \frac{\bar{\sigma}_1 - \bar{\sigma}_3}{2}$$

$$\phi_m = \sin^{-1}\left(\frac{q}{\bar{p}}\right)$$

$$\theta_p = \tan^{-1}\left[\frac{\tau_h}{\frac{(\bar{\sigma}_v - \bar{\sigma}_h)}{2} + q}\right]$$

$$\theta_q = 45 - \theta_p$$

$$\theta_f = 45 + \frac{\phi_m}{2} - \theta_p$$

$$\bar{\sigma}_1 = \bar{p} + q$$

$$\bar{\sigma}_3 = \bar{p} - q$$

FIGURE 5.3. MOHR'S CIRCLE OF STRESS FOR AN INFINITESIMAL ELEMENT OF SOIL AT THE CENTER OF THE NGI DIRECT SIMPLE SHEAR SAMPLE

where θ_p is the angle between the horizontal plane of the sample and the plane on which the major principal stress acts;

$$\theta_q = 45 - \theta_p \tag{5.5}$$

where θ_q is the angle between the horizontal plane of the sample and the plane on which the maximum shear stress acts;

$$\theta_f = 45 + \frac{\phi_m}{2} - \theta_p \tag{5.6}$$

where θ_f is the angle between the horizontal plane of the sample and the plane of maximum obliquity; and

$$\bar{\sigma}_1 = \bar{p} + q \tag{5.7}$$

$$\bar{\sigma}_3 = \bar{p} - q \tag{5.8}$$

where $\bar{\sigma}_1$ is the major principal effective stress, and $\bar{\sigma}_3$ is the minor principal effective stress. Note that ϕ_m is computed for the case of zero cohesion ($c = 0$).

All tests that included lateral stress measurements were analyzed on the basis of the assumptions and equations presented here. The tests without lateral stress measurements were analyzed in the conventional way (on the basis of $\bar{\sigma}_v$ and τ_h). Test results are presented in Part 7.

PART 6

DESCRIPTION OF THE SOILS TESTED

6.1 Introduction

To obtain an understanding of clay soil behavior in the field, the soil structure should be preserved as found in situ. Therefore, only undisturbed samples of cohesive soils were tested in the laboratory.

Two fine grained soils were studied: a Gulf of Alaska clay (from the Copper River prodelta) and Concord Blue clay. They are described in the following sections. Pertinent background information about these soils is noted, along with the reasons for obtaining laboratory test data.

6.2 Gulf of Alaska Clay

Petroleum related activities in the outer continental shelf region of the Gulf of Alaska may stimulate major marine construction in this area. Therefore, it is important to identify and evaluate the geological and geotechnical characteristics of the marine soils associated with this region.

Marine geologic studies were conducted by the United States Geological Survey (USGS) in the continental shelf and the upper continental slope regions of the Gulf of Alaska. Several areas of slope instability were discovered. One area of instability is the Copper River prodelta, from which the clay samples used in this study were obtained.

The Copper River is a major source of Holocene sediment, with an annual sediment discharge of 107×10^6 tons. Much of this sediment has accumulated on the prodelta, reaching a maximum thickness of 350 m, with an average thickness of 150 m. The rate of sedimentation is very high in this area, being on the order of 10-15 meters per 1,000 years (14).

Seismic reflection surveys of the Copper River prodelta show disrupted bedding and irregular topography, indicating submarine slides and slumps (14,35). This type of structure is evident across the entire span of the prodelta, an area of 1,700 km^2. The seafloor in this area has a slope of approximately 0.5° (14).

Submarine slope failures can occur on extremely flat terrain. Since the extent of many submarine slopes is fairly large, the infinite slope method of analysis can be used to advantage (71). Using this simple model (Figure 6.1), the equation for stability* (for the case of zero cohesion) is:

$$FS = \frac{\text{resisting force}}{\text{driving force}} = \left[1 - \frac{\Delta u}{\gamma' H \cos^2 i}\right] \frac{\tan \phi'}{\tan i} \qquad 6.1$$

where

FS = Factor of safety

Δu = Excess pore water pressure (in excess of hydrostatic)

γ' = Buoyant unit weight of soil = $\gamma_t - \gamma_w$

H = Depth of failure surface measured from the surface of the sediment

*Adopted from Hampton, et al (35).

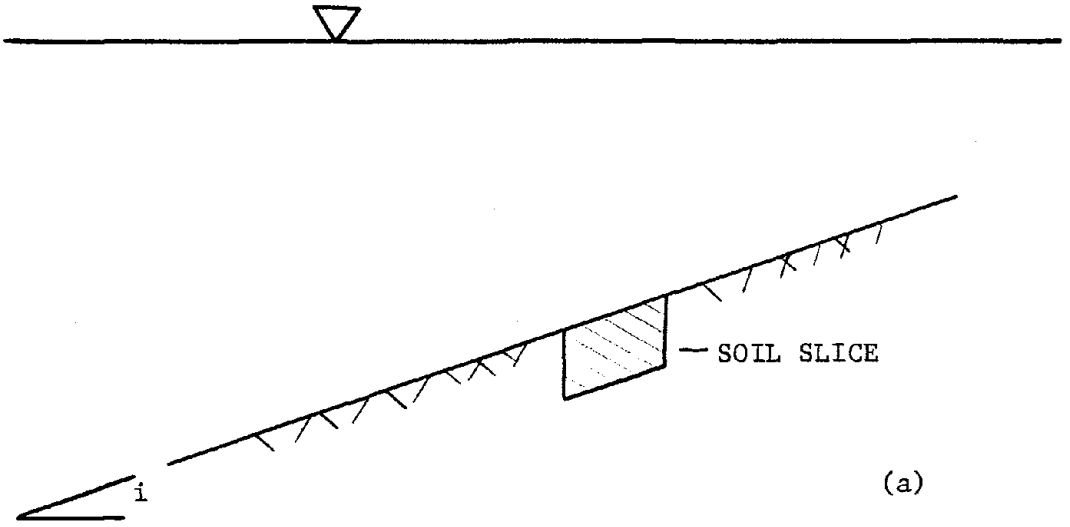

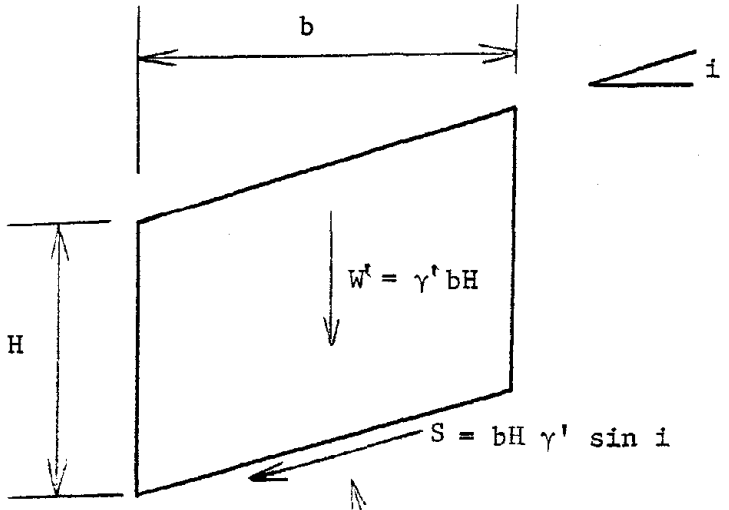

RESISTING FORCE = (N-U)tan ϕ

DRIVING FORCE = S

NOTE: $\gamma' = \gamma_t - \gamma_w$

Δu = PORE PRESSURE IN EXCESS OF HYDROSTATIC

FIGURE 6.1. SUBMARINE SLOPE STABILITY ANALYSIS: (a) SUBMARINE SLOPE; (b) SOIL SLICE USED FOR STABILITY ANALYSIS

i = Slope angle

ϕ' = Effective stress friction angle of soil

Any excess pore water pressure reduces the normal effective stress on the failure plane. The shearing resistance is thereby reduced, while the applied shear stress, caused by the weight of the soil, remains constant. The effective stress friction angle for the Copper River prodelta sediment is approximately 24° (35). If the excess pore pressure is zero, the theoretical maximum slope angle for this soil is also 24°.

Excess pore pressure in marine sediments can be produced by high rates of sedimentation, cyclic loading, and the presence of gas-charged sediments (90). For the Copper River prodelta, all of these factors are important and they must be taken into consideration. In determining the stability of submarine slopes, other factors should also be considered: removal of slope support by faulting or erosion, seismic forces and accelerations, and tectonic slope steepening.

A high rate of sedimentation causes a lag between sediment accumulation and subsequent consolidation, resulting in an accumulation of excess pore pressure. In the literature, this is frequently referred to as underconsolidation. Hampton, et al (35), investigated the significance of the excess pore pressures resulting from high sedimentation rates in the Copper River delta. The theoretical approach developed by Gibson (32) was used to determine the magnitude of the excess pore

pressures. Using the infinite slope method of analysis and the theoretical pore pressures, Hampton et al (35), determined that only slopes with an inclination less than 2.6° would be stable. This is a substantial decrease from the 24° angle determined for the case of zero excess pore pressure.

Excess pore pressures are also developed by earthquake loadings. The forces and accelerations generated by the earthquake increase the applied shear stresses acting on potential failure surfaces, causing further instability. Reimnitz (82) attributed the slump structures seen on seismic records from the Copper River prodelta to the 1964 Alaska earthquake.

Excess pore pressures can also be generated by storm waves. The waves induce pressure fluctuations on the seafloor. The magnitude of these pressure fluctuations depends upon wave height, wave length, and water depth. Hampton, et al (35), showed that wave induced pressure fluctuations are significant in water depths up to at least 150 m. The wave action can also cause erosion on the seafloor.

Indications of free gas were noted by seismic data in the Copper River prodelta. The gas could be methane generated within the Holocene sediments, or it could be gas that has been liberated from underlying rock and then migrated up fault planes (58).

In summary, all of the factors noted above can lead to the instability of submarine slopes. For the Copper River prodelta, the rapid rate of sedimentation is important. The Gulf of Alaska is also in an area of

intense seismic activity. Storms with large waves are common, especially in the winter months (16). Therefore, it is imperative to determine the behavior of these submarine soils under cyclic loading.

A four inch inside diameter undisturbed core sample was obtained from the United States Geological Survey for laboratory testing. The sample was taken in the Copper River prodelta, and it contained sediment from one to two meters depth below the seafloor. Pertinent geotechnical data is given in Table 6.1.

6.3 Concord Blue Clay

Concord Blue clay is a silty glacial lacustrine clay obtained from a site near Colden, New York, which is southeast of Buffalo. Undisturbed block samples, containing approximately one cubic foot of soil, were cut by hand from a test pit. The samples were taken at a depth of ten feet below the ground surface.

Concord Blue clay was selected for laboratory testing because high quality undisturbed samples are readily and economically available. Pertinent geotechnical data is presented in Table 6.2.

TABLE 6.1

GEOTECHNICAL DATA FOR THE

GULF OF ALASKA CLAY

SITE: COPPER RIVER PRODELTA

TYPE: 4 INCH DIAMETER UNDISTURBED CORES

GEOTECHNICAL DATA

WATER CONTENT	57% - 65%
LIQUID LIMIT	50%
PLASTIC LIMIT	27%
SPECIFIC GRAVITY	2.84*
FRICTION ANGLE	24°*
SENSITIVITY (FALL CONE)	3.8
CONSOLIDATION HISTORY	UNDERCONSOLIDATED
PERCENT SAND	1*
PERCENT SILT	34*
PERCENT CLAY	65*

*Data from Hampton, et al (35).

TABLE 6.2

GEOTECHNICAL DATA FOR

CONCORD BLUE CLAY

SITE: COLDEN, NEW YORK (SOUTHEAST OF BUFFALO)

TYPE: UNDISTURBED BLOCKS

GEOTECHNICAL DATA

WATER CONTENT	27% - 28%
LIQUID LIMIT	34%
PLASTIC LIMIT	21%
SPECIFIC GRAVITY	2.76*
FRICTION ANGLE	25°*
SENSITIVITY (FALL CONE)	1.4
CONSOLIDATION HISTORY	NORMALLY CONSOLIDATED

*Data from Egan and Sangrey (19).

PART 7

TEST RESULTS

7.1 Gulf of Alaska Clay

7.1.1 Introduction. All direct simple shear tests performed on the Gulf of Alaska clay are summarized in Table 7.1. An explanation for each column of data is given in Table 7.2.

Prior to shear, all samples were consolidated in the NGI direct simple shear device. The soil samples were consolidated to stresses greater than the in situ maximum preconsolidation stress. This procedure was used because it minimizes the effects of sample disturbance, and it ensures that the samples will be normally consolidated (60).

For all direct simple shear tests performed on the Gulf of Alaska clay, the horizontal (lateral) stresses acting on the soil sample during consolidation and shear were measured by using calibrated wire reinforced membranes. The horizontal stress is computed by the equation:

$$\bar{\sigma}_h = \frac{(r - r_i)}{(1 - \varepsilon_v)} \frac{1}{k} \qquad 7.1$$

where

r = Microstrain reading corresponding to the horizontal stress, $\bar{\sigma}_h$

r_i = Initial microstrain reading corresponding to zero horizontal stress

ε_v = Vertical strain in the sample

k = Membrane calibration factor (microinches per inch/unit stress)

TABLE 7.1

SUMMARY OF TESTS - GULF OF ALASKA CLAY

COLUMN 1	2	3	4	5	6	7	8	9	10	11	12
Test No.	A cm^2	SAMPLE PREPARATION					CONSOLIDATION				
		w_i %	e_i	H_i cm	S_u kg/cm^2	S_t	$\bar{\sigma}_{vo}$ kg/cm^2	$\bar{\sigma}_{vm}$ kg/cm^2	OCR	H_f cm	ε_v %
GOA1S	50.0	63.0	1.79	1.72	0.039	-	0.527	0.527	1.0	1.53	10.6
GOA2S	50.0	58.0	1.65	1.64	0.039	-	0.527	0.527	1.0	1.48	9.7
GOA3S	50.0	60.4	1.72	1.72	0.039	-	0.257	0.257	1.0	1.59	7.5
GOA4C	50.0	59.3	1.68	1.74	0.036	-	0.527	0.527	1.0	1.60	8.3
GOA5C	50.0	67.2	1.91	1.66	0.025	-	0.527	0.527	1.0	1.39	16.2
GOA6C	50.0	64.8	1.84	1.65	0.024	-	0.527	0.527	1.0	1.40	14.8
GOA7C	50.0	61.6	1.75	1.40	0.033	4.2	0.527	0.527	1.0	1.22	13.0
GOA8C	50.0	57.5	1.63	1.80	0.036	3.9	0.527	0.527	1.0	1.62	10.0
GOA9C	50.0	64.0	1.82	1.84	0.032	3.4	0.527	0.527	1.0	1.61	12.4

TABLE 7.1 (CONTINUED)

	13	14	15	16	17	18	19	20	21	22	23	24	
	CYCLIC LOADING						STATIC LOADING				AFTER TEST		
Test No.	τ_c kg/cm^2	τ_c/S_u %	N	γ_N kg/cm^2	u_N kg/cm^2	f Hz	S_u kg/cm^2	γ_f %	u_f kg/cm^2	RATE min/mm	w_f %	e_f	REMARKS
GOA1S	-	-	-	-	-	-	0.147	22.2	0.241	75	50.1	1.42	Bottom of core
GOA2S	-	-	-	-	-	-	0.134	16.9	0.270	75	51.5	1.46	Top of core
GOA3S	-	-	-	-	-	-	0.087	22.2	0.101	75	57.5	1.63	
GOA4C	0.047	30	1030	14.9	0.436	0.1	-	-	-	-	52.3	1.49	
GOA5C	0.056	36	925	19.1	0.436	0.1	-	-	-	-	52.9	1.50	
GOA6C	0.070	45	105	17.9	0.414	0.1	-	-	-	-	54.4	1.55	
GOA7C	0.084	54	60	27.5	0.425	0.1	-	-	-	-	45.7	1.30	
GOA8C	0.098	63	26	17.5	0.384	0.1	-	-	-	-	49.4	1.41	
GOA9C	0.035	23	3000	0.04	0.076	0.1	0.160	17.6	0.252	75	49.2	1.40	No failure in cyclic loading

TABLE 7.2

EXPLANATION FOR TABLES 7.1, 7.6, AND 7.7

Column	Symbol	Explanation
1		Test Number
2	A	Sample Cross Sectional Area
3	w_i	Water Content of Trimmings
4	e_i	Void Ratio of Trimmings
5	H_i	Sample Height Before Consolidation
6	S_u	Undrained Shear Strength (Swedish Fall Cone)
7	S_t	Sensitivity (Swedish Fall Cone)
8	$\bar{\sigma}_{vo}$	Final Consolidation Stress
9	$\bar{\sigma}_{vm}$	Maximum Consolidation Stress
10	OCR	Overconsolidation Ratio
11	H_f	Sample Height After Consolidation
12	ε_v	Vertical Strain After Consolidation
13	τ_c	Cyclic Shear Stress
14	τ_c/S_u	Cyclic Shear Stress as a Percentage of Peak Static Strength
15	N	Number of Cycles Tested
16	γ_N	Shear Strain at N Cycles
17	u_N	Pore Pressure at N Cycles
18	f	Frequency of Loading
19	S_u	Static Undrained Shear Strength (Peak of Stress-Strain Curve)
20	γ_f	Shear Strain at Peak of Stress-Strain Curve
21	u_f	Pore Pressure at Peak of Stress-Strain Curve
22		Strain Rate
23	w_f	Water Content of Sample (After Test)
24	e_f	Void Ratio of Sample (After Test)

The term $(1-\varepsilon_v)$ is a correction factor that takes into account the decrease in distance between the reinforcing wire windings caused by the vertical strain of the sample (8). This correction factor is necessary because the vertical distance between the wire windings is constant during the calibration of the membranes.

The static tests were performed under controlled strain conditions, and the cyclic tests were performed under controlled stress conditions. For the cyclic tests, a square wave load shape with complete stress reversal was used, and the cyclic loading frequency was 0.1 Hz. The standard 50 cm^2 sample size was used for all tests.

The results of a consolidation test, in the form of void ratio versus consolidation stress, are shown in Figure 7.1 (arithmetic) and Figure 7.2 (logarithmic).

In the following three sections, the test results for the Gulf of Alaska clay are presented. First, the coefficient of lateral stress at rest, K_o, is determined, based on the lateral stress measurements that were made during the consolidation phase of each test. The static test results are presented next, and this is followed by the cyclic loading test results. With the use of the equations presented in Part 5, various information is determined about the state of stress within the soil sample during static and cyclic shear.

It should be noted that whenever test results are presented graphically, the curves for individual tests represent a large number of data points,

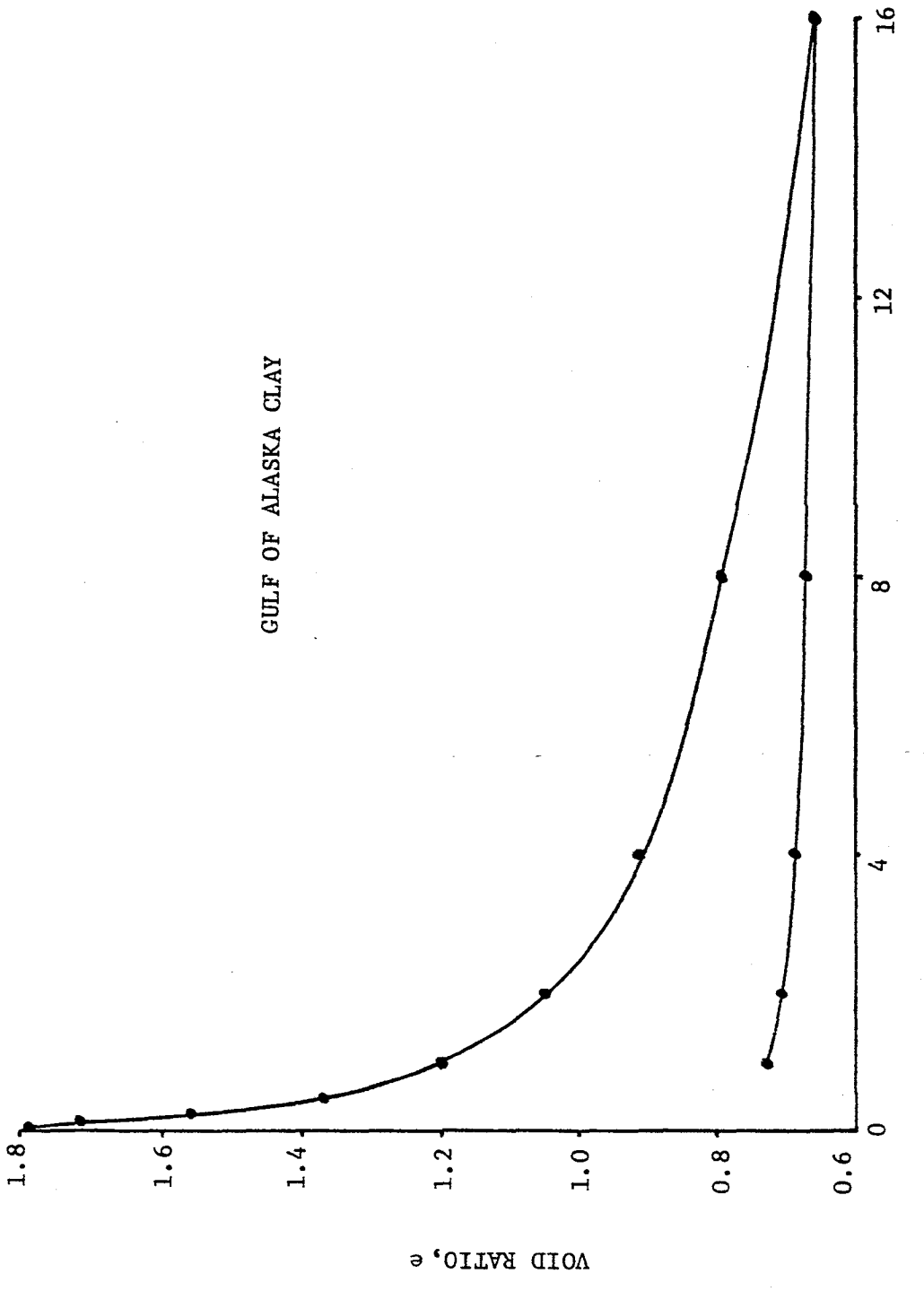

FIGURE 7.1. RESULTS OF OEDOMETER TEST - GULF OF ALASKA CLAY

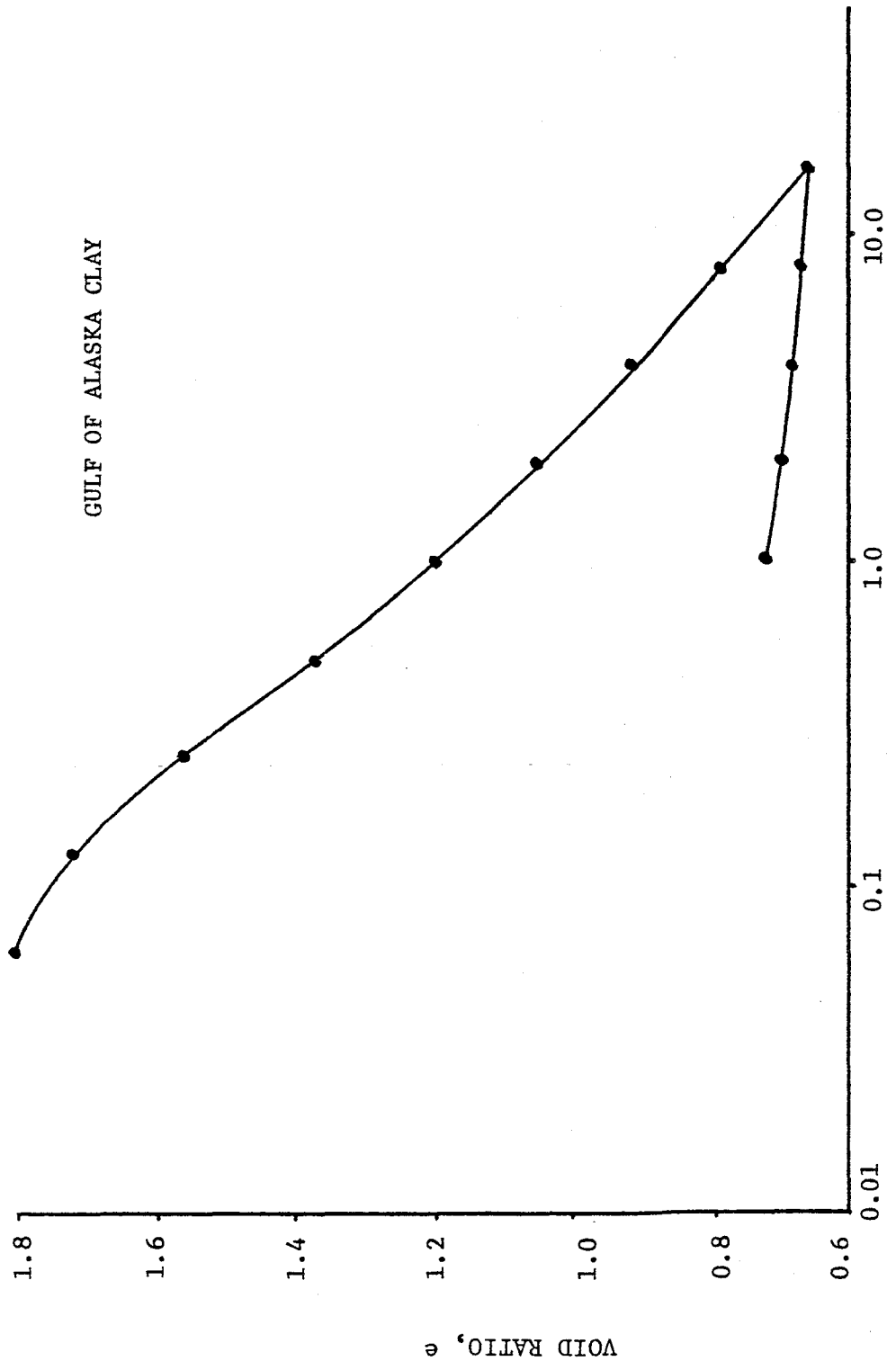

FIGURE 7.2. RESULTS OF OEDOMETER TEST - GULF OF ALASKA CLAY

typically, between 25 and 50. The curves depict a smooth fit through the data points and are representative of the actual data, excluding minor irregularities.

7.1.2 Determination of K_o. The horizontal (lateral) stresses acting on the soil samples were monitored during the consolidation phase of each test. The consolidation stress was applied in three increments, and for each vertical stress, the corresponding horizontal effective stress was measured after the completion of primary consolidation. The results are summarized in Table 7.3.

The measured horizontal effective stress is plotted versus the vertical effective stress in Figure 7.3. The data points tend to fall on a straight line, which does not pass through the origin. Fitting a straight line to the data by the method of least squares results in the equation:

$$\bar{\sigma}_h = 0.536\ \bar{\sigma}_v - 0.034 \qquad 7.2$$

where $\bar{\sigma}_h$ and $\bar{\sigma}_v$ are in kg/cm^2. Experimental evidence has shown that the K_o line for one dimensional consolidation is essentially straight (61). However, the K_o line should pass through the origin.

The reason that the least squares line does not pass through the origin can be attributed to the difficulty of obtaining an initial microstrain reading corresponding to zero horizontal stress. Since changes in the zero reading usually occur while the membrane is mounted on a sample, the recommended procedure is to take an initial reading after

TABLE 7.3

RESULTS OF LATERAL STRESS MEASUREMENTS DURING CONSOLIDATION - GULF OF ALASKA CLAY

TEST	FIRST CONSOLIDATION LOAD $\bar{\sigma}_v$ = 0.12 kg/cm^2		SECOND CONSOLIDATION LOAD $\bar{\sigma}_v$ = 0.24 kg/cm^2		THIRD CONSOLIDATION LOAD $\bar{\sigma}_v$ = 0.51 kg/cm^2		REMARKS
	$\bar{\sigma}_h$ (kg/cm^2)	$K_o = \bar{\sigma}_h / \bar{\sigma}_v$	$\bar{\sigma}_h$ (kg/cm^2)	$K_o = \bar{\sigma}_h / \bar{\sigma}_v$	$\bar{\sigma}_h$ (kg/cm^2)	$K_o = \bar{\sigma}_h / \bar{\sigma}_v$	
GOA1S	-	-	-	-	0.245	0.481	Data Not Taken for 1st and 2nd Loads
GOA2S	0.035	0.295	0.083	0.347	0.236	0.463	
GOA3S	0.042	0.351	0.094	0.392	-	-	3rd Load Not Applied
GOA4C	0.034	0.281	0.089	0.371	0.238	0.466	
GOA5C	-	-	-	-	-	-	Erroneous Initial Reading
GOA6C	-	-	-	-	-	-	Membrane Leak - Gradual Decrease in Reading with Time
GOA7C	0.026	0.216	0.094	0.393	0.232	0.455	
GOA8C	-	-	-	-	-	-	Membrane Leak - Gradual Decrease in Reading with Time
GOA9C	0.031	0.262	0.084	0.349	0.252	0.494	

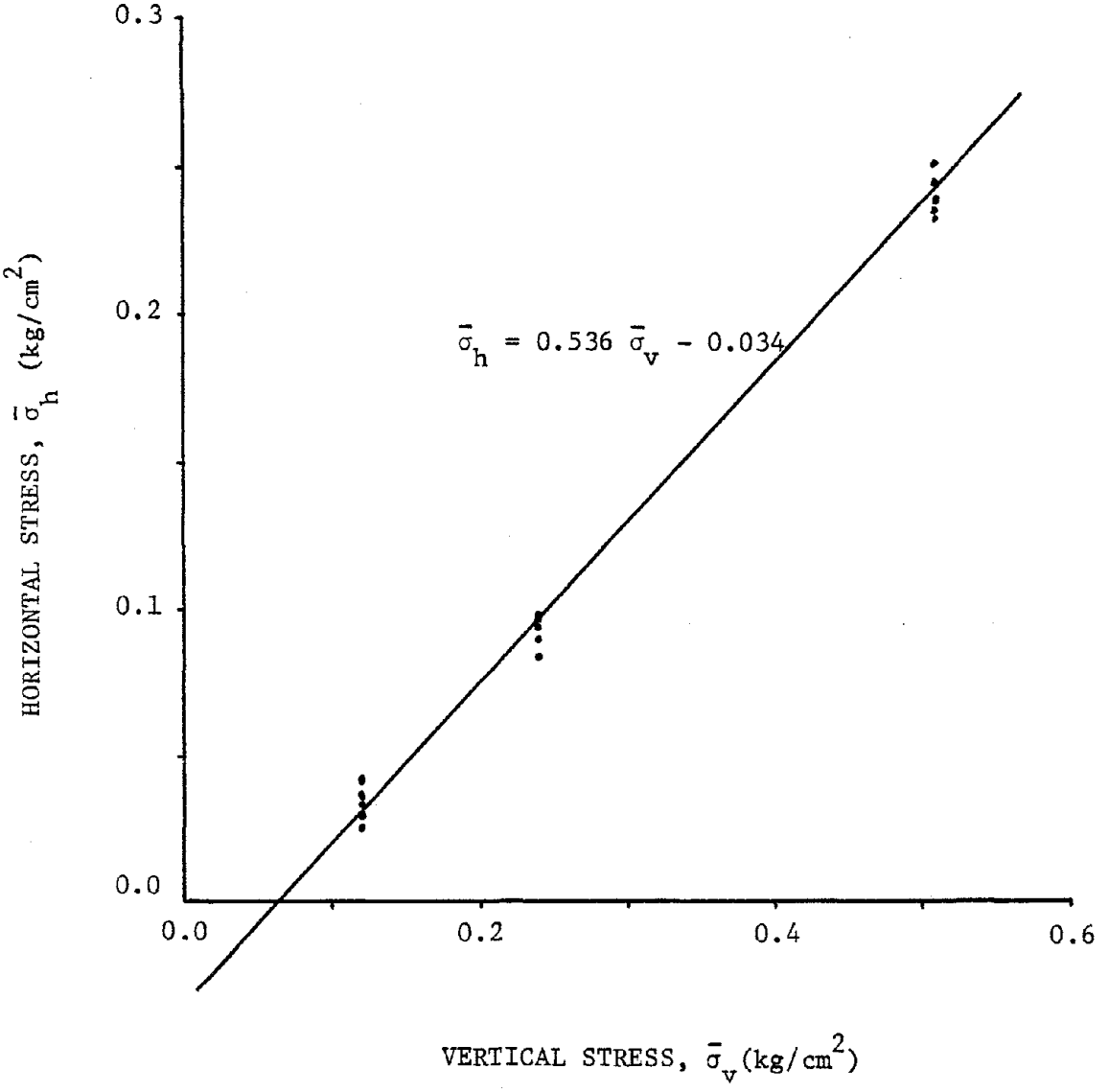

FIGURE 7.3. RESULTS OF LATERAL STRESS MEASUREMENTS MADE DURING CONSOLIDATION - GULF OF ALASKA CLAY

sample preparation is completed (8). This procedure was followed for all tests.

It seems unlikely that the horizontal stress acting on the sample will be zero after sample preparation is completed. During sample preparation, the wire reinforced rubber membrane is stretched in the expander and then released around the sample. Because of this procedure, it seems probable that the membrane exerts a horizontal stress on the sample. Furthermore, during sample preparation, the upper cap is placed on top of the sample. The cap exerts a vertical stress of 0.017 kg/cm^2 (1.7 kN/m^2) on the sample.

Therefore, after sample preparation is completed, a known vertical stress and an unknown horizontal stress are acting on the sample. Ideally, however, both the vertical stress and the horizontal stress should be zero in order to obtain a true initial microstrain reading. These two situations are contrasted in Figure 7.4a.

Further insight may be gained by studying the diagram in Figure 7.4b. In the primed coordinate system, stresses are measured relative to the assumed initial stress conditions ($\bar{\sigma}_h = \bar{\sigma}_v = 0$) acting on the sample. The data points obtained for each test were plotted relative to this coordinate system. The unprimed coordinate system corresponds to the actual (true) stresses acting on the sample.

After sample preparation is completed, it is known that the actual vertical stress acting on the sample is 0.017 kg/cm^2 (1.7 kN/m^2).

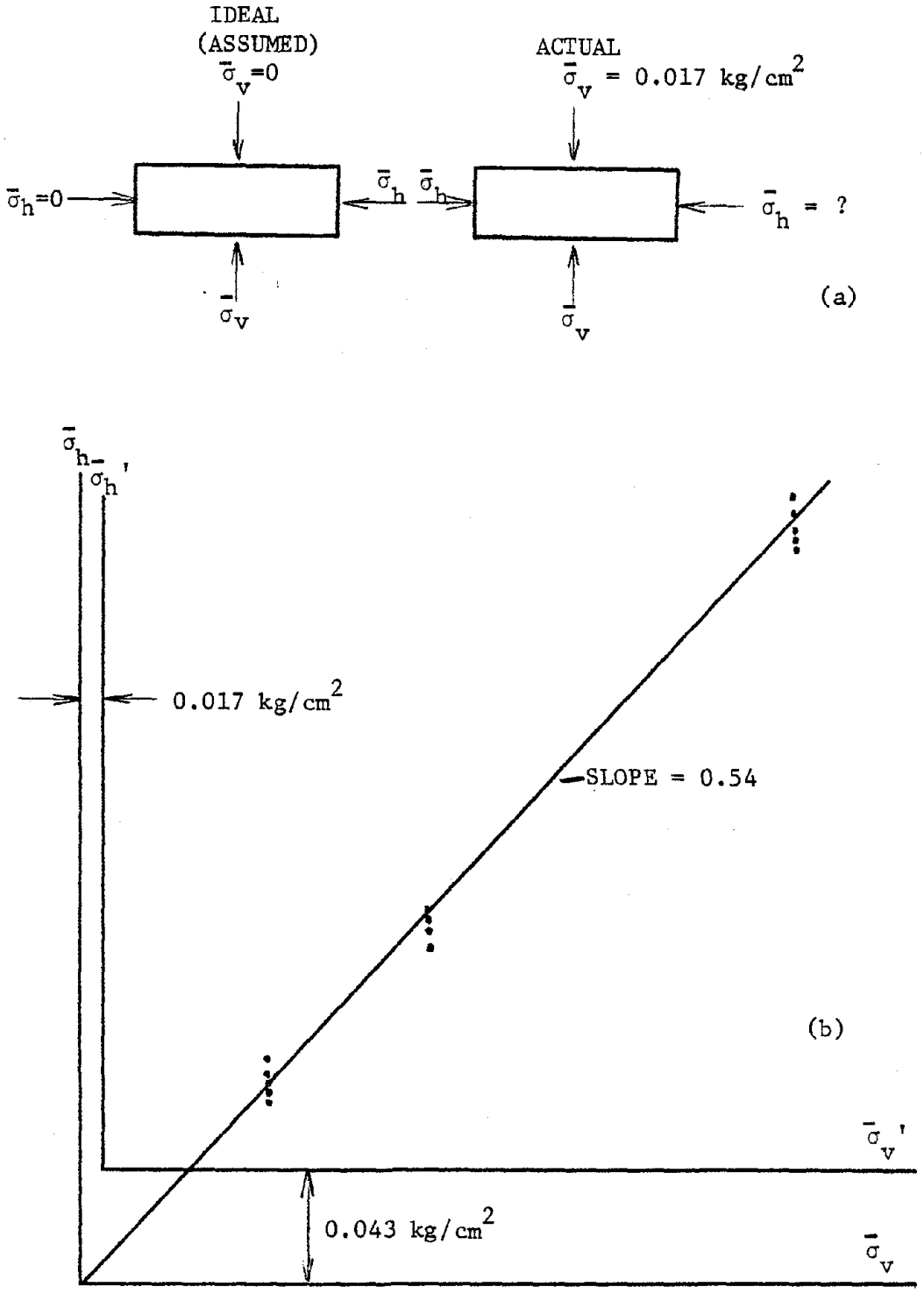

FIGURE 7.4. STRESSES ACTING ON THE SOIL SAMPLE AFTER SAMPLE PREPARATION IS COMPLETED: (a) COMPARISON OF IDEAL AND ACTUAL STRESSES ACTING ON THE SAMPLE; (b) DETERMINATION OF THE INITIAL HORIZONTAL STRESS ACTING ON THE SAMPLE

Therefore, the true $\bar{\sigma}_h$ axis can be drawn offset to the $\bar{\sigma}'_h$ axis, as shown. If the true relationship between the horizontal effective stress and the vertical effective stress is linear, then this line can be extended until it intersects the $\bar{\sigma}_h$ axis. The true $\bar{\sigma}_v$ axis must also pass through this point of intersection, as shown.

The actual stresses acting on the soil sample when the initial microstrain reading was taken can now be found from Figure 7.4b:

$$(\bar{\sigma}_v)_{initial} = 0.017 \text{ kg/cm}^2 \ (1.7 \text{ kN/m}^2)$$

$$(\bar{\sigma}_h)_{initial} = 0.043 \text{ kg/cm}^2 \ (4.2 \text{ kN/m}^2) \qquad 7.3$$

Note that the deduced initial value of the horizontal stress is an average value for all tests. The coefficient of lateral stress at rest, K_o, is equal to the slope of the straight line (Figure 7.4b):

$$K_{o \text{ Gulf of Alaska Clay}} = 0.54 \qquad 7.4$$

Note that this value of K_o is also an average value for all tests on the Gulf of Alaska clay.

The measured value of K_o (equal to the slope of the straight line) agrees favorably with values of K_o derived from empirical relationships. For example, the following relationship is commonly used for normally consolidated clays (11):

$$K_o = 0.95 - \sin\phi = 0.543 \qquad 7.5$$

Alpan (1) recommends an alternative relationship for normally consolidated clays:

$$K_o = 0.19 + 0.233 \log PI = 0.507 \qquad 7.6$$

where PI is the plasticity index, in percent. Brooker and Ireland (11) developed a chart relating K_o, overconsolidation ratio, and plasticity index; for this relationship:

$$K_o = 0.56 \qquad 7.7$$

Note that these three empirical values of K_o were computed using the data in Table 6.1.

In summary, it will be assumed that the true relationship between the measured horizontal effective stress and the vertical effective stress is linear. Accordingly, the coefficient of lateral stress at rest is equal to the slope of this line, and it is a constant.

A true initial microstrain reading, corresponding to zero horizontal stress, can now be computed by rearranging Equation 7.1 and substituting $K_o = 0.54$:

$$K_o \bar{\sigma}_v = \bar{\sigma}_h = \frac{(r-r_i)}{(1-\varepsilon_v)} \frac{1}{k}$$

$$r_i = r - K_o \bar{\sigma}_v (1-\varepsilon_v)k \qquad 7.8$$

where r is the measured microstrain reading corresponding to the final consolidation stress, $\bar{\sigma}_v$. This procedure was used to calculate an initial microstrain reading for all tests performed on the Gulf of Alaska clay.

7.1.3 Static Test Results. The results of the static tests were used primarily as a basis of comparison for the cyclic loading tests. This is a common practice in geotechnical engineering. For example, cyclic stresses are often expressed as a percentage of the static shear strength. An additional objective was simply to obtain static test data, including lateral stress measurements, and to analyze this data using the equations presented in Part 5.

Stress-strain curves for the static tests are shown in Figure 7.5. The shear stress was normalized by dividing it by the consolidation stress, $\bar{\sigma}_{vo}$. Tests 1, 2, and 3 were true static tests; Test 9 was performed following a sequence of cyclic loading that did not cause failure.

There is some scatter in the stress-strain curves, but the reason for it is not evident. Since there is a lack of conclusive evidence to prove otherwise, it will be assumed that the observed scatter is random in nature. The scatter can be attributed to the basic heterogeneity of the soil and to the sources of error inherent in laboratory testing (41). The magnitude of the scatter is typical for laboratory tests of this nature.

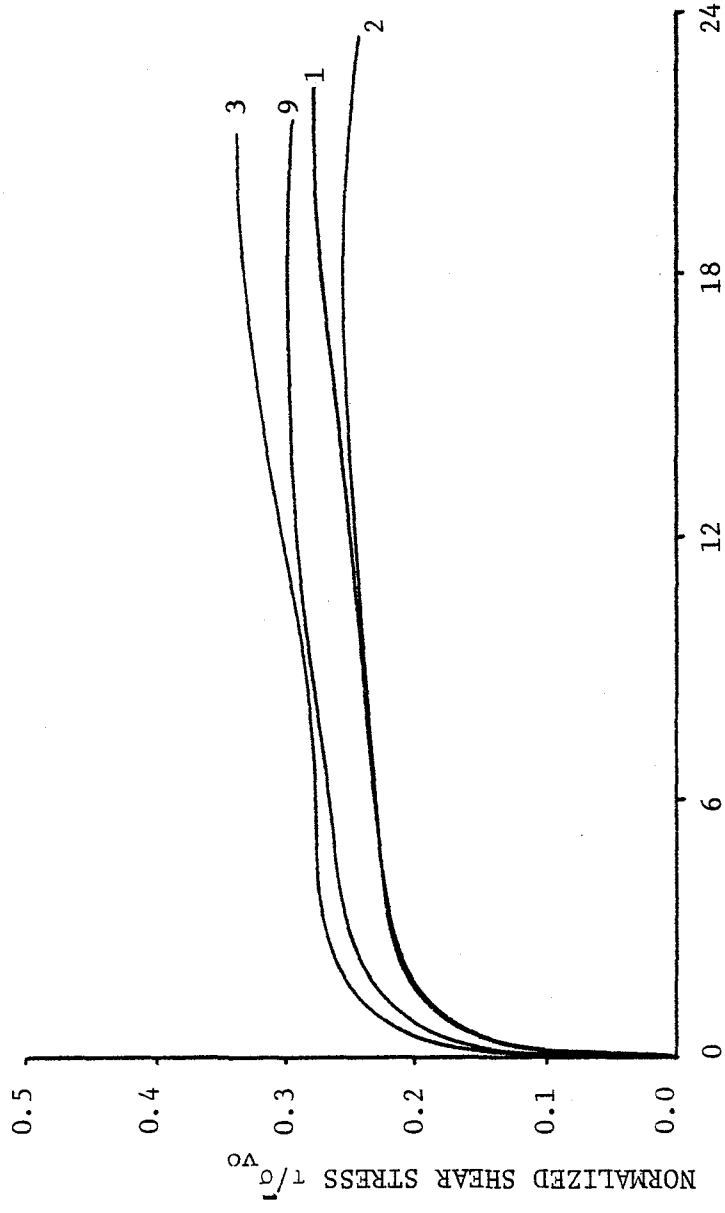

FIGURE 7.5. NORMALIZED STRESS-STRAIN CURVES FOR STATIC TESTS - GULF OF ALASKA CLAY

During cyclic loading, the sample for Test 9 developed a shear strain of only 0.04 percent. Previous research has shown that cyclic shear strains of this magnitude will have little effect on the results of a subsequent static test (73,107). Therefore, it seems reasonable that the stress-strain curve for this test should fall within the scatter of the other stress-strain curves.

The nominal value of the undrained shear strength is dependent on the failure criterion that is used. Typically, it is assumed that failure occurs either at the peak of the stress-strain curve or at some specified value of shear strain, such as two or three percent. For the data shown in Figure 7.5, the average normalized undrained shear strength is 0.293 at peak shear stress, and it is 0.239 at three percent shear strain. For practical purposes, a shear strain of three percent (or even less) constitutes failure for most geotechnical engineering applications, and this is the failure criterion that was used for this investigation.

Ladd and Edgers (59) have compiled undrained shear strength data (measured in direct simple shear tests) for 13 clays of varying composition, Atterberg limits, and sensitivity. They found that the normalized undrained shear strength ($S_u/\overline{\sigma}_{vo}$ at peak shear stress) is approximately 0.21 for clays with a plasticity index between 10 and 25 percent. The measured normalized undrained shear strength of the Gulf of Alaska clay is slightly higher than 0.21, indicating reasonable test results.

Excess pore pressure is plotted versus shear strain in Figure 7.6. The pore pressure was also normalized by dividing it by the consolidation stress. The curves for Tests 1, 2, and 3 follow a sequence directly opposite to that of the stress-strain curves shown in Figure 7.5; that is, the test with the lowest stress-strain curve had the highest pore pressures. However, the curve for Test 9 does not fit into this pattern. The average normalized pore pressure is 0.311 at 3 percent shear strain, and it is 0.428 at 15 percent shear strain.

Stress paths, with shear stress plotted versus vertical normal effective stress, are presented in Figure 7.7. The stress paths for Tests 1, 2, and 3 are typical for a normally consolidated clay (59,73). However, the stress path for Test 9 is similar in shape to a stress path for a lightly overconsolidated clay (59,73); that is, the initial part of the stress path is relatively steep.

The pore pressures that are generated by low level cyclic loading reduce the effective stresses within a soil sample. This causes the soil to behave as if it were overconsolidated (73,107). However, this "apparent overconsolidation" is not identical to true overconsolidation. For "apparent overconsolidation", the volume of the sample remains constant during unloading, whereas for true overconsolidation, the volume of the sample is allowed to change during unloading. If the change in volume that occurs during rebound is small, the difference between "apparent overconsolidation" and true overconsolidation will also be small. This is the case for the Gulf of Alaska clay (see Figures 7.1 and

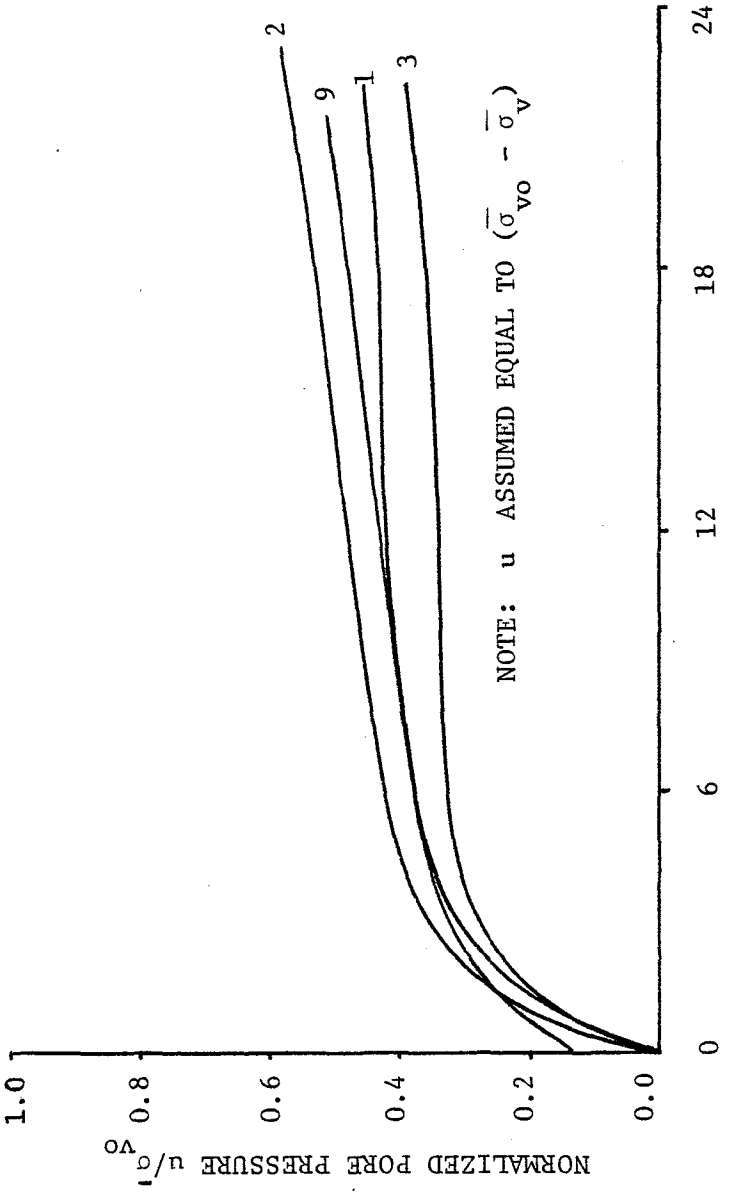

FIGURE 7.6. NORMALIZED PORE PRESSURE VERSUS SHEAR STRAIN FOR STATIC TESTS - GULF OF ALASKA CLAY

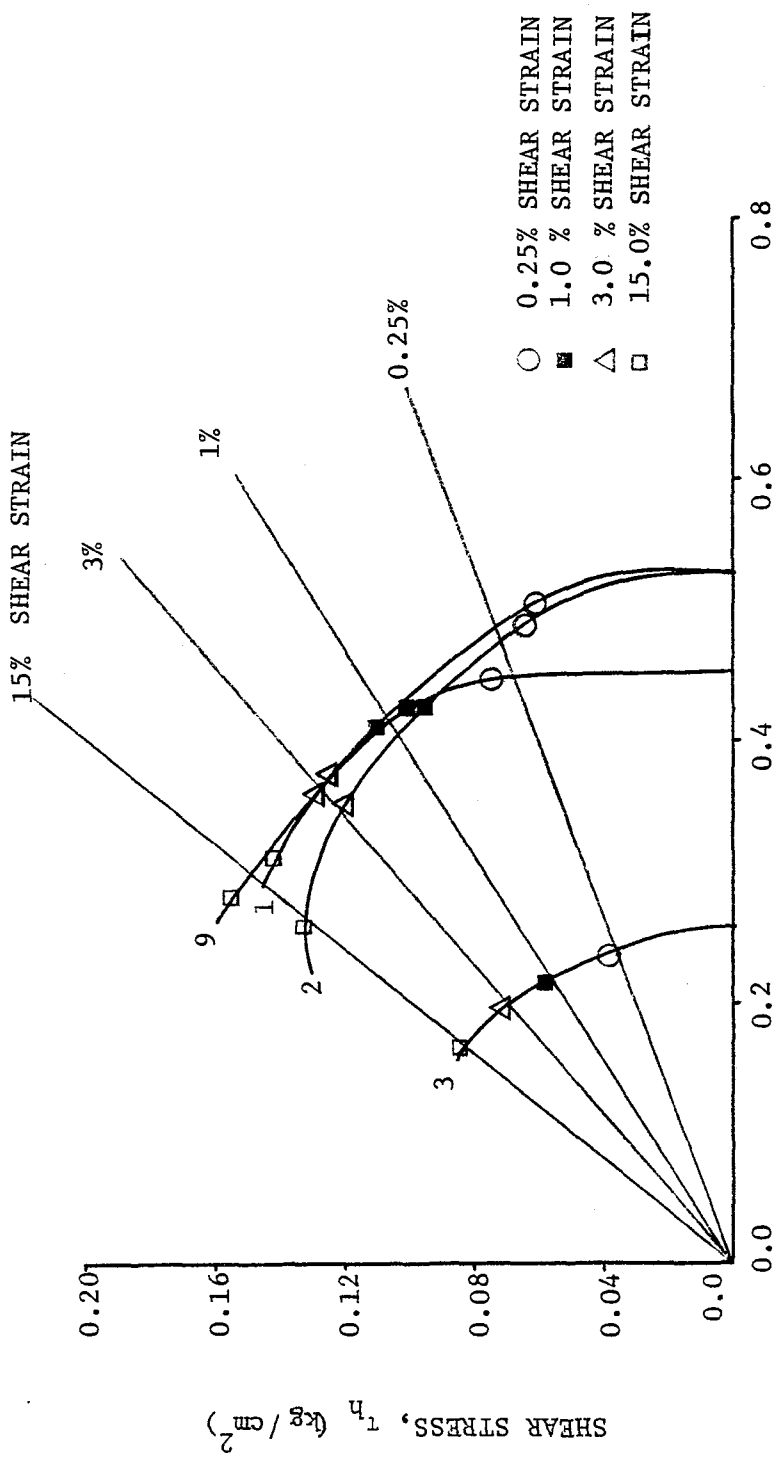

FIGURE 7.7. STRESS PATHS (τ_h VERSUS $\bar{\sigma}_v$) FOR STATIC TESTS - GULF OF ALASKA CLAY. STRAIN CONTOURS ARE ALSO SHOWN

7.2). Therefore, the "apparent overconsolidation" model provides a simple qualitative description for the static loading behavior of the Gulf of Alaska clay after it has been subjected to low level cyclic loading.

Typically, for direct shear tests and direct simple shear tests, it is assumed that the horizontal plane of the sample is the plane of maximum obliquity. The angle of internal friction, ϕ, can then be computed from the equation:

$$\tan \phi = \tau_h / \bar{\sigma}_v \qquad 7.9$$

where τ_h is the maximum applied shear stress on the horizontal plane of the sample, and $\bar{\sigma}_v$ is the normal effective stress on this plane. The angle ϕ can also be evaluated as a function of shear strain by substituting suitable values of τ_h and $\bar{\sigma}_v$ into Equation 7.9. In this case, the computed value of ϕ represents the mobilized friction angle at the corresponding shear strain. For the Gulf of Alaska clay, the average value of the angle of internal friction is 27.9° at peak shear stress, and the average value of the mobilized friction angle is 18.8° at 3 percent shear strain and 25.7° at 15 percent shear strain.

Strain contours are also shown in Figure 7.7. Since the strain contours are straight lines passing through the origin, they are equivalent to the average values of ϕ determined previously. For example, the contour for three percent shear strain corresponds to a (mobilized) friction angle of 18.8° (the strain contour shown in Figure 7.7 is not inclined at 18.8° since the scales on the two axes are unequal).

The relationship between normalized shear modulus and shear strain is presented in Figure 7.8. In this report, the shear modulus is defined as a secant modulus:

$$G = \tau_h/\gamma \qquad 7.10$$

where τ_h is the shear stress applied to the sample, and γ is the corresponding shear strain. The data for all four tests tend to form a narrow band. The scatter in the stress-strain curves (Figure 7.5) is not evident here because the shear modulus is plotted on a log scale.

The relationship between the vertical normal stress and shear strain is presented in Figure 7.9, and the relationship between the horizontal normal stress and shear strain is presented in Figure 7.10. Both the vertical normal stress and the horizontal normal stress were normalized by dividing them by the consolidation stress. Since it is assumed that excess pore pressures do not develop in the sample during shear, the measured normal stresses are effective stresses. The vertical normal effective stress decreases throughout each test; this decrease corresponds to the buildup of pore pressures that would have occurred during an undrained test. The horizontal normal effective stress first decreases slightly, reaching a minimum value at approximately four percent shear strain, and thereafter, it gradually increases.

Modeling the direct simple shear soil sample as an elastic-plastic material, Prevost and Höeg (79) determined that the octahedral normal total stress ($=[\sigma_v + 2\ \sigma_h]/3$) increases when the sample is subjected to an increment of simple shear strain. Since the vertical normal total

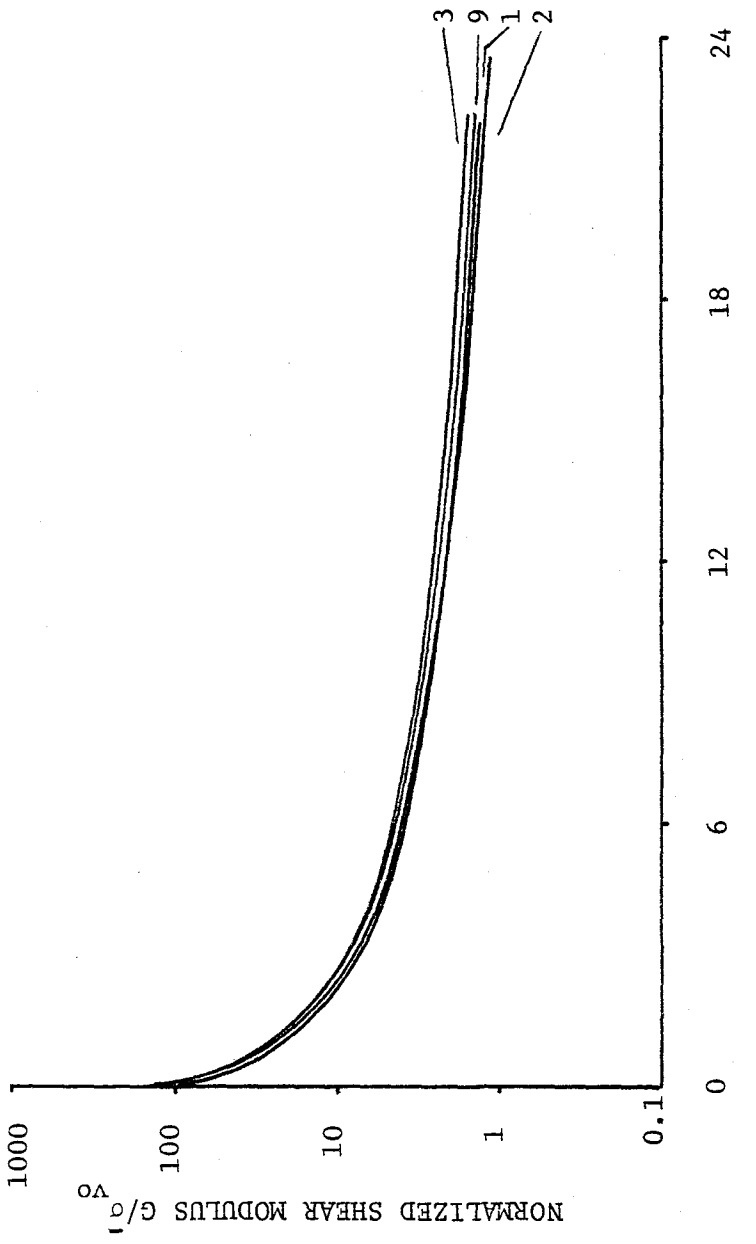

FIGURE 7.8. NORMALIZED SHEAR MODULUS VERSUS SHEAR STRAIN FOR STATIC TESTS - GULF OF ALASKA CLAY

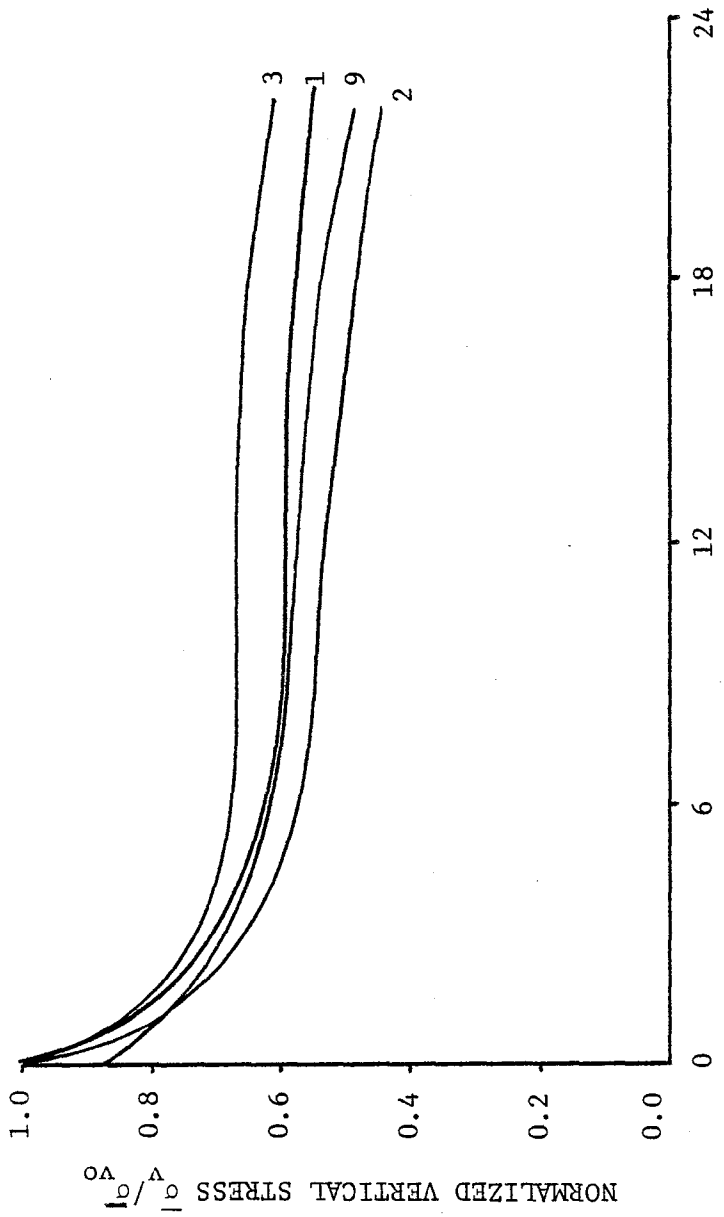

FIGURE 7.9. NORMALIZED VERTICAL STRESS VERSUS SHEAR STRAIN FOR STATIC TESTS - GULF OF ALASKA CLAY

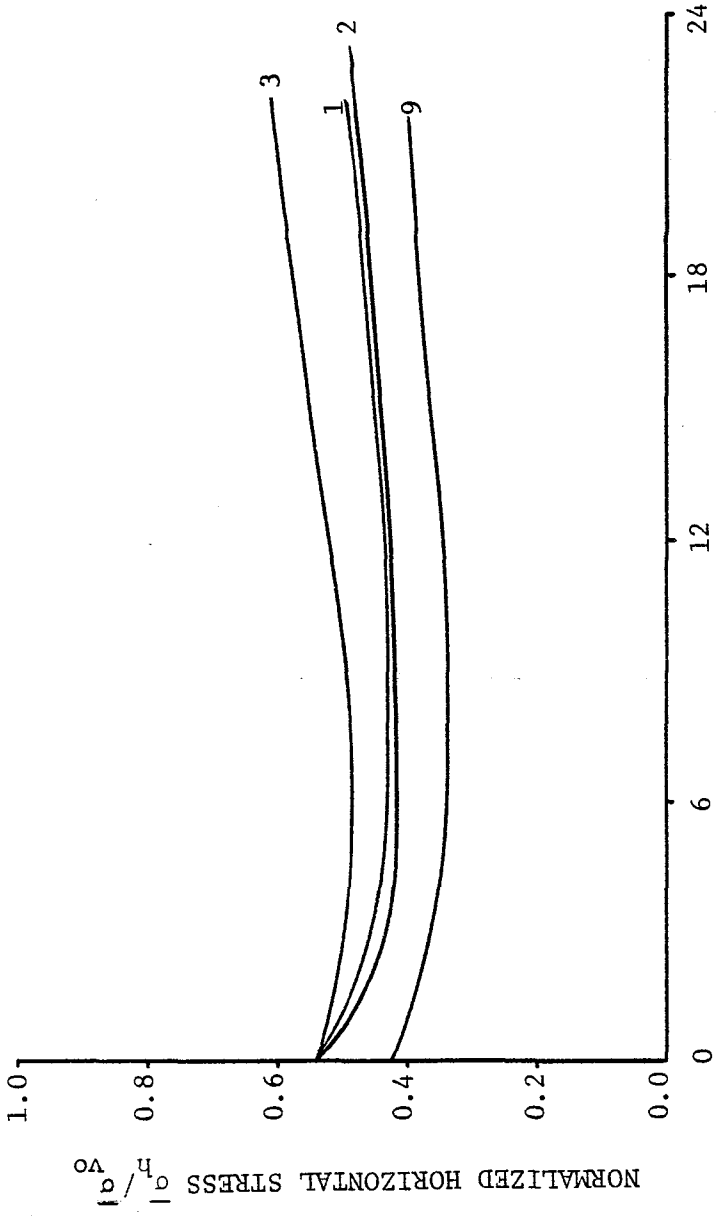

FIGURE 7.10. NORMALIZED HORIZONTAL (LATERAL) STRESS VERSUS SHEAR STRAIN FOR STATIC TESTS - GULF OF ALASKA CLAY

stress remains constant during a constant volume test, this implies that the horizontal normal total stress increases. By combining the results shown in Figures 7.6 and 7.10, and noting that total stress is equal to effective stress plus pore pressure, it can be seen that the horizontal normal total stress does increase during static shear, as predicted.

The coefficent of lateral stress, K, is defined as the ratio of the horizontal normal stress, $\bar{\sigma}_h$, to the vertical normal stress, $\bar{\sigma}_v$. The relationship between the coefficient of lateral stress and shear strain is shown in Figure 7.11. Initially, at zero shear strain, the coefficient of lateral stress corresponds to at rest conditions (K_o). The coefficient of lateral stress increases throughout each test, and at large shear strains, it approaches a value of unity. At 3 percent shear strain, the average coefficient of lateral stress is 0.63, and at 15 percent shear strain, it is 0.79.

The ratio of the minor principal stress, $\bar{\sigma}_3$, to the major principal stress, $\bar{\sigma}_1$, will be defined as the principal stress ratio, R, in this report. The relationship between the principal stress ratio and shear strain is presented in Figure 7.12. At zero shear strain, the principal stress ratio is equal to the coefficient of lateral stress at rest, K_o. The principal stress ratio decreases throughout each test, although at large shear strains, it remains relatively constant. At 3 percent shear strain, the average principal stress ratio is 0.35, and at 15 percent shear strain, it is 0.27.

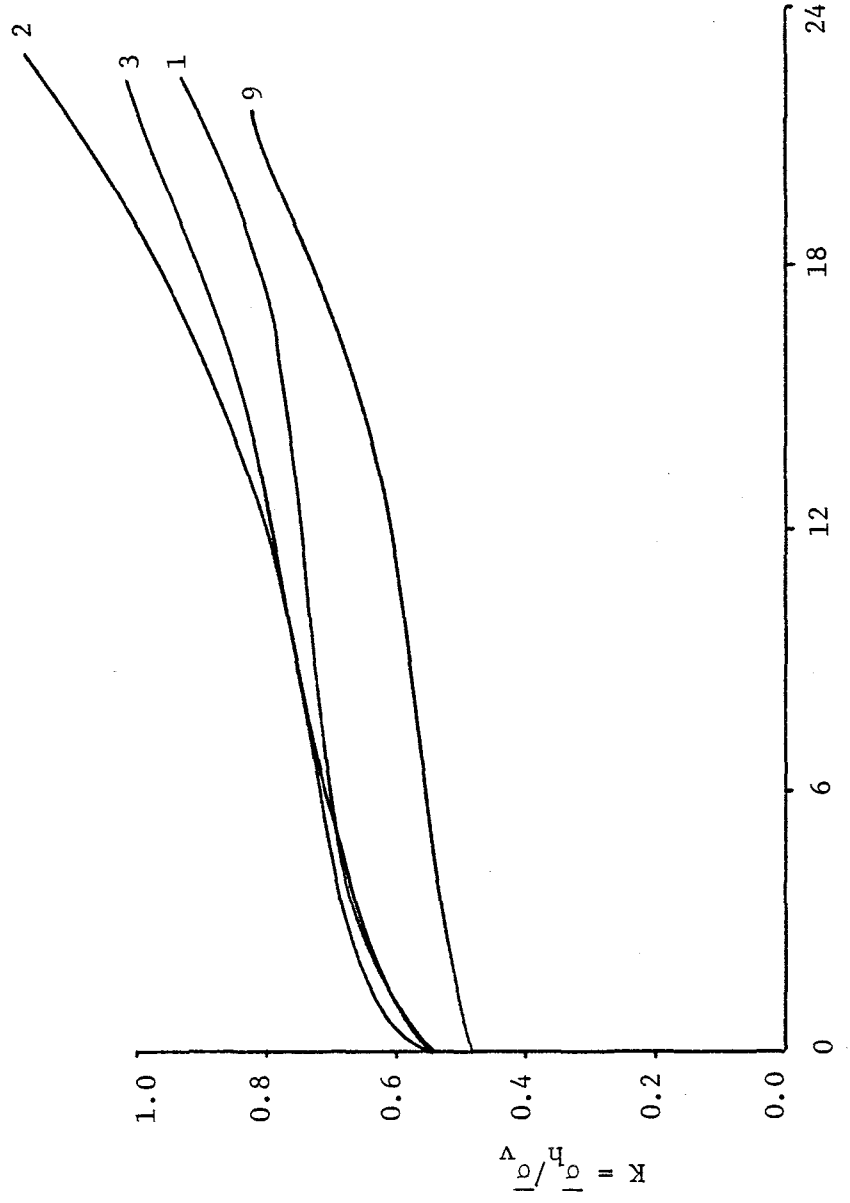

FIGURE 7.11. THE COEFFICIENT OF LATERAL STRESS, $K = \bar{\sigma}_h/\bar{\sigma}_v$, VERSUS SHEAR STRAIN FOR STATIC TESTS - GULF OF ALASKA CLAY

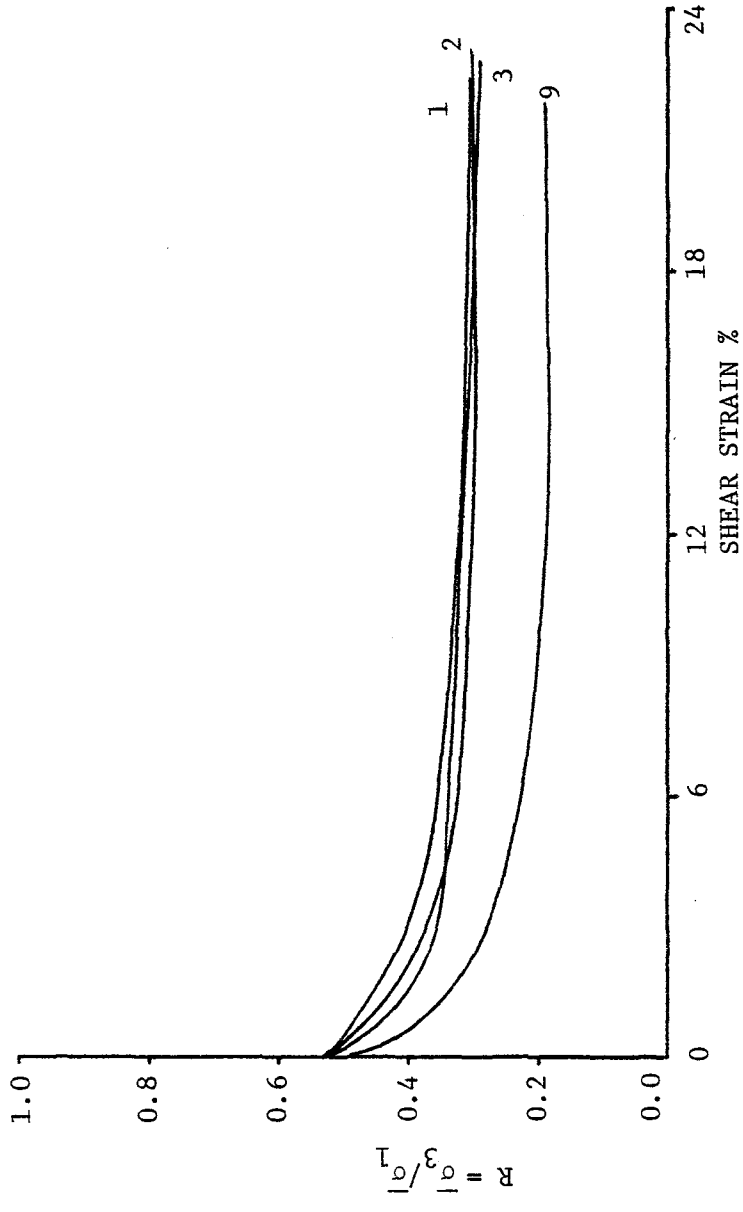

FIGURE 7.12. THE PRINCIPAL STRESS RATIO, $R = \bar{\sigma}_3/\bar{\sigma}_1$, VERSUS SHEAR STRAIN FOR STATIC TESTS - GULF OF ALASKA CLAY

The angles θ_q, θ_f, and θ_p were defined in Part 5 as:

1. θ_q is the angle between the horizontal plane of the sample and the plane on which the maximum shear stress acts.
2. θ_f is the angle between the horizontal plane of the sample and the plane of maximum obliquity.
3. θ_p is the angle between the horizontal plane of the sample and the major principal plane.

The relationship between θ_q and shear strain is presented in Figure 7.13. Initially, at zero shear strain, θ_q is 45°. The angle θ_q decreases rapidly at small shear strains, and thereafter, it decreases gradually for the remainder of each test. At large shear strains, θ_q approaches a value of zero. Therefore, for large shear strains, the horizontal plane of the sample is approximately the plane on which the maximum shear stress acts. Roscoe, et al (87), using the Cambridge simple shear device, found similar results for sands.

The relationship between θ_p and shear strain is presented in Figure 7.14. Initially, at zero shear strain, the horizontal plane is the major principal plane ($\theta_p = 0$). The angle θ_p increases throughout each test, and at large shear strains, θ_p approaches 45°. This result is equivalent to the previous observation that θ_q approaches a value of zero at large shear strains.

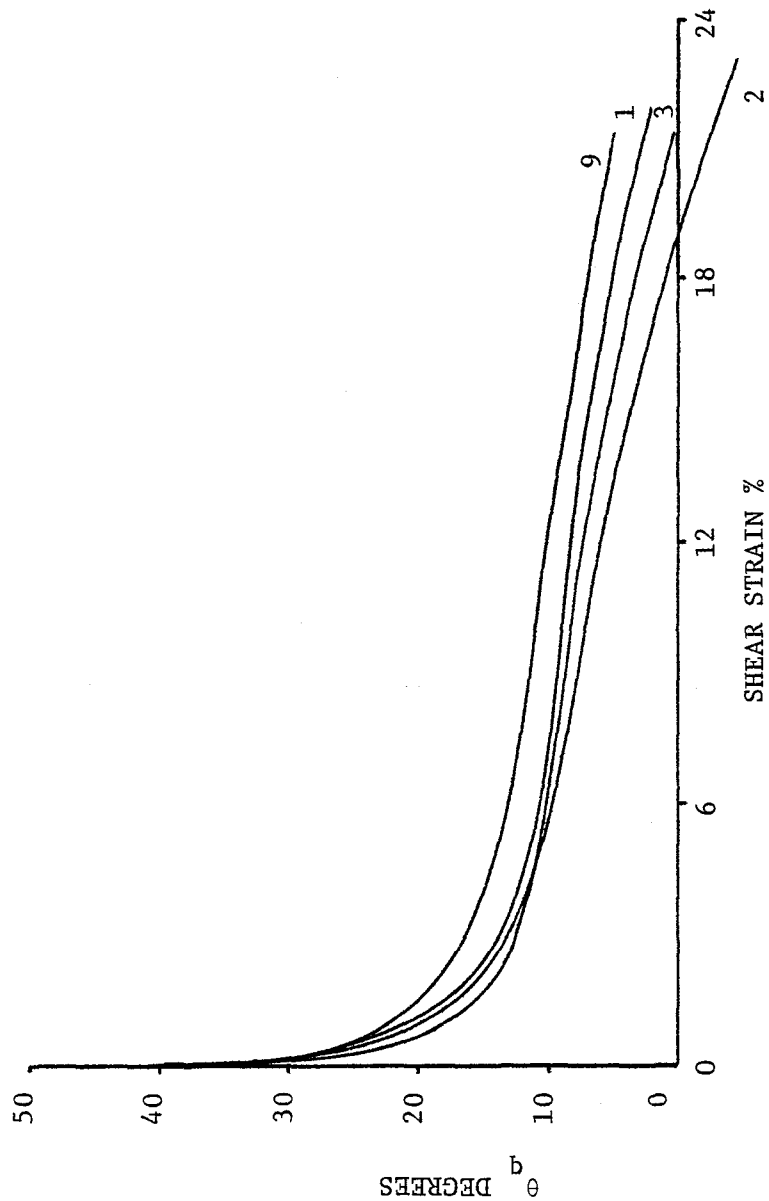

FIGURE 7.13. THE ANGLE BETWEEN THE HORIZONTAL PLANE OF THE SAMPLE AND THE PLANE OF MAXIMUM SHEAR STRESS VERSUS SHEAR STRAIN FOR STATIC TESTS - GULF OF ALASKA CLAY

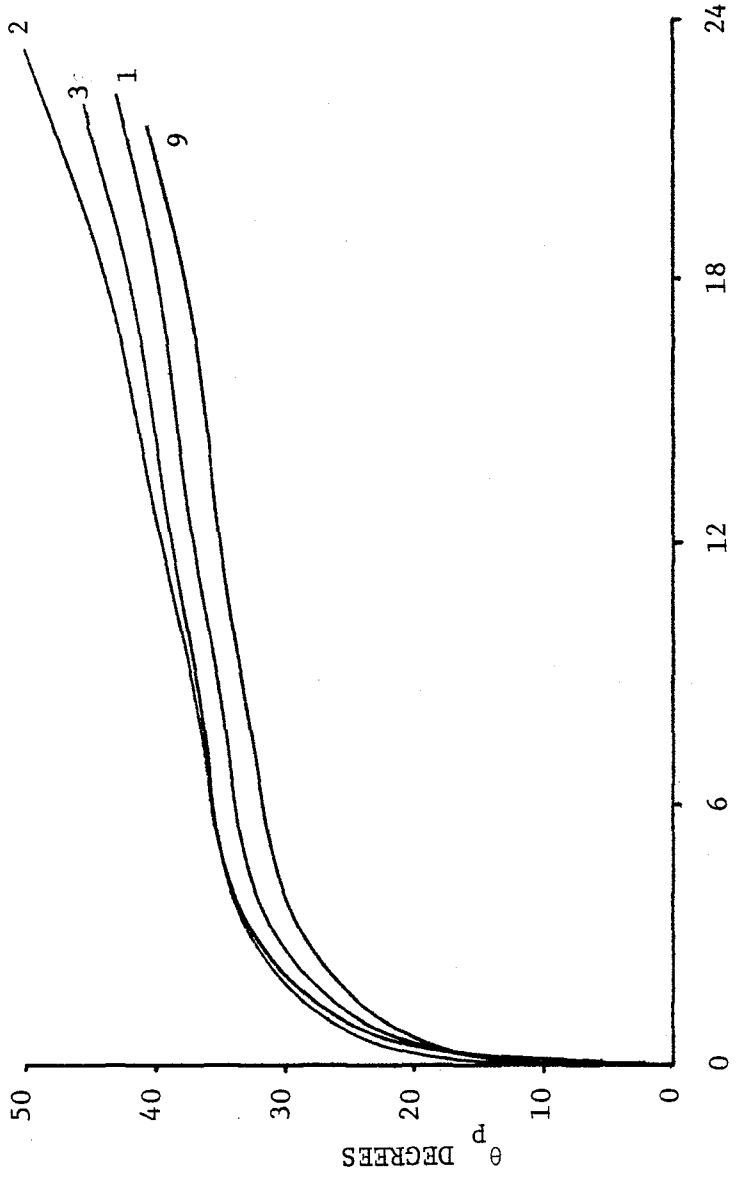

FIGURE 7.14. THE ANGLE BETWEEN THE HORIZONTAL PLANE OF THE SAMPLE AND THE MAJOR PRINCIPAL PLANE VERSUS SHEAR STRAIN FOR STATIC TESTS - GULF OF ALASKA CLAY

The relationship between θ_f and shear strain is presented in Figure 7.15. The angle θ_f decreases throughout each test, and at large shear strains, the average value of θ_f is approximately 25°. The large values of θ_f (Figure 7.15) indicate that the horizontal plane of the sample is not the plane of maximum obliquity. Roscoe, et al (87), found similar results for sands.

As mentioned in Part 5, there is sufficient information available to determine $q - \bar{p}$ data, since lateral stresses were measured. Accordingly, the mobilized angle of internal friction, ϕ_m, can be determined by means of Equation 5.3:

$$\phi_m = \sin^{-1} (q/\bar{p}) \qquad 7.11$$

The mobilized angle of internal friction is a function of shear strain, and this relationship is presented in Figure 7.16a. The data for Tests 1, 2,and 3 show little scatter, and the curves for these three tests form a narrow band in the figure. However, the values of ϕ_m for Test 9 seem to be unreasonably high. It was noted previously that non-failure cyclic loading of normally consolidated clays tends to make them behave as if they were overconsolidated. In fact, Andersen (2,3) concluded that cyclic loading of normally consolidated clays causes the cohesion parameter, c, to increase, while the angle of internal friction remains unchanged. This behavior as an overconsolidated clay, with a nonzero cohesion parameter, will cause the computed

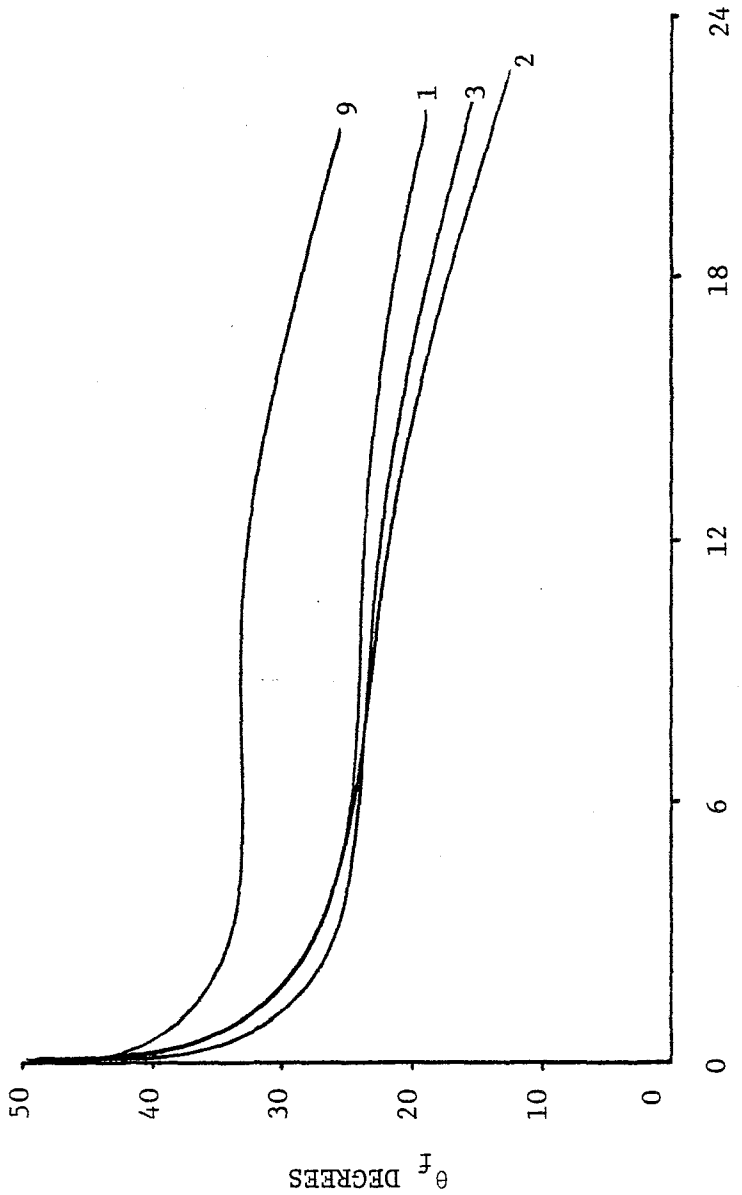

FIGURE 7.15. THE ANGLE BETWEEN THE HORIZONTAL PLANE OF THE SAMPLE AND THE PLANE OF MAXIMUM OBLIQUITY VERSUS SHEAR STRAIN FOR STATIC TESTS - GULF OF ALASKA CLAY

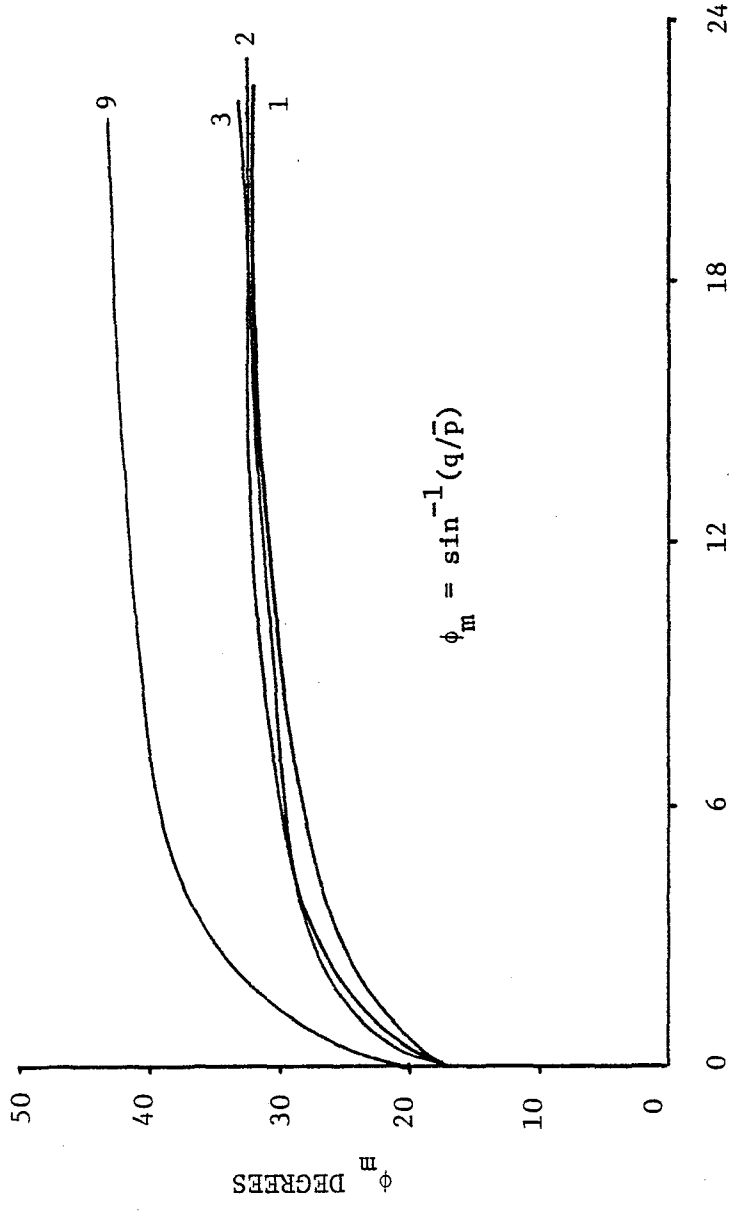

FIGURE 7.16a. THE MOBILIZED ANGLE OF INTERNAL FRICTION VERSUS SHEAR STRAIN FOR STATIC TESTS - GULF OF ALASKA CLAY

values of ϕ_m to be too high because the computations were based on the assumption of zero cohesion.

It is of interest to compare the average values of ϕ_m (for Tests 1,2, and 3) with the average values of ϕ that were determined on the basis of the stresses acting on the horizontal plane of the sample ($\tan \phi = \tau_h/\bar{\sigma}_v$). Accordingly, the average values of ϕ_m and ϕ are presented in Figure 7.16b as a function of shear strain. As can be seen in this figure, ϕ_m is always greater than ϕ, and at large shear strains, the difference between the two is about 7°. At zero shear strain, ϕ_m is greater than zero since the samples were consolidated under K_o conditions.

A $q - \bar{p}$ stress plot is shown in Figure 7.17. The K_o line, shown in the figure, corresponds to the measured coefficient of lateral stress at rest ($K_o = 0.54$). Strain contours (based on Tests 1, 2, and 3) are also shown. Since the strain contours are straight lines passing through the origin, they are equivalent to the average values of ϕ_m determined previously*.

The stress paths for Tests 1, 2, and 3 begin at the K_o line and end near the strain contour for 15 percent shear strain. The stress path for Test 9 extends beyond this strain contour.

---

*If the q and $\bar{p}$ axes have the same scales, the strain contours would be inclined at an angle $\alpha = \tan^{-1}(\sin \phi_m)$.

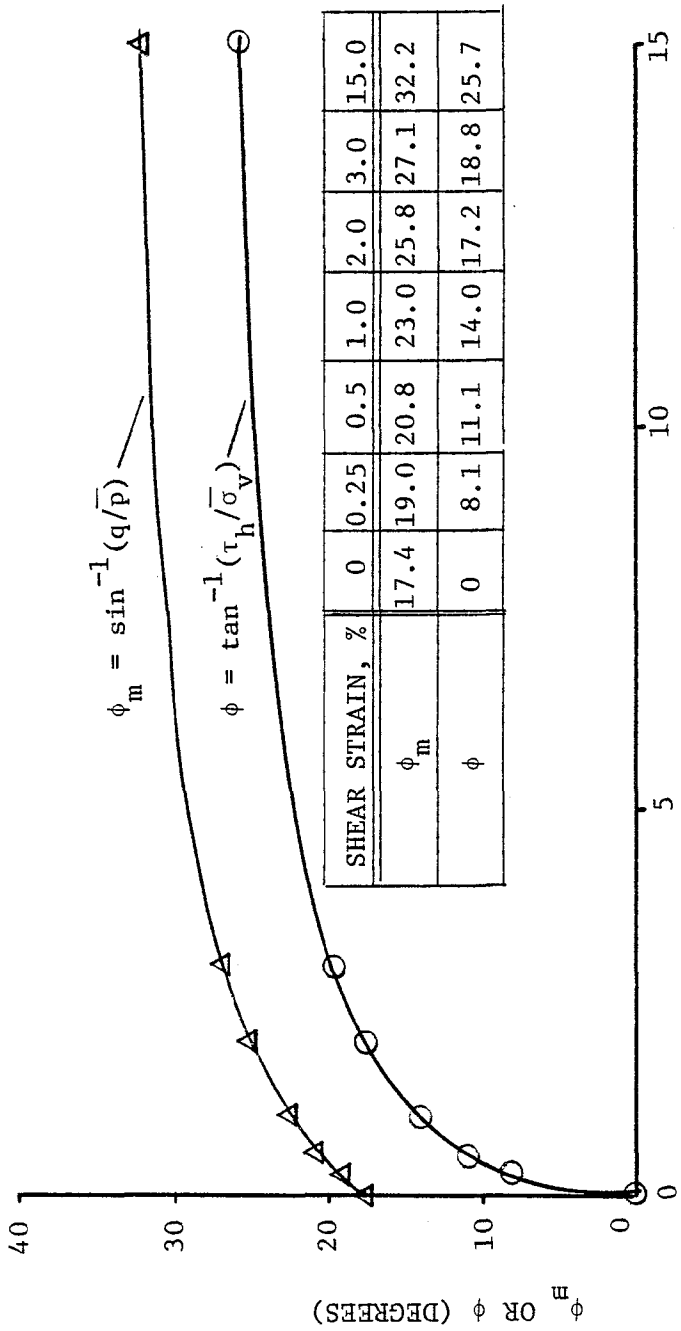

SHEAR STRAIN, %	0	0.25	0.5	1.0	2.0	3.0	15.0
ϕ_m	17.4	19.0	20.8	23.0	25.8	27.1	32.2
ϕ	0	8.1	11.1	14.0	17.2	18.8	25.7

FIGURE 7.16b. AVERAGE VALUES OF ϕ_m AND ϕ VERSUS SHEAR STRAIN FOR STATIC TESTS - GULF OF ALASKA CLAY

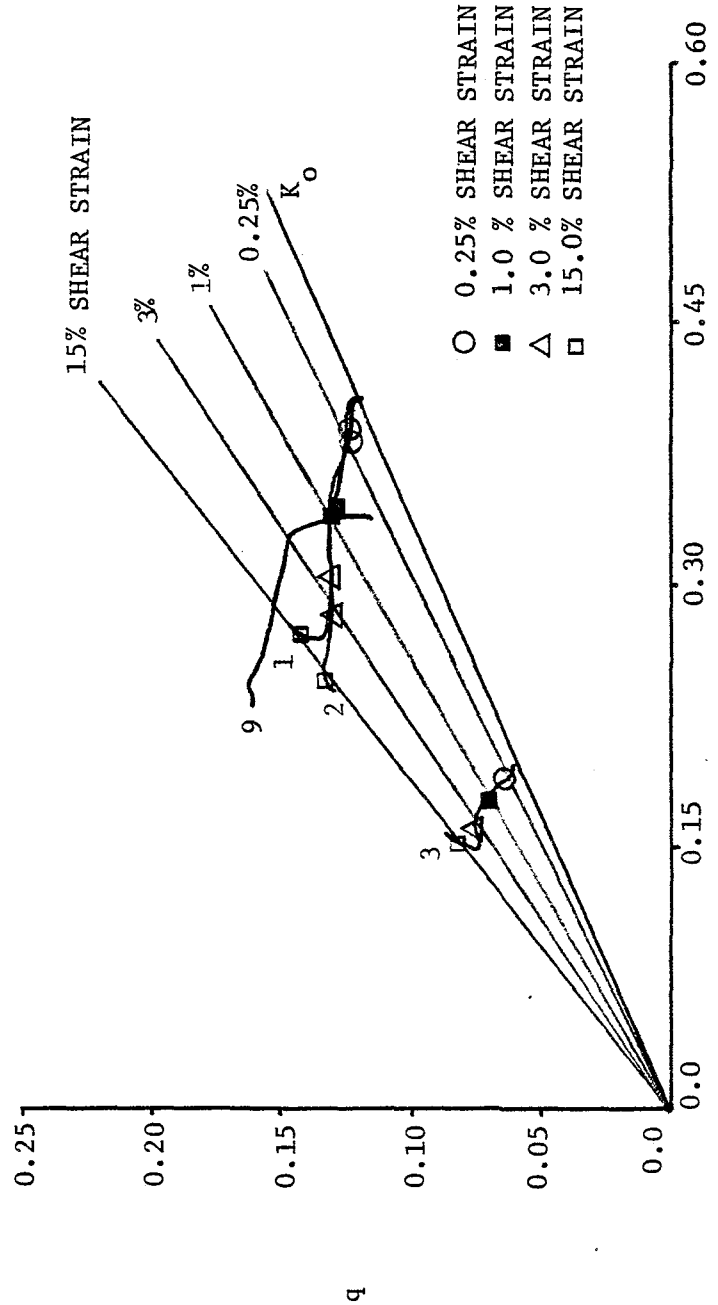

FIGURE 7.17. STRESS PATHS (q-$\bar{p}$) FOR STATIC TESTS - GULF OF ALASKA CLAY. STRAIN CONTOURS ARE ALSO SHOWN

7.1.4 Cyclic Loading Test Results. Six cyclic loading tests were performed on the Gulf of Alaska clay, each with a different cyclic shear stress. The cyclic shear stresses used for each test are summarized below:

Test	τ_c (kg/cm^2)	τ_c/S_u (%)*
4	0.047	30
5	0.056	36
6	0.070	45
7	0.084	54
8	0.098	63
9	0.035	23

The relationship between cyclic shear strain and the number of loading cycles is presented in Figure 7.18. The cyclic shear strain is one-half of the peak to peak shear strain. Typically, the cyclic shear strains increase gradually until failure is imminent, after which they increase very rapidly. In Test 9, there were no indications of imminent failure, even after 3,000 loading cycles.

Normalized pore pressure is plotted versus the number of loading cycles in Figure 7.19. These curves represent the excess pore pressures that were generated by the cyclic loading. It should be noted that when the normalized pore pressure in the sample approaches a value of approximately 0.4, the rate of pore pressure generation (per cycle) accelerates, and failure occurs with further cyclic loading.

*S_u is the peak static undrained shear strength corresponding to the consolidation stress used in the cyclic loading tests (S_u = 0.155 kg/cm^2).

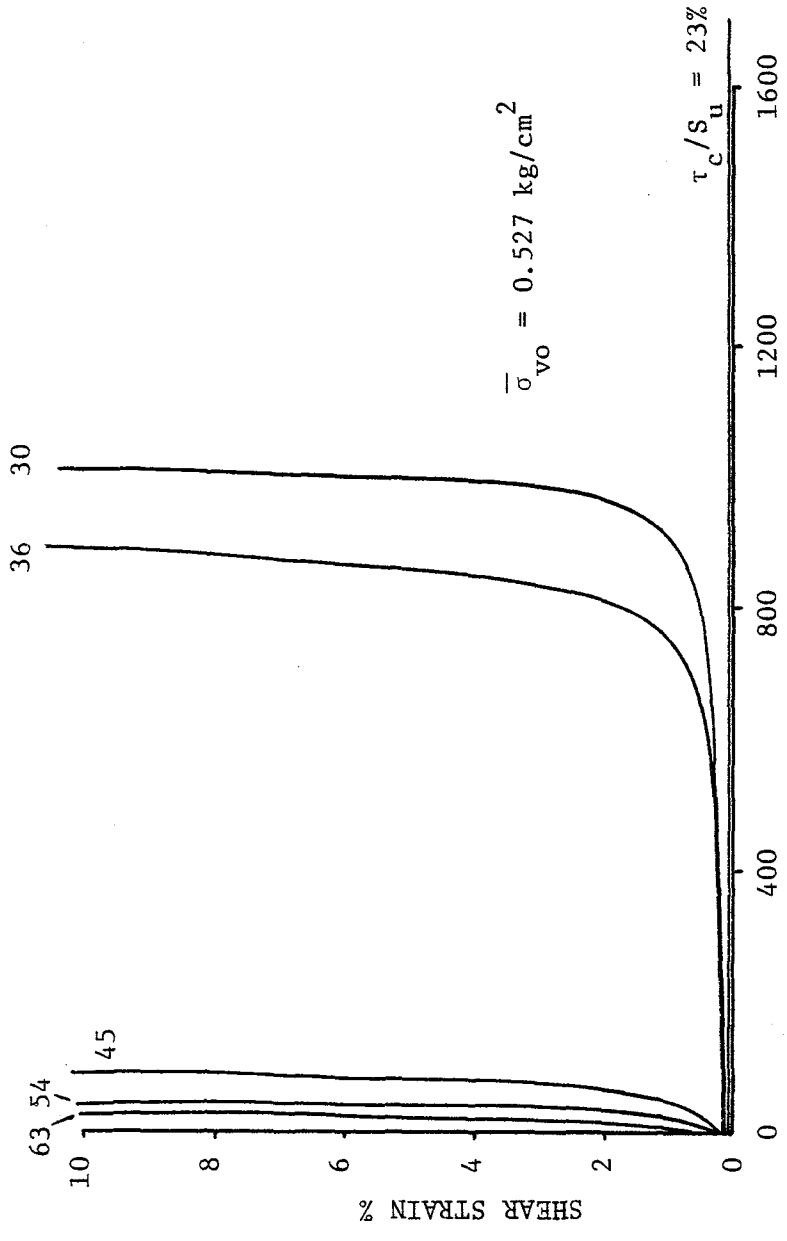

FIGURE 7.18. CYCLIC SHEAR STRAIN VERSUS NUMBER OF LOADING CYCLES - GULF OF ALASKA CLAY

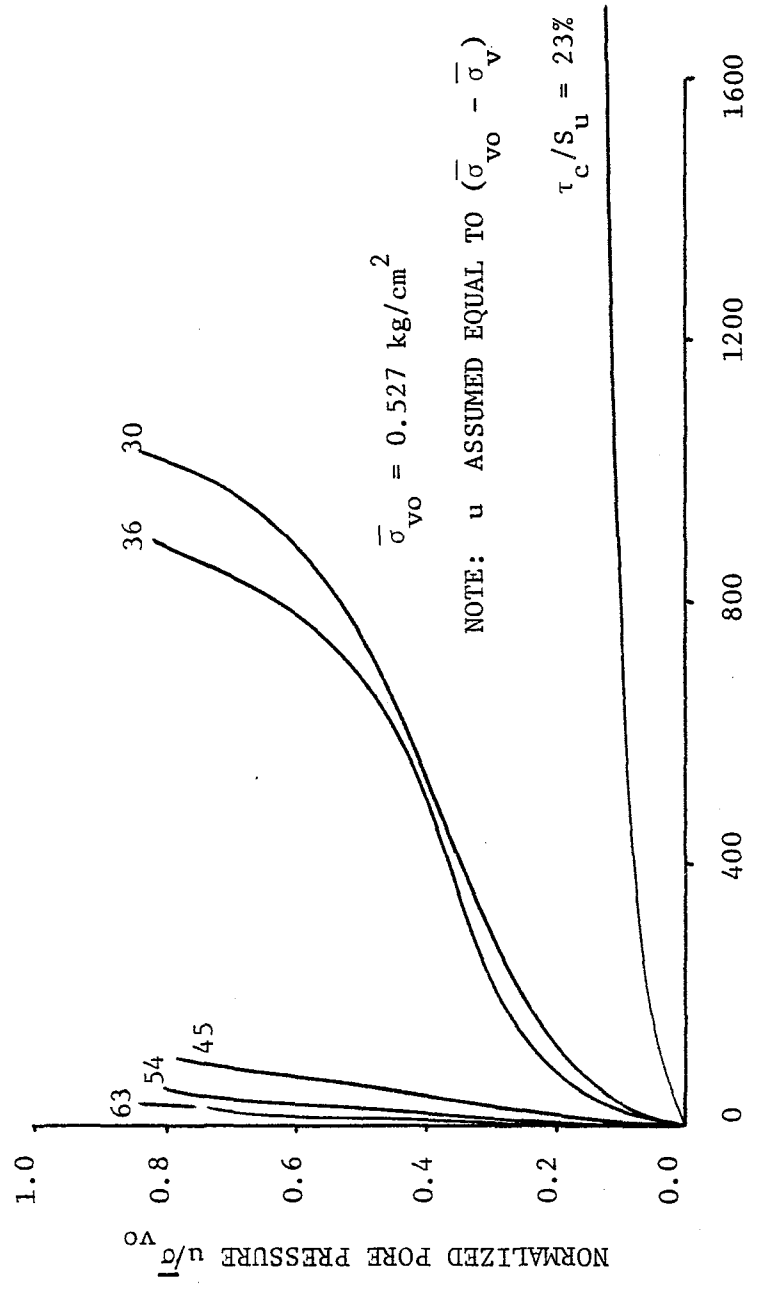

FIGURE 7.19. NORMALIZED PORE PRESSURE VERSUS NUMBER OF LOADING CYCLES - GULF OF ALASKA CLAY

In Test 9, the pore pressure and the cyclic shear strain remained approximately constant during the latter part of the test. This implies that the sample was in a state of non-failure equilibrium. Consequently, the critical level of repeated loading for the Gulf of Alaska clay is estimated to be about 25 percent of the peak static undrained shear strength.

Stress paths (τ_c versus $\bar{\sigma}_v$) are shown in Figure 7.20a. Only the positive peak points of the stress paths are shown; that is, when the shear stress has its maximum positive value. The actual stress paths would cycle above and below the $\bar{\sigma}_v$ axis.

Strain contours are also shown in Figure 7.20a. Since the strain contours were approximated by straight lines passing through the origin, they can be expressed equivalently as average values of the mobilized friction angle for cyclic loading, $(\phi)_c$, which is defined by the equation:

$$\tan (\phi)_c = \tau_c/\bar{\sigma}_v \qquad 7.12$$

The average values of $(\phi)_c$, determined from the cyclic loading tests, are presented in Table 7.4. For comparison, the values of ϕ that were computed from the static tests are also presented in this table.

TABLE 7.4

COMPARISON OF AVERAGE VALUES OF ϕ AND $(\phi)_c$ AT DIFFERENT SHEAR STRAINS - GULF OF ALASKA CLAY

SHEAR STRAIN	0.25%	0.5%	1.0%	2.0%	3.0%	15.0%
ϕ	8.1	11.1	14.0	17.2	18.8	25.7
$(\phi)_c$	9.3	11.7	14.9	18.6	20.9	31.7

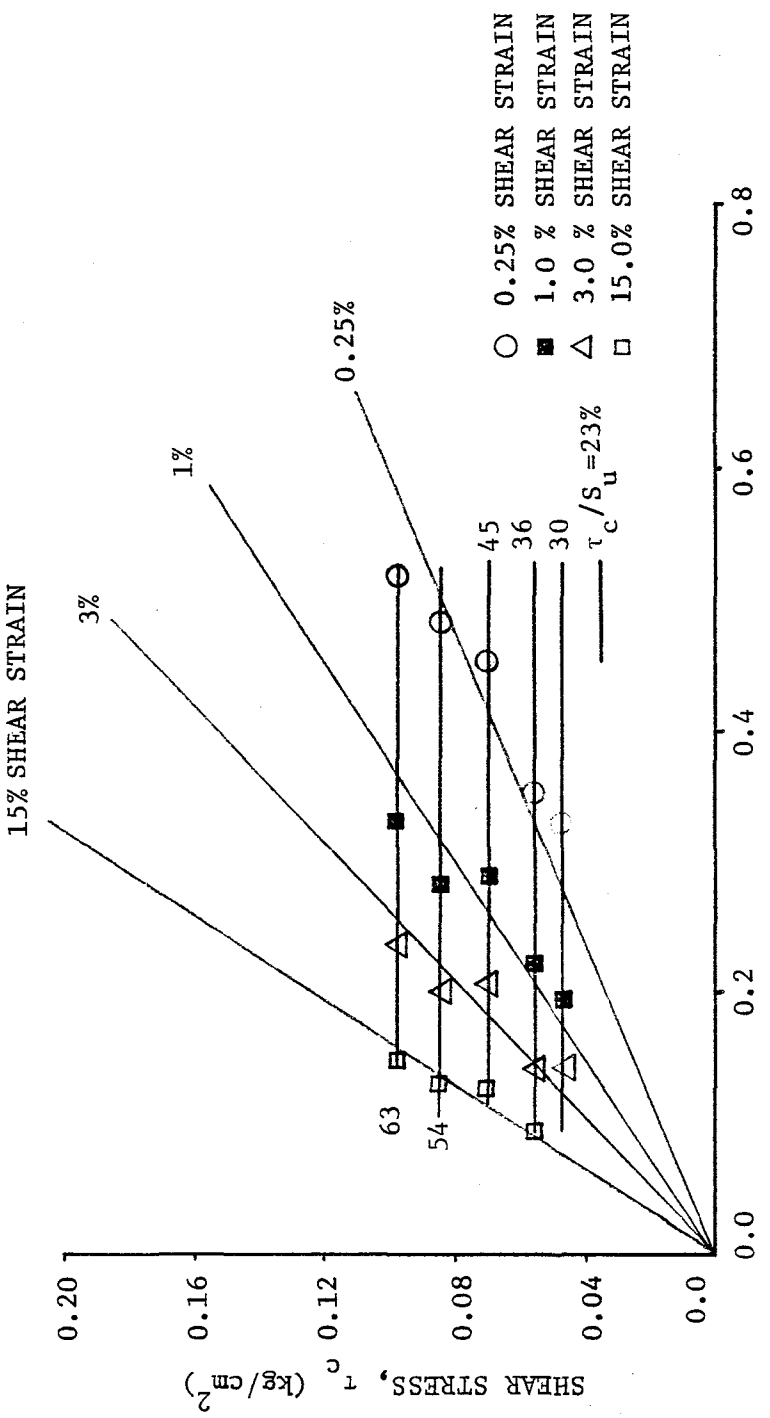

FIGURE 7.20a. STRESS PATHS (τ_c VERSUS $\bar{\sigma}_v$) FOR CYCLIC LOADING TESTS - GULF OF ALASKA CLAY. STRAIN CONTOURS ARE ALSO SHOWN

The values of $(\phi)_c$ are consistently higher than the values of ϕ, but the difference between the two values is small, except at large shear strains. This implies that the strain contours for the static and the cyclic loading tests are also quite similar, as shown in Figure 7.20b. Therefore, for the Gulf of Alaska clay, the strain behavior of the sample during cyclic loading can be approximately predicted from the static test results if the effective stresses in the sample can be determined.

The relationship between normalized shear modulus and the number of loading cycles is presented in Figure 7.21. The shear modulus decreases gradually with increasing number of loading cycles until failure is imminent; thereafter, the shear modulus decreases rapidly. As the cyclic shear stress increases, the initial shear modulus (for the first loading cycle) decreases.

The relationship between the vertical normal stress and the number of loading cycles is presented in Figure 7.22, and the relationship between the horizontal normal stress and the number of loading cycles is presented in Figure 7.23. Both of these stresses were normalized by dividing them by the consolidation stress. The vertical normal stress decreases with increasing number of loading cycles; this decrease is directly related to the increase in excess pore pressure that would occur in an undrained test. The measured horizontal stress also decreases with increasing number of loading cycles.

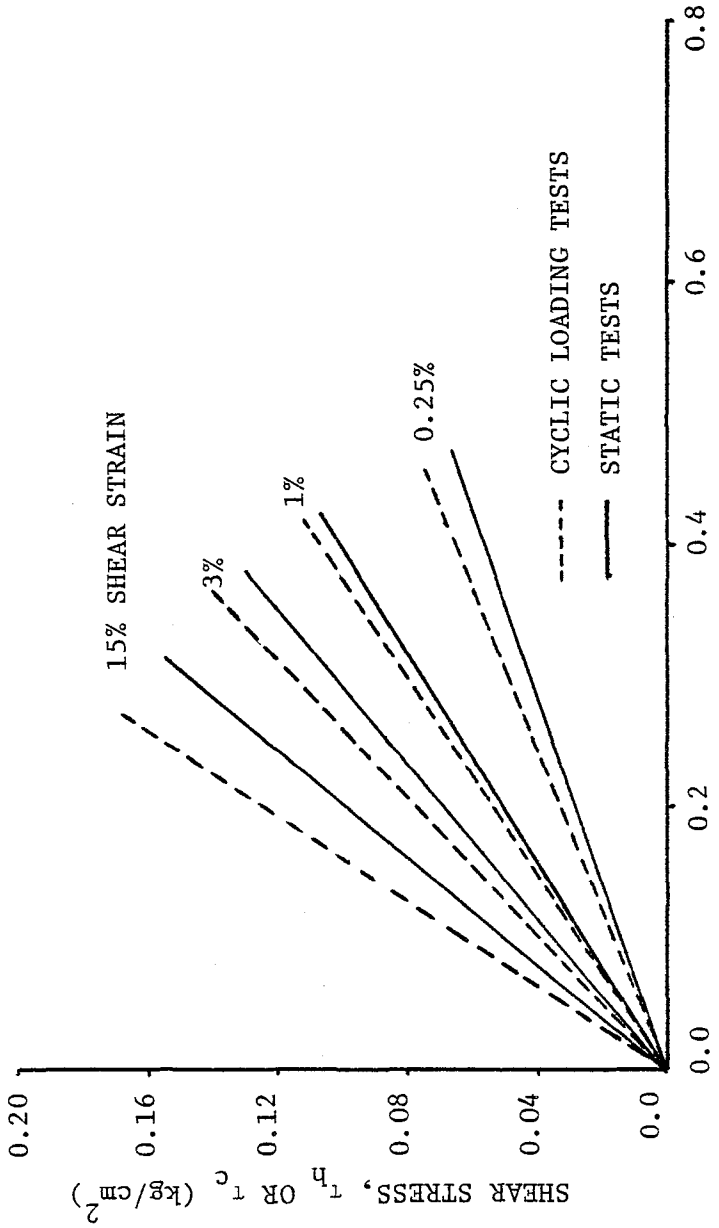

FIGURE 7.20b. COMPARISON OF STRAIN CONTOURS (τ VERSUS $\bar{\sigma}_v$ STRESS PLOT) FOR STATIC AND CYCLIC LOADING TESTS - GULF OF ALASKA CLAY

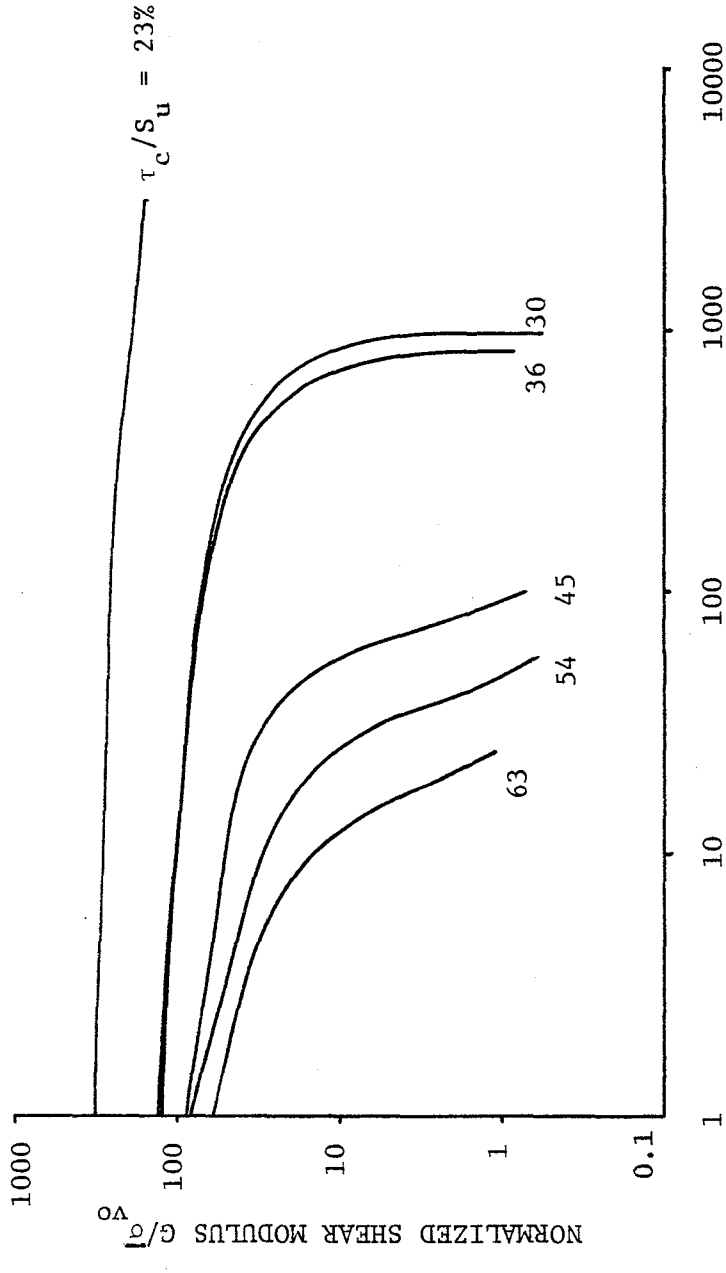

FIGURE 7.21. NORMALIZED SHEAR MODULUS VERSUS NUMBER OF LOADING CYCLES - GULF OF ALASKA CLAY

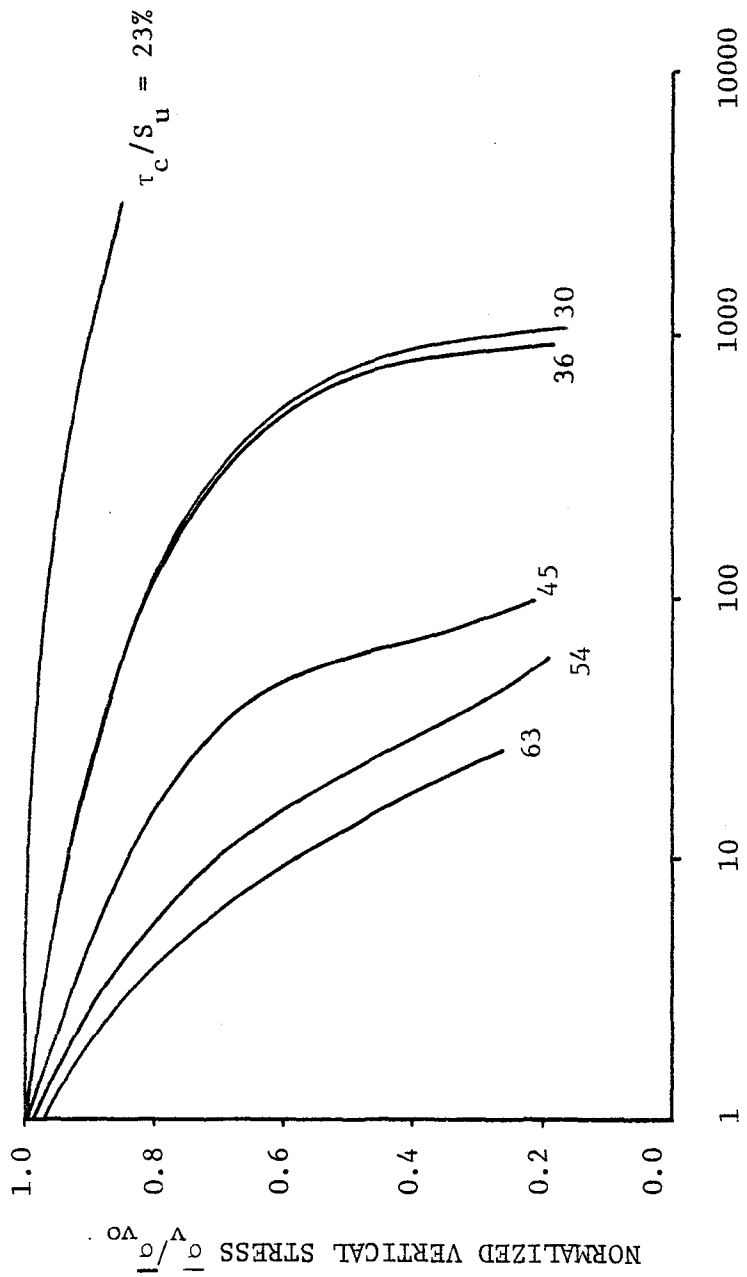

FIGURE 7.22. NORMALIZED VERTICAL STRESS VERSUS NUMBER OF LOADING CYCLES - GULF OF ALASKA CLAY

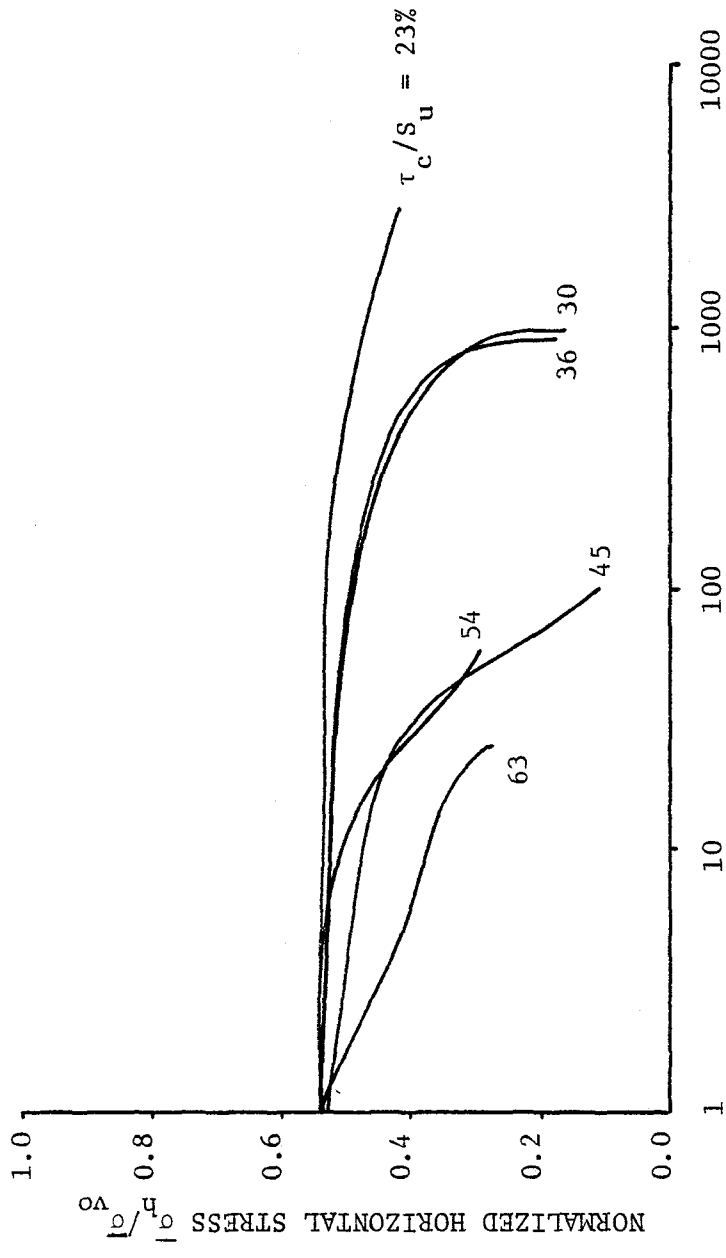

FIGURE 7.23. NORMALIZED HORIZONTAL (LATERAL) STRESS VERSUS NUMBER OF LOADING CYCLES - GULF OF ALASKA CLAY

The coefficient of lateral stress is plotted versus the number of loading cycles in Figure 7.24. As for the static tests, the coefficient of lateral stress tends to increase, and it approaches a value of unity at large shear strains. At 3 percent shear strain, the average value of K is 0.81, and at 15 percent shear strain, it is 0.92.

The principal stress ratio, R, is plotted versus the number of loading cycles in Figure 7.25. As the shear strains increase, the principal stress ratio decreases. At 3 percent shear strain, the average value of R is 0.38, and at 15 percent shear strain, it is 0.20.

The relationships between the angles θ_q, θ_p, and θ_f and the number of loading cycles are presented in Figures 7.26 to 7.28. As the shear strains increase, θ_q approaches 0°, and θ_p approaches 45°. Therefore, at large shear strains, the horizontal plane of the soil sample is approximately the plane on which the maximum shear stress acts. It is also evident from Figure 7.28 (θ_f versus number of cycles) that the horizontal plane of the sample is never the plane of maximum obliquity at any time during the test.

As mentioned previously, there is sufficient information available to determine $q - \bar{p}$ data for the cyclic loading tests, since lateral stresses were measured. Accordingly, the mobilized angle of internal friction for cyclic loading can be determined by means of Equation 5.3:

$$(\phi_m)_c = \sin^{-1} (q/\bar{p}) \qquad 7.13$$

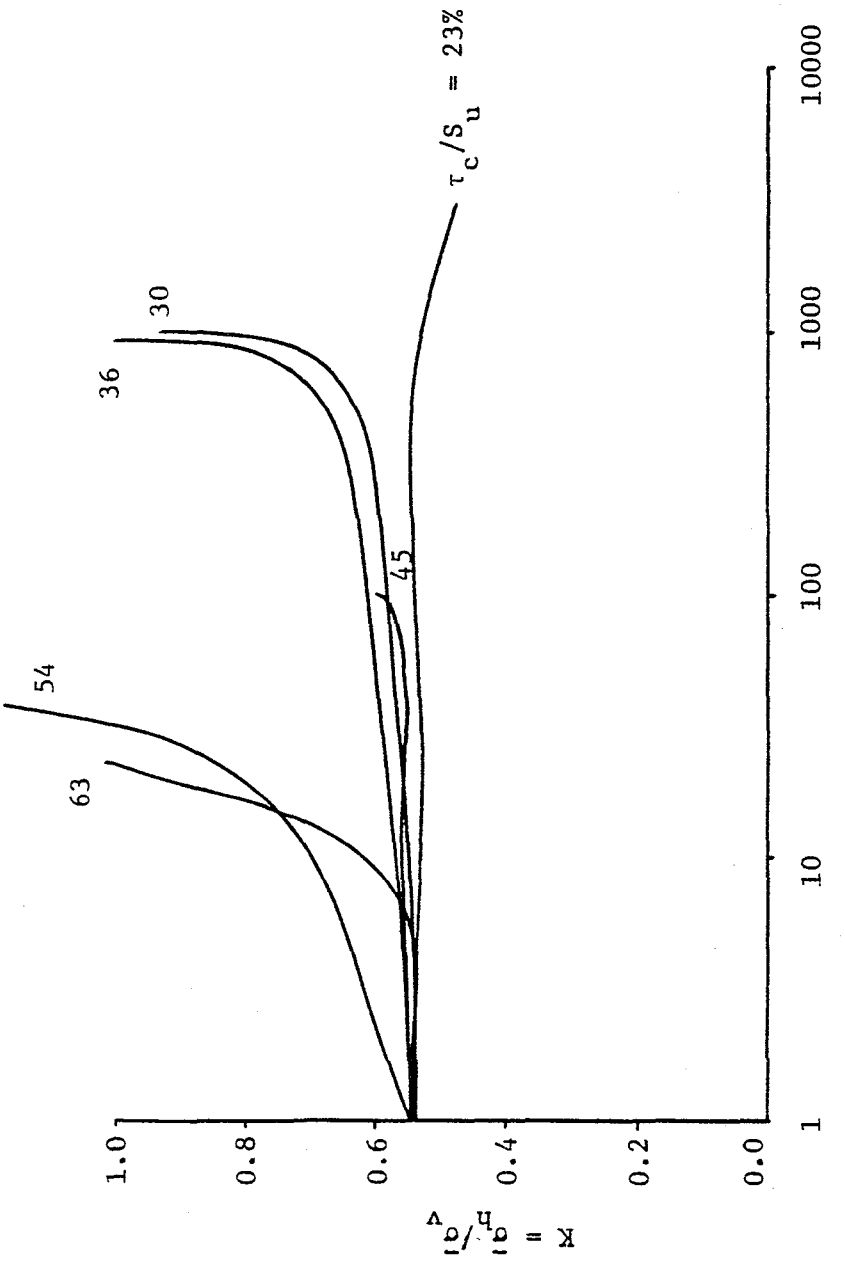

FIGURE 7.24. THE COEFFICIENT OF LATERAL STRESS, $K = \bar{\sigma}_h/\bar{\sigma}_v$, VERSUS NUMBER OF LOADING CYCLES - GULF OF ALASKA CLAY

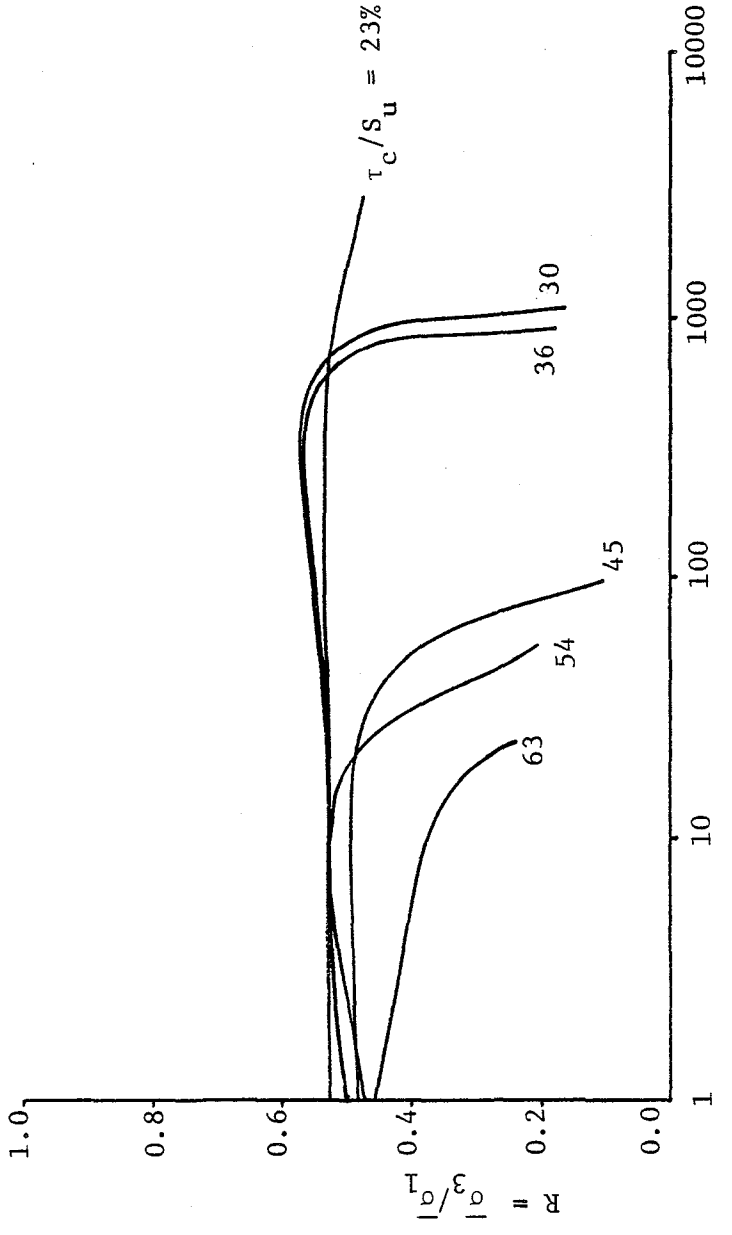

FIGURE 7.25. THE PRINCIPAL STRESS RATIO, $R = \bar{\sigma}_3/\bar{\sigma}_1$, VERSUS NUMBER OF LOADING CYCLES - GULF OF ALASKA CLAY

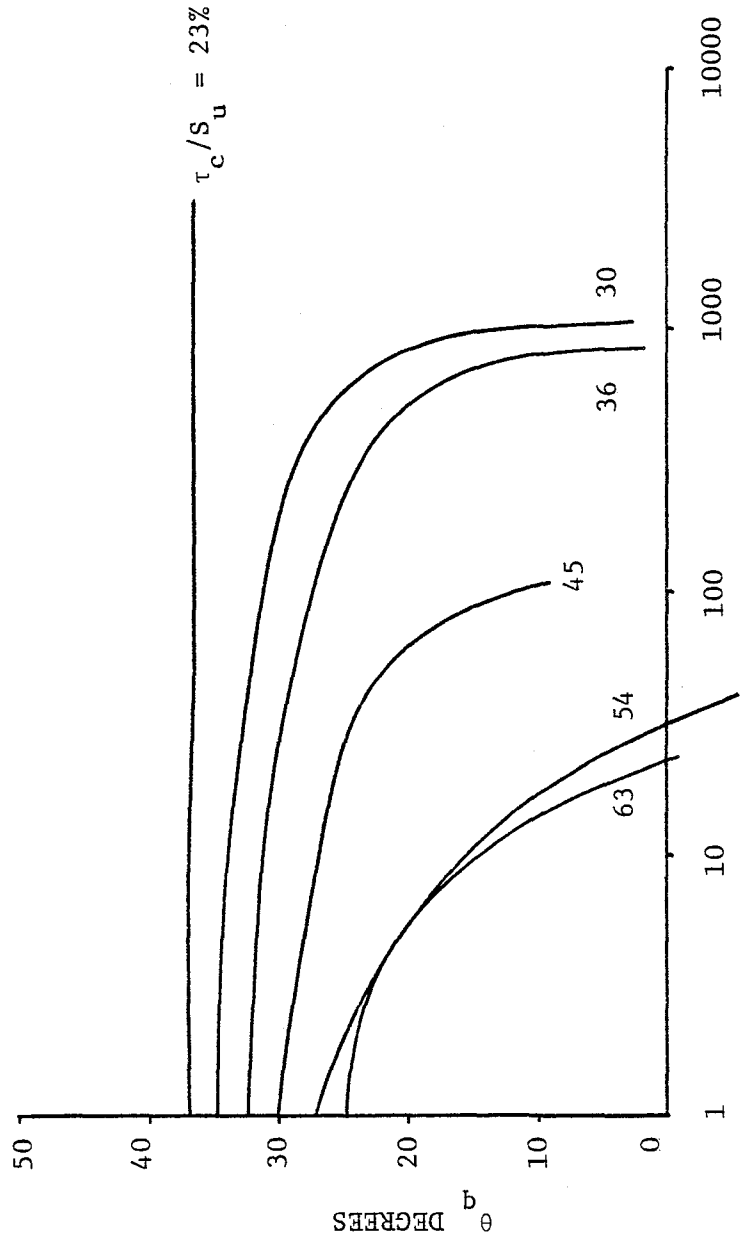

FIGURE 7.26. THE ANGLE BETWEEN THE HORIZONTAL PLANE OF THE SAMPLE AND THE PLANE OF MAXIMUM SHEAR STRESS VERSUS NUMBER OF LOADING CYCLES - GULF OF ALASKA CLAY

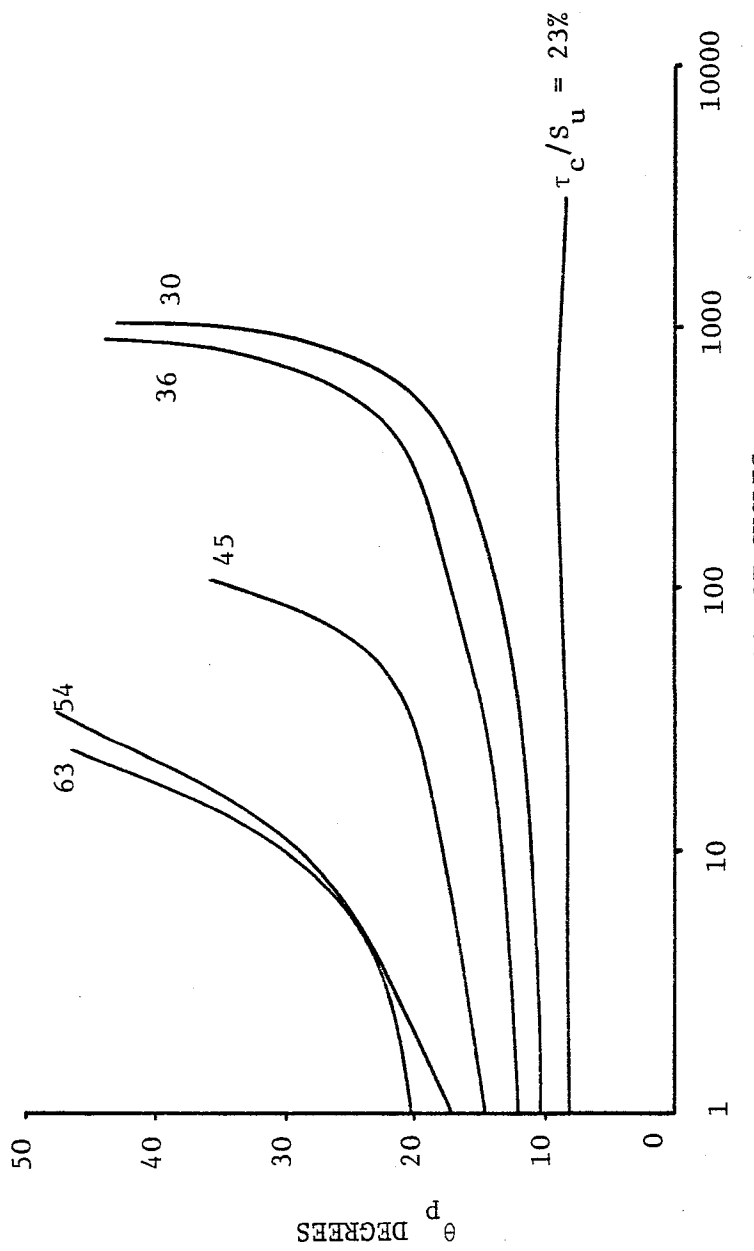

FIGURE 7.27. THE ANGLE BETWEEN THE HORIZONTAL PLANE OF THE SAMPLE AND THE MAJOR PRINCIPAL PLANE VERSUS NUMBER OF LOADING CYCLES - GULF OF ALASKA CLAY

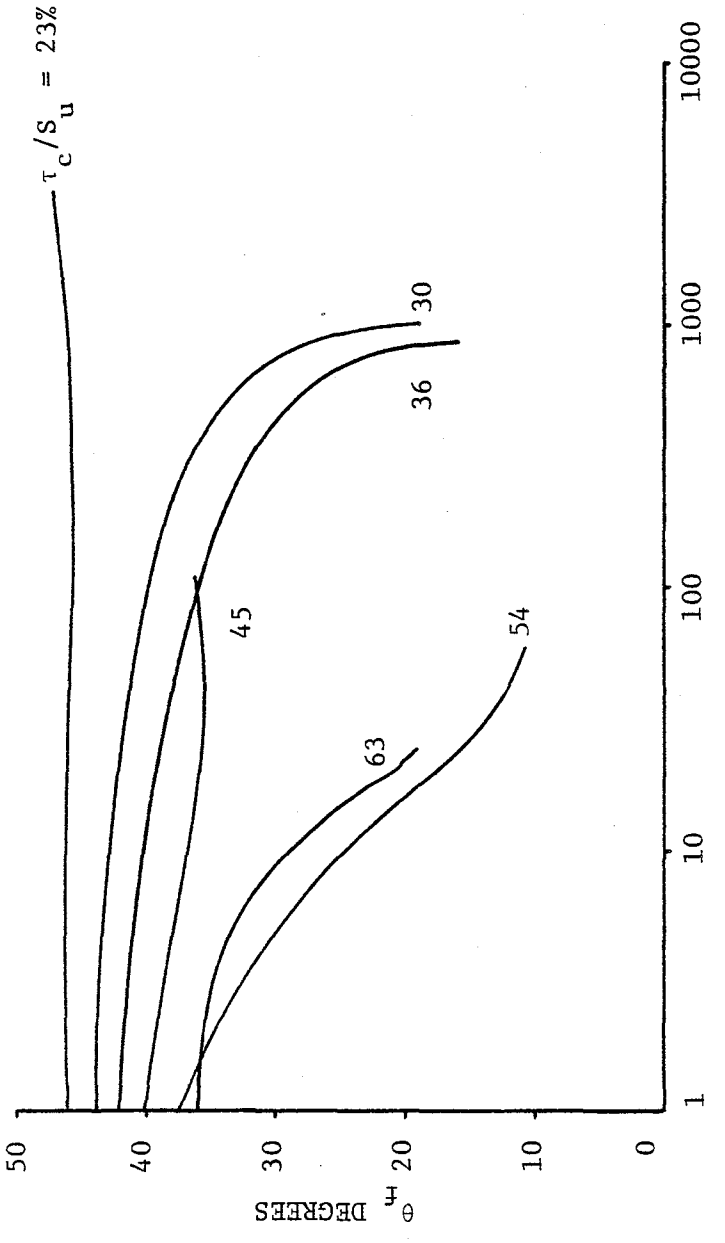

FIGURE 7.28. THE ANGLE BETWEEN THE HORIZONTAL PLANE OF THE SAMPLE AND THE PLANE OF MAXIMUM OBLIQUITY VERSUS NUMBER OF LOADING CYCLES - GULF OF ALASKA CLAY

The relationship between $(\phi_m)_c$ and the number of loading cycles is shown in Figure 7.29.

A q - $\bar{p}$ stress plot is shown in Figure 7.30. The K_o line corresponds to the measured coefficient of lateral stress at rest (K_o = 0.54). Only the positive peak points of the stress path are shown; that is, when the shear stress has its maximum positive value. The stress paths do not begin at the K_o line because the first data point is for the first loading cycle, and therefore, τ_h is not equal to zero.

Strain contours are also shown in Figure 7.30. Since the strain contours were approximated by straight lines passing through the origin, they can be expressed alternatively as average values of $(\phi_m)_c$. In Table 7.5, the average values of $(\phi_m)_c$, determined from the cyclic loading tests, are compared with the values of ϕ_m that were computed from the static tests. The average values of $(\phi_m)_c$ and ϕ_m are also compared in Figure 7.31.

TABLE 7.5

COMPARISON OF AVERAGE VALUES OF ϕ_m AND $(\phi_m)_c$ AT DIFFERENT SHEAR STRAINS - GULF OF ALASKA CLAY

Shear Strain	0.25%	0.5%	1.0%	2.0%	3.0%	15.0%
ϕ_m	19.0	20.8	23.0	25.8	27.1	32.2
$(\phi_m)_c$	19.0	19.8	22.4	24.9	27.1	41.3

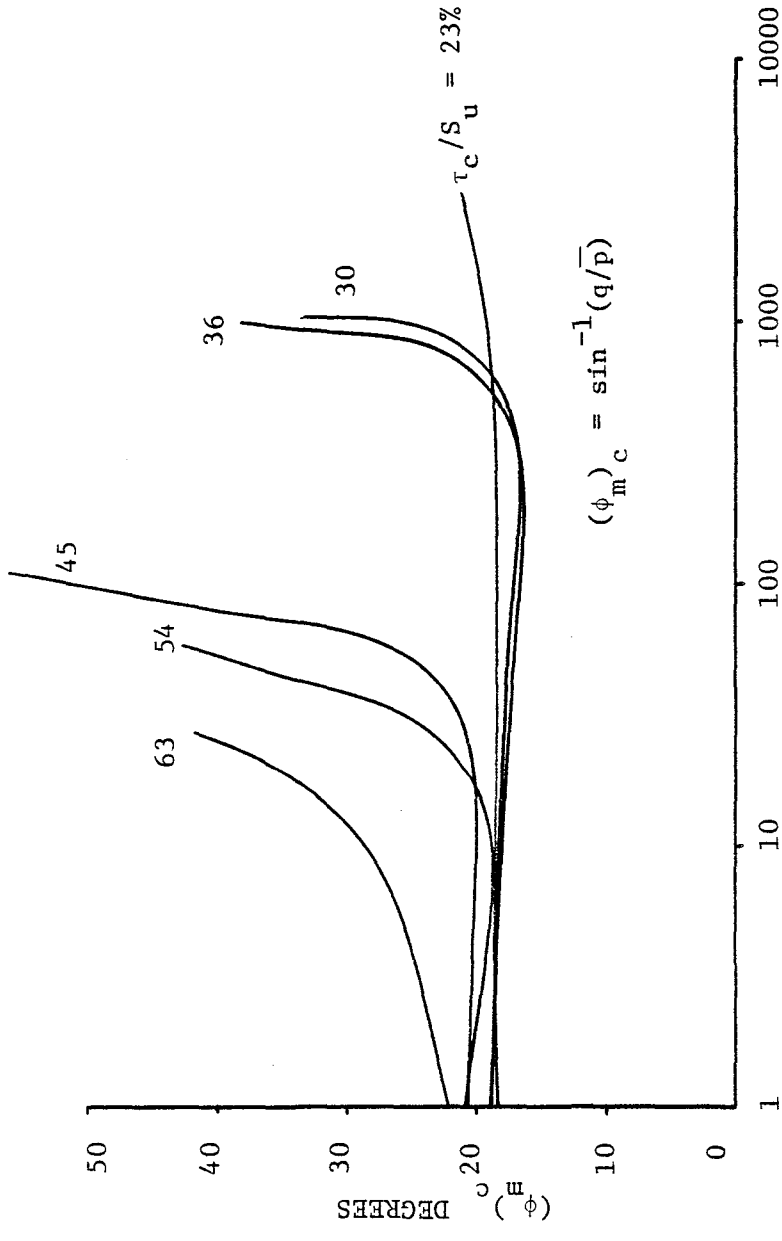

FIGURE 7.29. THE MOBILIZED ANGLE OF INTERNAL FRICTION VERSUS NUMBER OF LOADING CYCLES - GULF OF ALASKA CLAY

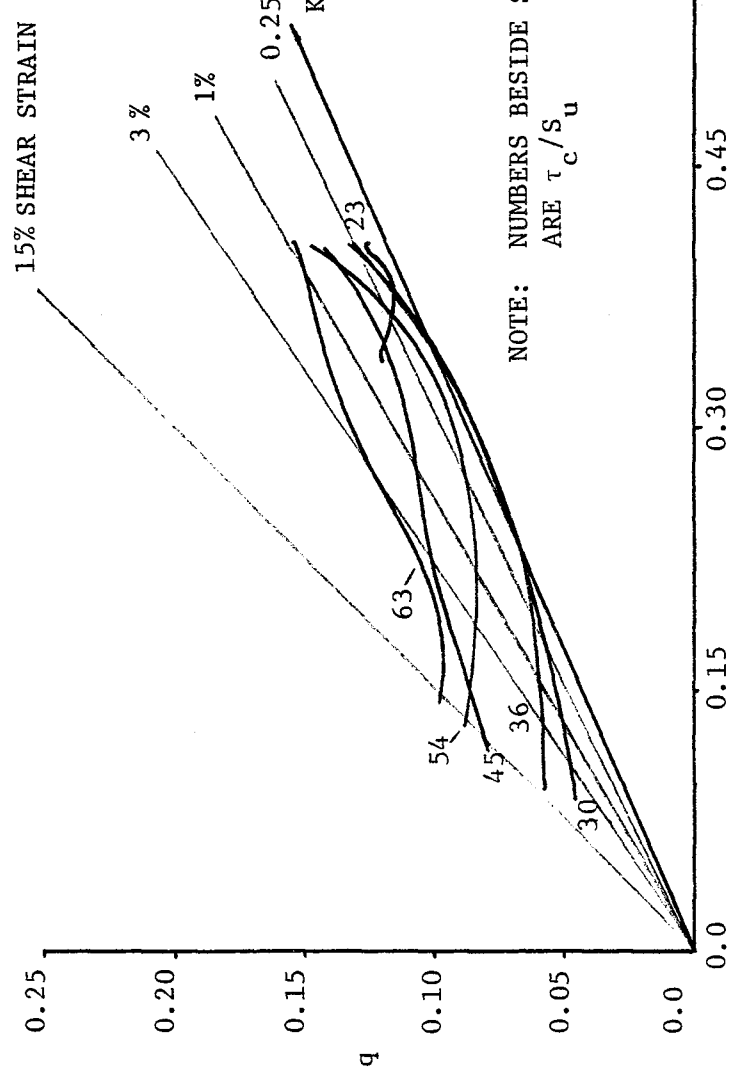

FIGURE 7.30. STRESS PATHS $(q-\bar{p})$ FOR CYCLIC LOADING TESTS - GULF OF ALASKA CLAY. STRAIN CONTOURS ARE ALSO SHOWN, BUT THE DATA POINTS HAVE BEEN OMITTED FOR CLARITY

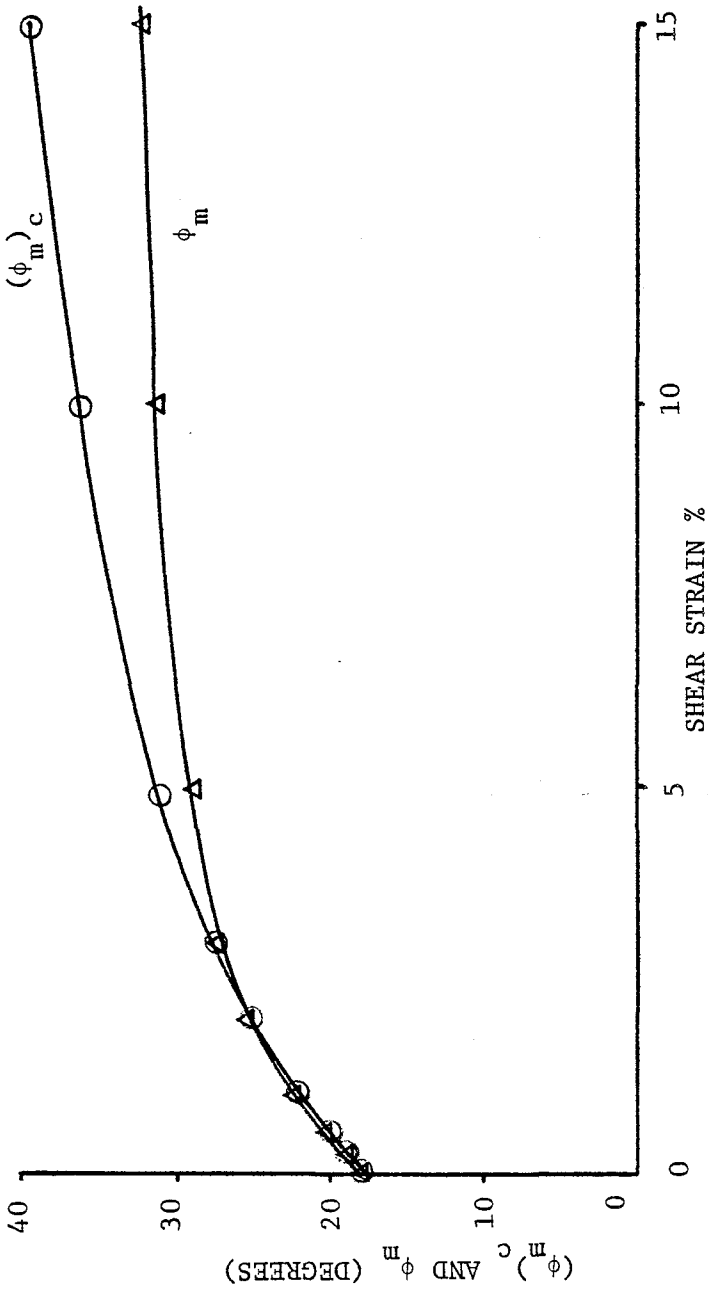

FIGURE 7.31. AVERAGE VALUES OF $(\phi_m)_c$ AND ϕ_m VERSUS SHEAR STRAIN - GULF OF ALASKA CLAY

The values of $(\phi_m)_c$ computed from the cyclic test results are virtually identical to the values of ϕ_m computed from the static test results, except at 15 percent shear strain. Consequently, the strain contours for the static tests and the cyclic loading tests are virtually identical, except at large shear strains.

Conventionally, cyclic loading strength is expressed as the number of loading cycles to failure, where failure is a specified shear strain level. This relationship is presented in Figure 7.32, in which the cyclic stress ratio (τ_c/S_u) is plotted versus the number of loading cycles. Several curves are shown, each corresponding to a different cyclic shear strain. It is evident that the curves are asymptotic to a lower bound cyclic stress level, which corresponds to the critical level of repeated loading for the Gulf of Alaska clay.

7.2 Concord Blue Clay

7.2.1 Introduction. All direct simple shear tests performed on the Concord Blue clay are summarized in Tables 7.6 (normally consolidated samples) and 7.7 (lightly overconsolidated samples). The columns of data are explained in Table 7.2.

Prior to shear, all samples were consolidated in the NGI direct simple shear device. The soil samples were consolidated to stresses greater than the in situ maximum preconsolidation stress. A series of 10 tests were performed on samples that were normally consolidated (OCR = 1) in the laboratory. Another series of 9 tests were performed on samples that

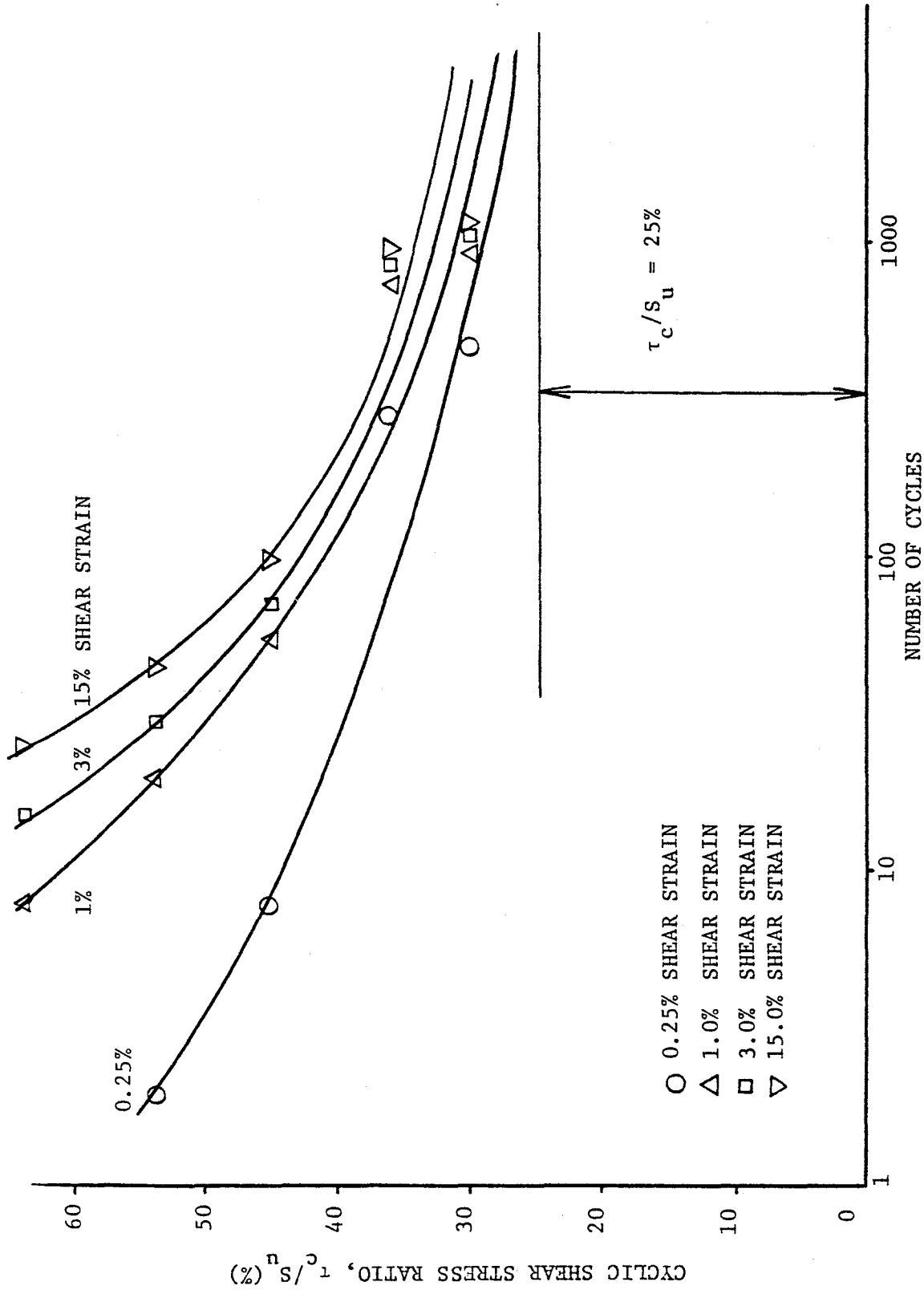

FIGURE 7.32. CYCLIC SHEAR STRESS RATIO VERSUS NUMBER OF LOADING CYCLES TO VARIOUS STRAIN LEVELS - GULF OF ALASKA CLAY

TABLE 7.6

SUMMARY OF TESTS - CONCORD BLUE CLAY (OCR = 1)

COLUMN	1	2	3	4	5	6	7	8	9	10	11	12
			SAMPLE PREPARATION					CONSOLIDATION				
Test No.		A cm^2	w_i %	e_i	H_1 cm	S_u kg/cm^2	S_t	$\bar{\sigma}_{vo}$ kg/cm^2	$\bar{\sigma}_{vm}$ kg/cm^2	OCR	H_f cm	ε_v %
CBC1S		17.8	28.4	0.785	1.75	-	-	1.12	1.12	1.0	1.69	3.4
CBC2S		17.8	27.8	0.767	1.54	0.58	-	3.37	3.37	1.0	1.44	6.6
CBC3												
CBC4												
CBC5C		17.8	28.2	0.781	1.49	0.46	-	3.37	3.37	1.0	1.44	3.0
CBC6C		17.8	28.1	0.776	1.97	0.43	-	3.37	3.37	1.0	1.84	6.6
CBC7C		17.8	27.4	0.759	2.05	-	-	3.37	3.37	1.0	1.90	6.9
CBC8C		17.8	27.6	0.762	1.58	-	-	3.37	3.37	1.0	1.47	6.9
CBC9C		17.8	27.0	0.759	1.42	0.46	-	3.37	3.37	1.0	1.33	6.8
CBC10C		17.8	27.9	0.770	1.49	-	-	3.37	3.37	1.0	1.39	6.4

TABLE 7.6 (CONTINUED)

	13	14	15	16	17	18	19	20	21	22	23	24	
	CYCLIC LOADING						STATIC LOADING				AFTER TEST		
Test No.	τ_c kg/cm^2	τ_c/S_u %	N	γ_N kg/cm^2	u_N kg/cm^2	f Hz	S_u kg/cm^2	γ_f %	u_f kg/cm^2	RATE min/mm	w_f %	e_f	REMARKS
CBC1S	-	-	-	-	-	-	0.347	12.2	0.302	30	28.7	0.792	Not corrected for false deformation
CBC2S	-	-	-	-	-	-	0.744	10.3	1.260	200	-	-	
CBC3													Large stone in Sample - Test Terminated
CBC4													
CBC5C	0.352	44	570	28.1	3.044	0.5	-	-	-	-	26.0	0.718	
CBC6C	0.437	54	27	9.2	2.621	0.5	-	-	-	-	25.1	0.693	
CBC7C	0.296	37	1360	10.7	2.923	0.5	-	-	-	-	25.5	0.704	
CBC8C	0.212	26	5960	14.4	3.024	0.5	-	-	-	-	26.5	0.731	
CBC9C	0.156	19	3000	0.04	0.292	0.5	0.772	8.63	1.310	100	25.8	0.712	No failure in cyclic loading
CBC10C	0.184	23	5000	0.13	0.726	0.5	0.675	14.1	1.613	100	-	-	No failure in cyclic loading

TABLE 7.7

SUMMARY OF TESTS - CONCORD BLUE CLAY (OCR = 2)

COLUMN	1	2	3	4	5	6	7	8	9	10	11	12
			SAMPLE PREPARATION					CONSOLIDATION				
Test No.	A cm^2	w_i %	e_i	H_i cm	S_u kg/cm^2	S_t	$\bar{\sigma}_{vo}$ kg/cm^2	$\bar{\sigma}_{vm}$ kg/cm^2	OCR	H_f cm	ε_v %
CBC11S	17.8	28.5	0.787	2.03	0.31	-	3.37	6.74	2.0	1.91	5.5
CBC12S	17.8	29.2	0.806	1.74	0.31	-	1.68	3.37	2.0	1.61	7.7
CBC13C	17.8	29.1	0.803	1.52	0.31	-	1.68	3.37	2.0	1.41	7.4
CBC14C	17.8	28.6	0.789	1.77	0.31	-	1.68	3.37	2.0	1.63	7.7
CBC15C	17.8	28.5	0.787	1.78	0.37	-	1.68	3.37	2.0	1.65	7.3
CBC16C	17.8	29.2	0.806	1.98	0.37	-	1.68	3.37	2.0	1.84	7.2
CBC17C	17.8	29.8	0.822	1.89	0.37	-	1.68	3.37	2.0	1.74	8.3
CBC18C	17.8	29.5	0.817	1.54	0.37	-	1.68	3.37	2.0	1.39	9.4
CBC19C	17.8	29.2	0.806	1.78	0.31	-	1.68	3.37	2.0	1.63	8.2

TABLE 7.7 (CONTINUED)

	13	14	15	16	17	18	19	20	21	22	23	24	
	CYCLIC LOADING						STATIC LOADING				AFTER TEST		
Test No.	τ_c kg/cm^2	τ_c/S_u %	N	γ_N kg/cm^2	u_N kg/cm^2	f Hz	S_u kg/cm^2	γ_f %	u_f kg/cm^2	RATE min/mm	w_f %	e_f	REMARKS
CBC11S	-	-	-	-	-	-	1.106	10.8	0.171	75	25.1	0.693	
CBC12S	-	-	-	-	-	-	0.692	12.5	-0.020	75	27.4	0.756	
CBC13C	0.219	36	625	12.0	1.411	0.5	-	-	-	-	26.5	0.731	
CBC14C	0.191	32	789	11.7	1.512	0.5	-	-	-	-	26.5	0.731	
CBC15C	0.163	27	3630	11.3	1.512	0.5	-	-	-	-	26.6	0.734	
CBC16C	0.185	31	1286	9.2	1.411	0.5	-	-	-	-	26.4	0.729	
CBC17C	0.350	58	30	15.6	1.210	0.5	-	-	-	-	26.8	0.740	
CBC18C	0.124	21	4280	8.5	1.462	0.5	-	-	-	-	26.9	0.742	
CBC19C	0.067	11	6000	0.05	-0.010	0.5	0.568	11.0	0.161	75	26.0	0.718	No failure in cyclic loading

were overconsolidated in the laboratory to an overconsolidation ratio of two (OCR = 2).

The static tests were performed under controlled strain conditions, and the cyclic tests were performed under controlled stress conditions. The small sample size was used for all tests. For the cyclic tests, a square wave load shape was used, with complete stress reversal. The cyclic loading frequency was 0.5 Hz. Horizontal (lateral) stress measurements were not taken for any of these tests.

In the following sections, the test results for Concord Blue clay are presented. First, the test results for the normally consolidated samples are presented, and this is followed by the test results for the lightly overconsolidated samples.

7.2.2 Normally Consolidated Samples. Four static tests were performed. Tests 1 and 2 were true static tests; Tests 9 and 10 were performed following a sequence of cyclic loading in which failure did not occur.

Static stress-strain curves are shown in Figure 7.33. The shear stress was normalized by dividing it by the consolidation stress. For Tests 9 and 10, the soil samples developed only small shear strains (0.04 and 0.13 percent) during cyclic loading. Therefore, it seems reasonable that the stress-strain curves for these two tests should be similar to the curves for the true static tests (73,107). The average normalized undrained shear strength is 0.240 at peak shear

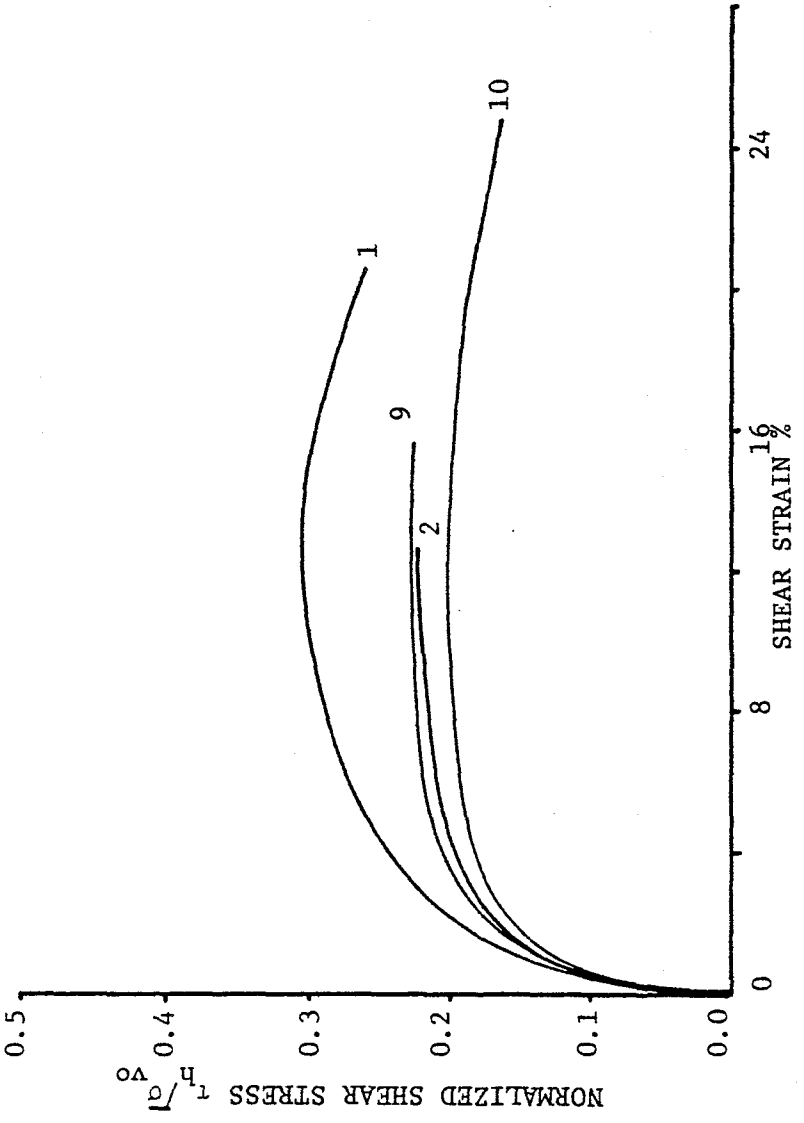

FIGURE 7.33. NORMALIZED STRESS-STRAIN CURVES FOR STATIC TESTS - NORMALLY CONSOLIDATED CONCORD BLUE CLAY

stress, and it is 0.192 at three percent shear strain. The normalized undrained shear strength of the normally consolidated Concord Blue clay is slightly higher than the value of 0.21 proposed by Ladd and Edgers (59).

The pore pressure versus shear strain curves for the static tests are shown in Figure 7.34. The pore pressure was normalized by dividing it by the consolidation stress. The average normalized pore pressure is 0.277 at 3 percent shear strain, and it is 0.418 at 15 percent shear strain.

Six cyclic loading tests (Tests 5 - 10) were performed on the normally consolidated Concord Blue clay, each with a different cyclic shear stress. The cyclic shear stresses used for each test are summarized below:

TEST	τ_c (kg/cm^2)	τ_c/S_u (%)*
5	0.352	44
6	0.437	54
7	0.296	37
8	0.212	26
9	0.156	19
10	0.184	23

For the cyclic tests, the relationship between cyclic shear strain and the number of loading cycles is shown in Figure 7.35, and the relationship between excess pore pressure and the number of loading cycles is

*S_u is the peak static undrained shear strength corresponding to the consolidation stress used in the cyclic loading tests (S_u = 0.809 kg/cm^2).

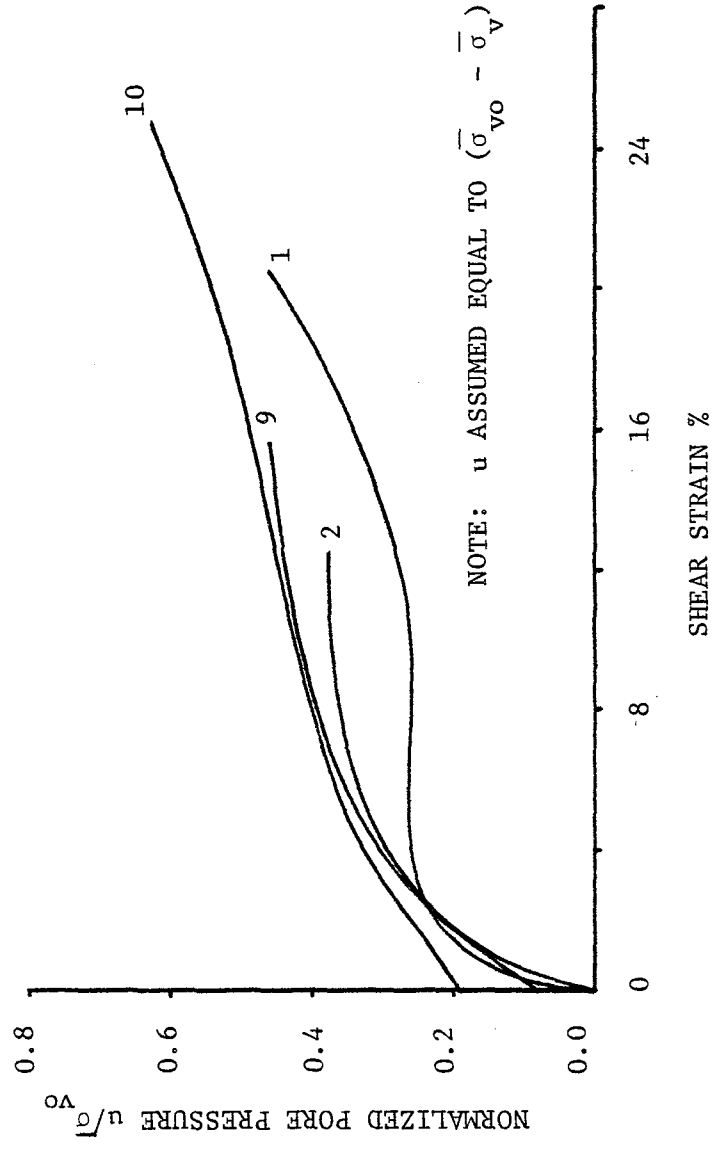

FIGURE 7.34. NORMALIZED PORE PRESSURE VERSUS SHEAR STRAIN FOR STATIC TESTS - NORMALLY CONSOLIDATED CONCORD BLUE CLAY

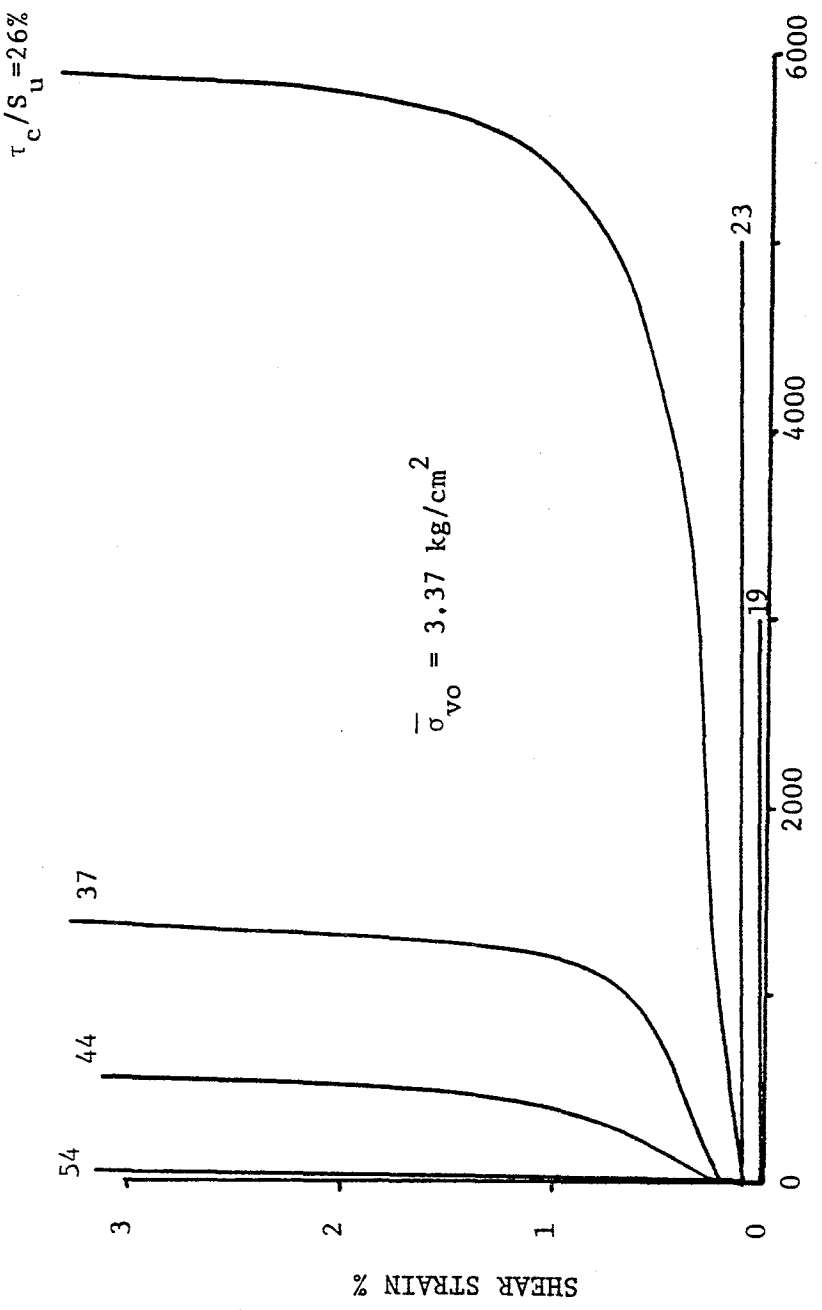

FIGURE 7.35. CYCLIC SHEAR STRAIN VERSUS NUMBER OF LOADING CYCLES - NORMALLY CONSOLIDATED CONCORD BLUE CLAY

shown in Figure 7.36. As mentioned previously, the cyclic shear strain is one-half of the peak to peak shear strain. The curves shown in Figures 7.35 and 7.36 are typical for normally consolidated clays (2,3). It should be noted that when the normalized pore pressure in the sample approaches a value of approximately 0.4 or 0.5, the rate of pore pressure generation (per cycle) accelerates, and failure occurs with further cyclic loading.

The samples for Tests 9 and 10 showed no indications of imminent failure during cyclic loading. Test 9 was terminated after 3,000 loading cycles, and Test 10 was terminated after 5,000 cycles. The shear strains and the pore pressures remained approximately constant during the latter part of these two tests. This implies that the samples for Tests 9 and 10 were in a state of non-failure equilibrium (93). Consequently, the critical level of repeated loading for normally consolidated Concord Blue clay is estimated to be about 25 percent of the peak static undrained shear strength. The critical level of repeated loading for the (normally consolidated) Gulf of Alaska clay was also found to be approximately 25 percent.

The relationship between the cyclic stress ratio, τ_c/S_u, and the number of cycles to failure (specified by a cyclic shear strain) is shown in Figure 7.37. Curves are shown for several shear strain levels. The critical level of repeated loading can also be found from this figure, as shown.

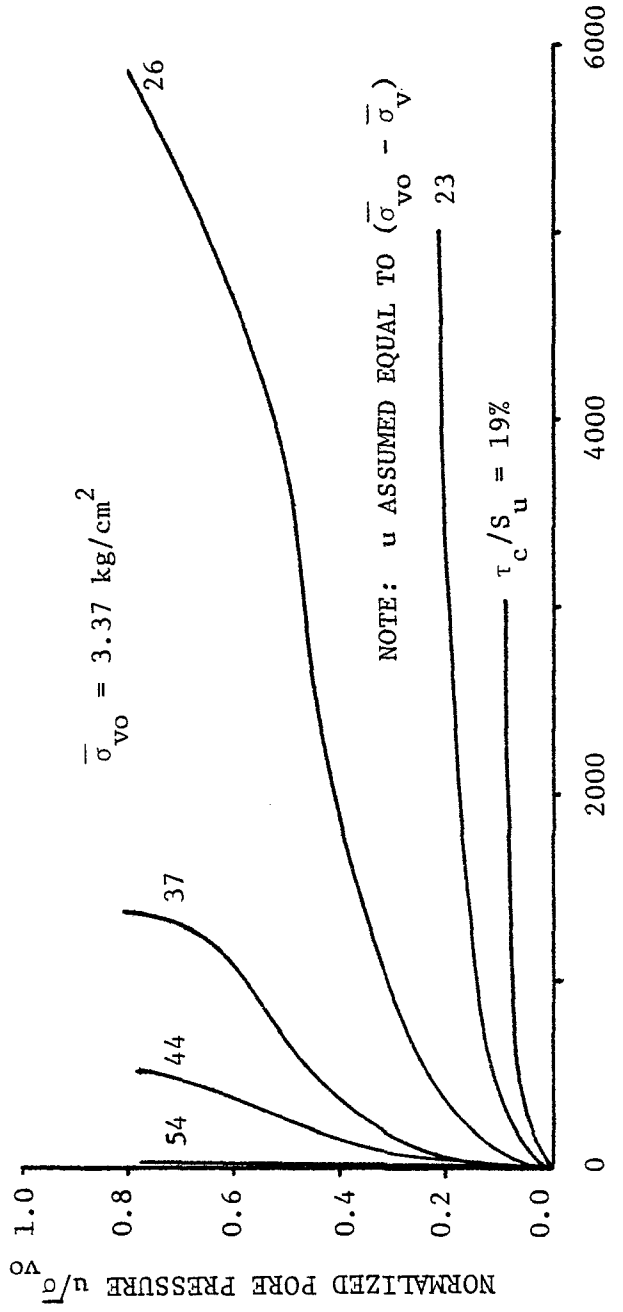

FIGURE 7.36. NORMALIZED PORE PRESSURE VERSUS NUMBER OF LOADING CYCLES - NORMALLY CONSOLIDATED CONCORD BLUE CLAY

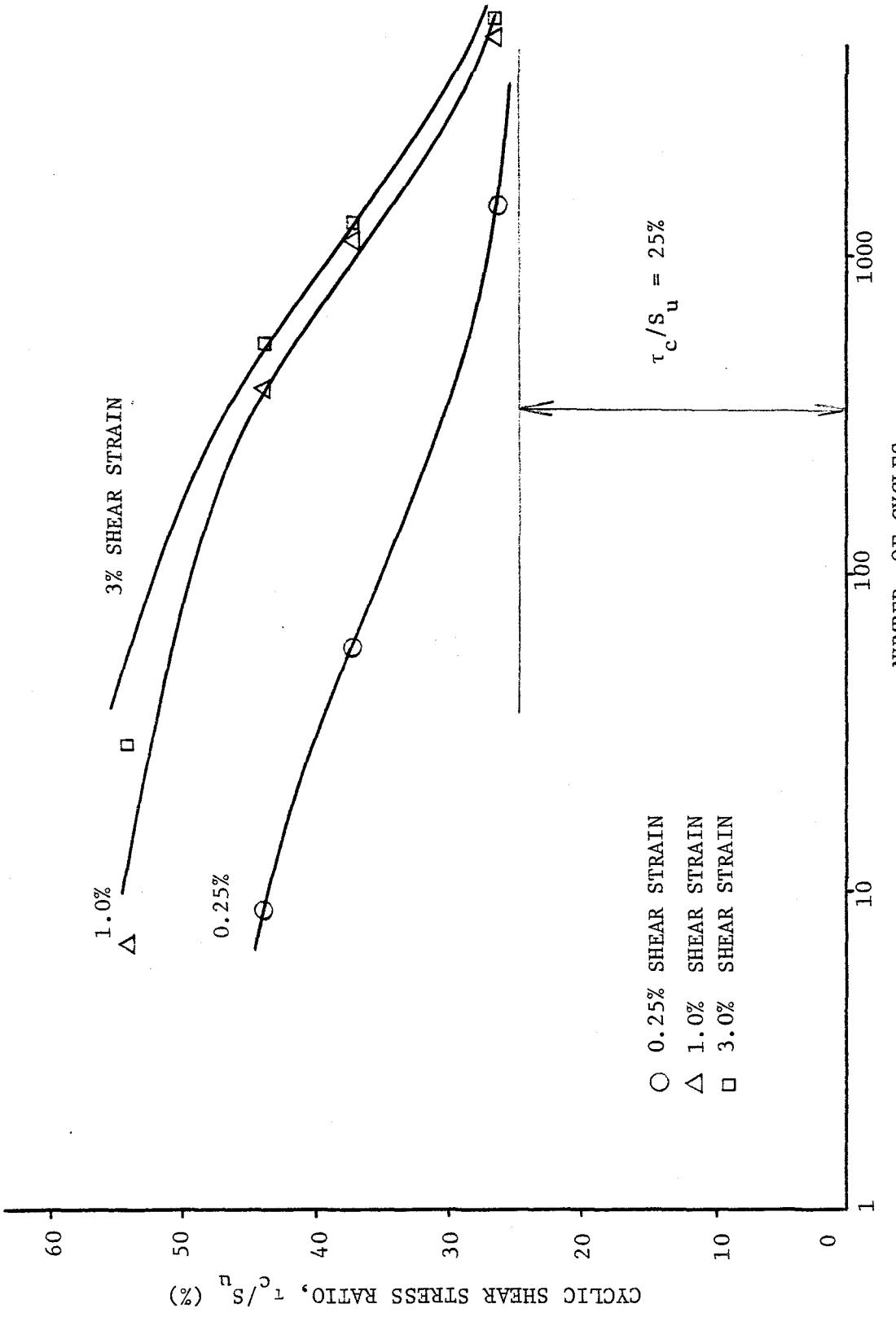

FIGURE 7.37. CYCLIC SHEAR STRESS RATIO VERSUS NUMBER OF LOADING CYCLES TO VARIOUS STRAIN LEVELS - NORMALLY CONSOLIDATED CONCORD BLUE CLAY

Stress paths (τ versus $\bar{\sigma}_v$) for the static tests are shown in Figure 7.38, and stress paths for the cyclic tests are shown in Figure 7.39. For the cyclic tests, only the positive peak points of the stress paths are shown; the actual stress path would cycle above and below the $\bar{\sigma}_v$ axis. Several strain contours are also shown in the figures.

The mobilized angle of friction for the static tests ($\tan \phi = \tau_h/\bar{\sigma}_v$) is compared with the mobilized angle of friction for cyclic loading ($\tan(\phi)_c = \tau_c/\bar{\sigma}_v$) in Table 7.8.

TABLE 7.8

COMPARISON OF AVERAGE VALUES OF ϕ AND $(\phi)_c$ AT DIFFERENT SHEAR STRAINS - NORMALLY CONSOLIDATED CONCORD BLUE CLAY

Shear Strain	0.25%	0.5%	1.0%	2.0%	3.0%	15.0%
ϕ	4.3	7.0	9.5	12.9	14.9	22.4
$(\phi)_c$	5.7	8.4	11.8	17.7	23.0	44.9

The values of $(\phi)_c$ are consistently higher than the values of ϕ, especially at large shear strains. Similar results were found for the Gulf of Alaska clay, except that the discrepancy between $(\phi)_c$ and ϕ is smaller. Consequently, for the normally consolidated Concord Blue clay, the strain contours for the static tests and the cyclic tests (at the same shear strain) do not coincide, except at small shear strains.

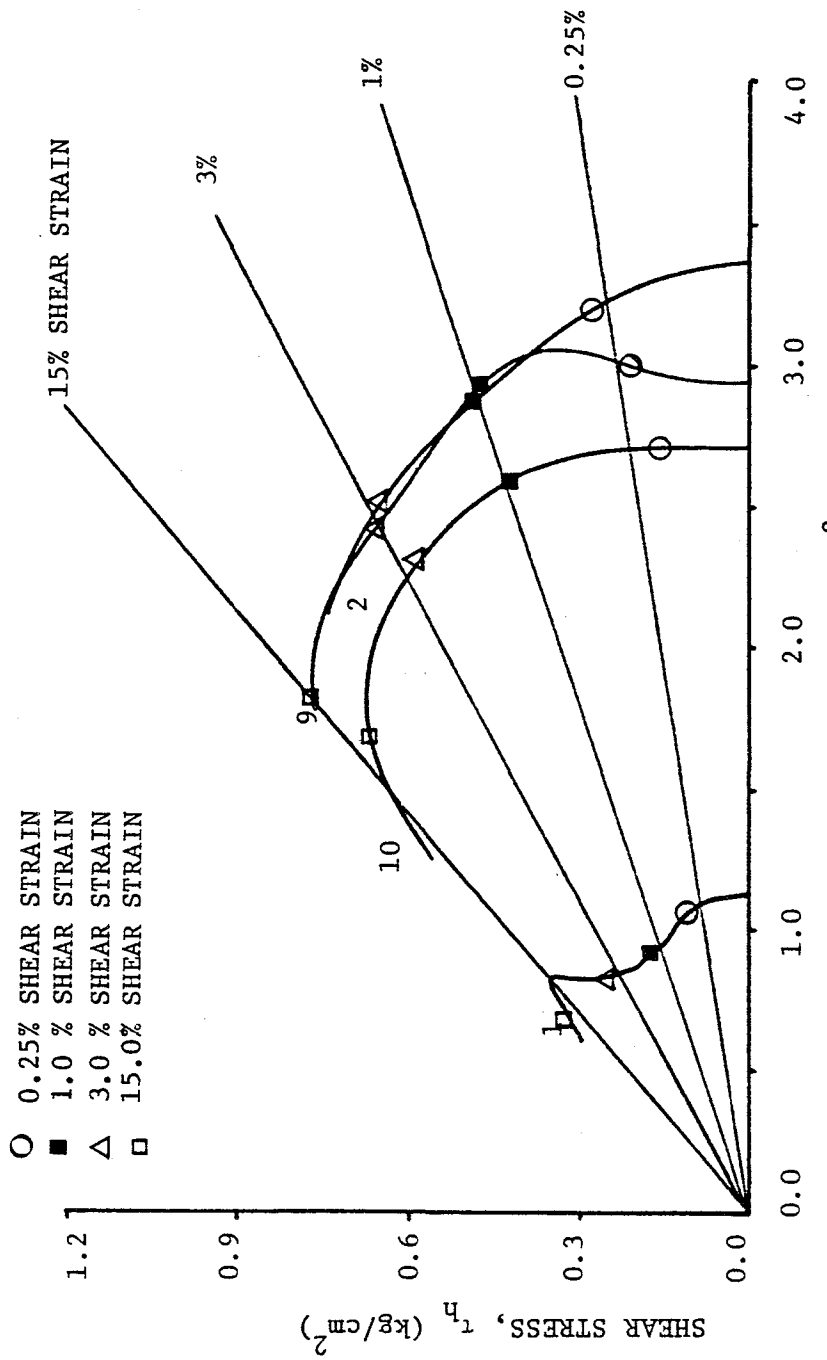

FIGURE 7.38. STRESS PATHS (τ_h VERSUS $\bar{\sigma}_v$) FOR STATIC TESTS - NORMALLY CONSOLIDATED CONCORD BLUE CLAY. STRAIN CONTOURS ARE ALSO SHOWN

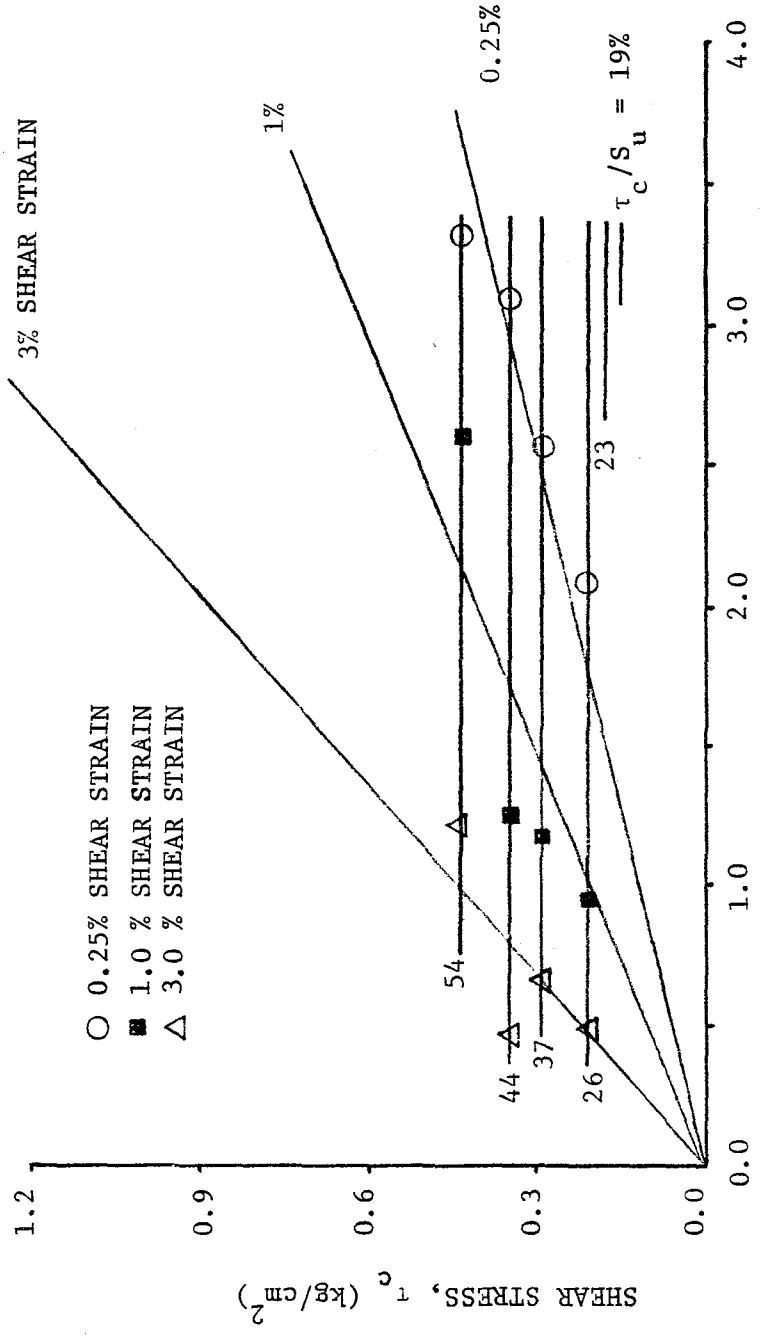

FIGURE 7.39. STRESS PATHS (τ_c VERSUS $\bar{\sigma}_v$) FOR CYCLIC LOADING TESTS - NORMALLY CONSOLIDATED CONCORD BLUE CLAY. STRAIN CONTOURS ARE ALSO SHOWN

7.2.3 Lightly Overconsolidated Samples. Three static tests were performed. Tests 11 and 12 were true static tests; static Test 19 was performed following a sequence of cyclic loading that did not cause failure.

The static stress-strain curves are shown in Figure 7.40. The average normalized undrained shear strength is 0.358 at peak shear stress, and it is 0.299 at 3 percent shear strain. The normalized peak undrained shear strength for the lightly overconsolidated Concord Blue clay is considerably higher than it is for the normally consolidated Concord Blue clay ($S_u/\overline{\sigma}_{vo} = 0.24$). This observation is consistent with published literature (59,60,73).

The relationship between normalized excess pore pressure and shear strain for the static tests is shown in Figure 7.41. Initially, at small shear strains, the pore pressures are negative. As the shear strains increase, the pore pressures become positive. The average normalized pore pressure is -0.069 at 3 percent shear strain, and it is 0.113 at 15 percent shear strain.

Seven cyclic loading tests (Tests 13 - 19) were performed on the lightly overconsolidated Concord Blue clay, each with a different cyclic shear stress. The cyclic shear stresses used for each test are summarized below:

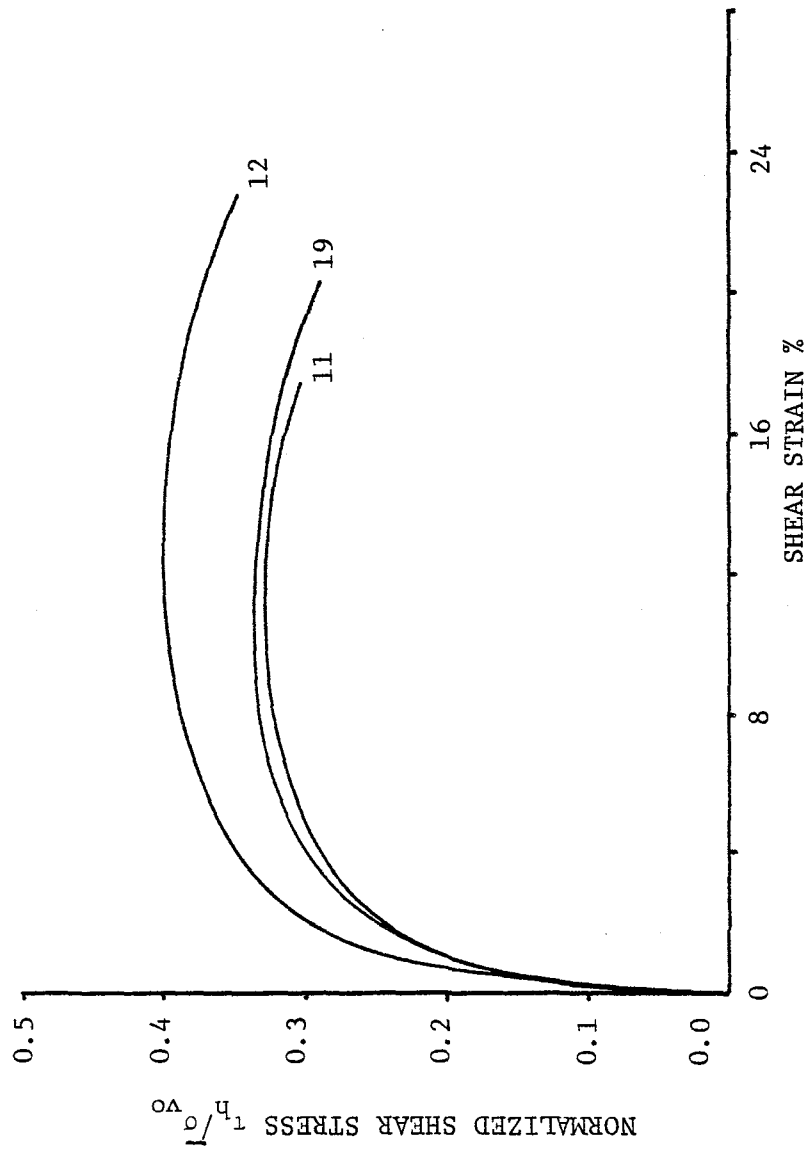

FIGURE 7.40. NORMALIZED STRESS-STRAIN CURVES FOR STATIC TESTS - LIGHTLY OVER-CONSOLIDATED CONCORD BLUE CLAY

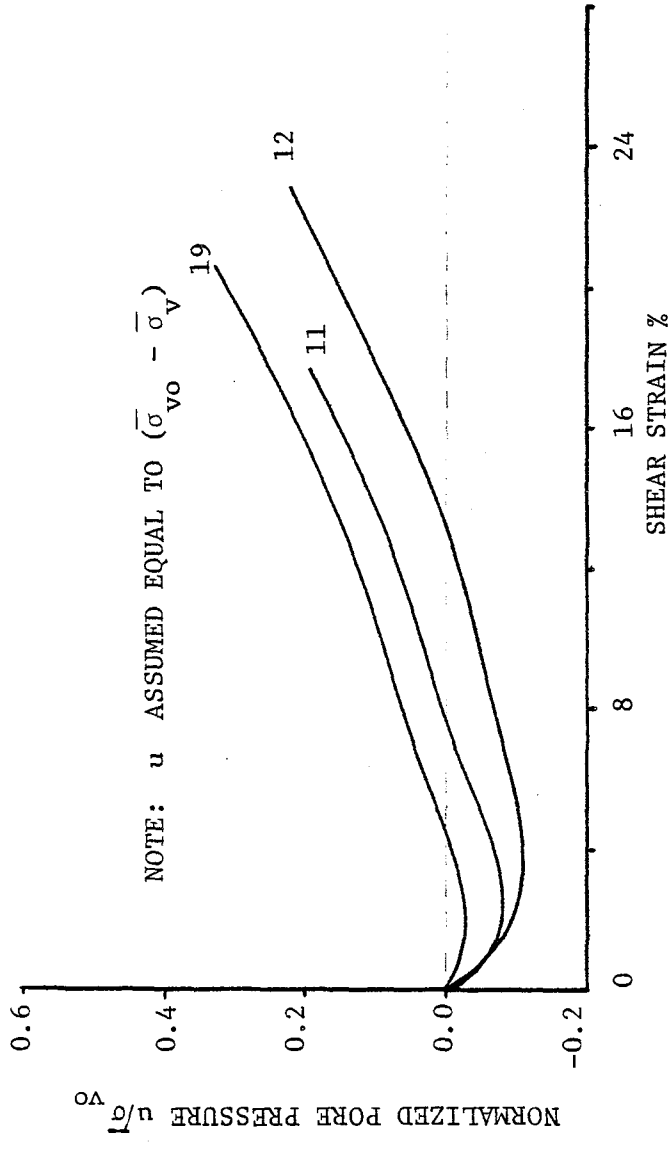

FIGURE 7.41. NORMALIZED PORE PRESSURE VERSUS SHEAR STRAIN FOR STATIC TESTS - LIGHTLY OVERCONSOLIDATED CONCORD BLUE CLAY

Test	τ_c (kg/cm^2)	τ_c/S_u (%) *
13	0.219	36
14	0.191	32
15	0.163	27
16	0.185	31
17	0.350	58
18	0.124	21
19	0.067	11

Cyclic shear strain is plotted versus the number of loading cycles in Figure 7.42. For Test 19, the cyclic shear strain remained constant throughout the latter part of the test, and the sample showed no indications of impending failure, even after 6,000 loading cycles.

Normalized pore pressure is plotted versus the number of loading cycles in Figure 7.43. Typically, negative pore pressures develop at the beginning of the test. However, the pore pressures increase rapidly, and they are positive during the latter part of the test. In Test 19, the pore pressure was approximately zero throughout the test. It should be noted that when the normalized pore pressure in the sample approaches a value of approximately 0.4, the rate of pore pressure generation (per cycle) accelerates, and failure occurs with further cyclic loading.

*S_u = 0.601 kg/cm^2.

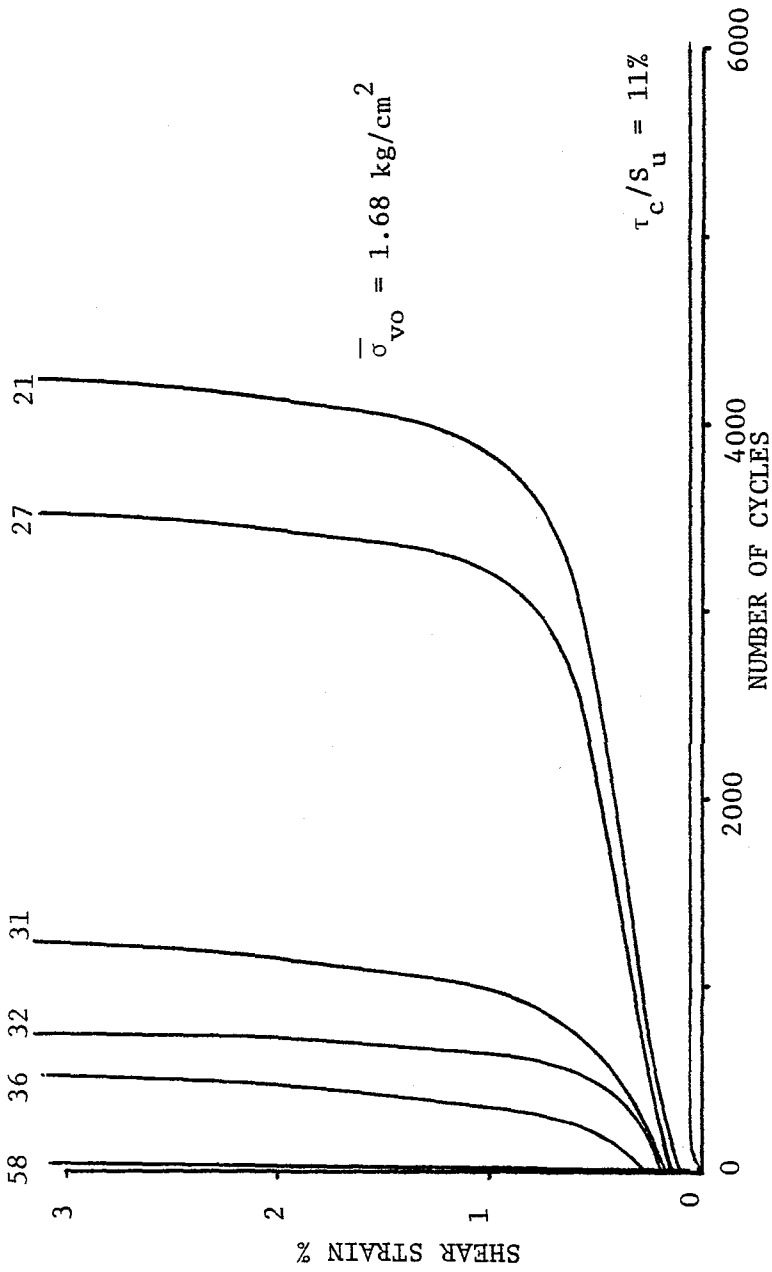

FIGURE 7.42. CYCLIC SHEAR STRAIN VERSUS NUMBER OF LOADING CYCLES - LIGHTLY OVER-CONSOLIDATED CONCORD BLUE CLAY

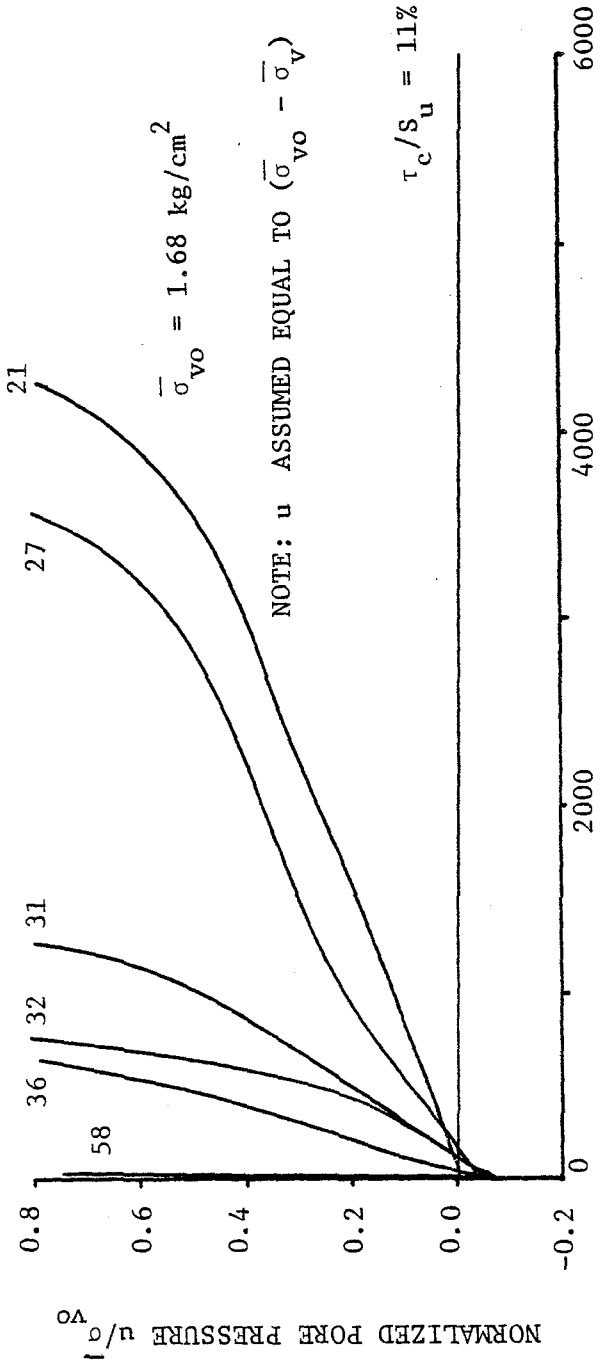

FIGURE 7.43. NORMALIZED PORE PRESSURE VERSUS NUMBER OF LOADING CYCLES - LIGHTLY OVERCONSOLIDATED CONCORD BLUE CLAY

Based on the results of the cyclic loading tests, the critical level of repeated loading (93) for the lightly overconsolidated Concord Blue clay is estimated to be approximately 15 percent of the peak static undrained shear strength.

The relationship between the cyclic stress ratio, τ_c/S_u, and the number of cycles to failure (specified by a cyclic shear strain) is shown in Figure 7.44. Curves are shown for several shear strain levels. The critical level of repeated loading can also be found from this figure, as shown.

Stress paths (τ versus $\bar{\sigma}_v$) for the static and the cyclic tests are shown in Figures 7.45 and 7.46. Several strain contours are also shown in these figures. The stress paths for the static tests are typical for a lightly overconsolidated clay (59,73).

The mobilized angle of friction for the static tests ($\tan \phi = \tau_h/\bar{\sigma}_v$) is compared with the mobilized angle of friction for cyclic loading ($\tan(\phi)_c = \tau_c/\bar{\sigma}_v$) in Table 7.9.

TABLE 7.9

COMPARISON OF AVERAGE VALUES OF ϕ AND $(\phi)_c$ AT DIFFERENT SHEAR STRAINS - LIGHTLY OVERCONSOLIDATED CONCORD BLUE CLAY

Shear Strain	0.25%	0.5%	1.0%	2.0%	3.0%	15.0%
ϕ	6.0	8.7	11.4	14.1	15.6	21.6
$(\phi)_c$	7.5	9.2	11.6	15.7	19.9	37.4

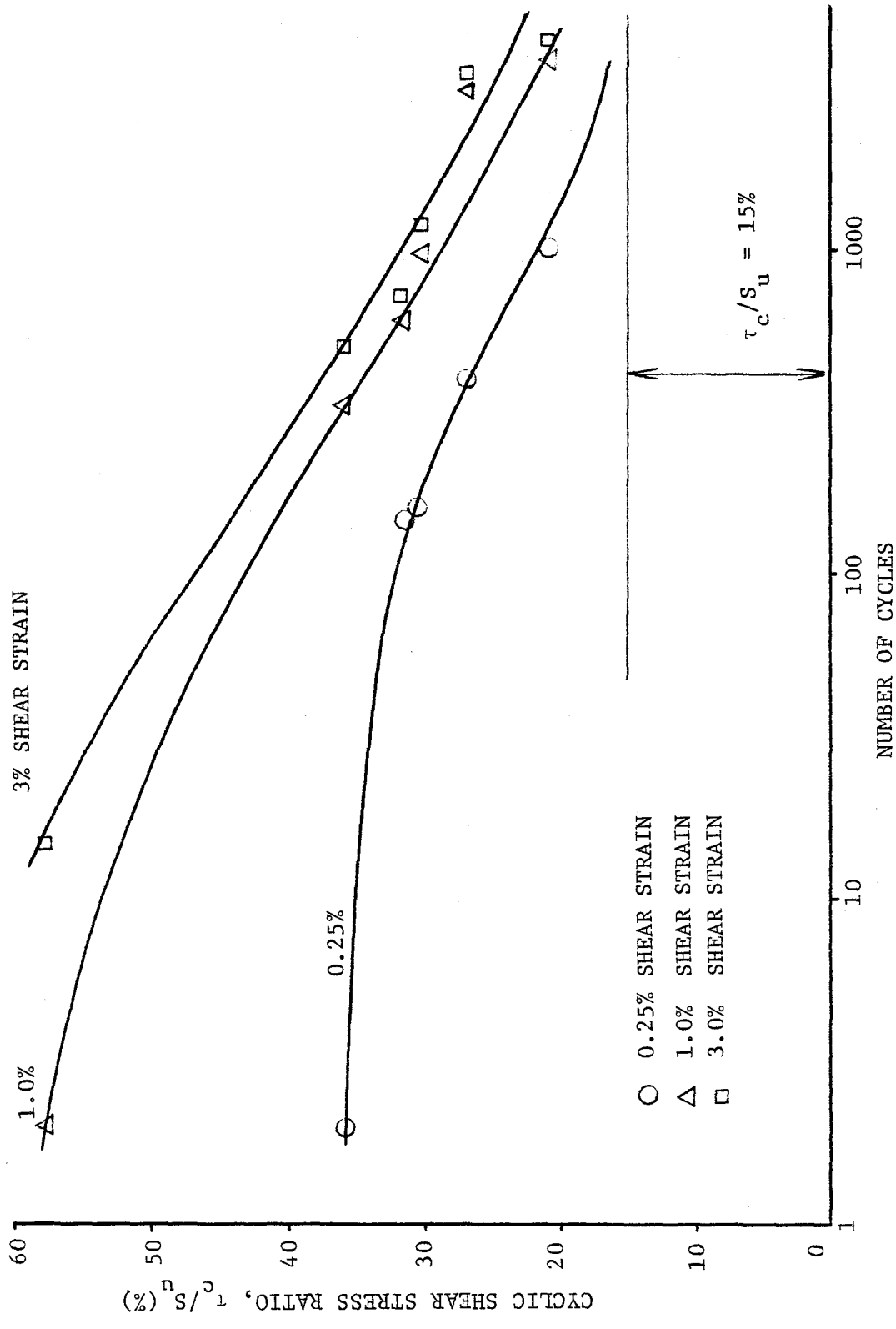

FIGURE 7.44. CYCLIC SHEAR STRESS RATIO VERSUS NUMBER OF LOADING CYCLES TO VARIOUS STRAIN LEVELS - LIGHTLY OVER-CONSOLIDATED CONCORD BLUE CLAY

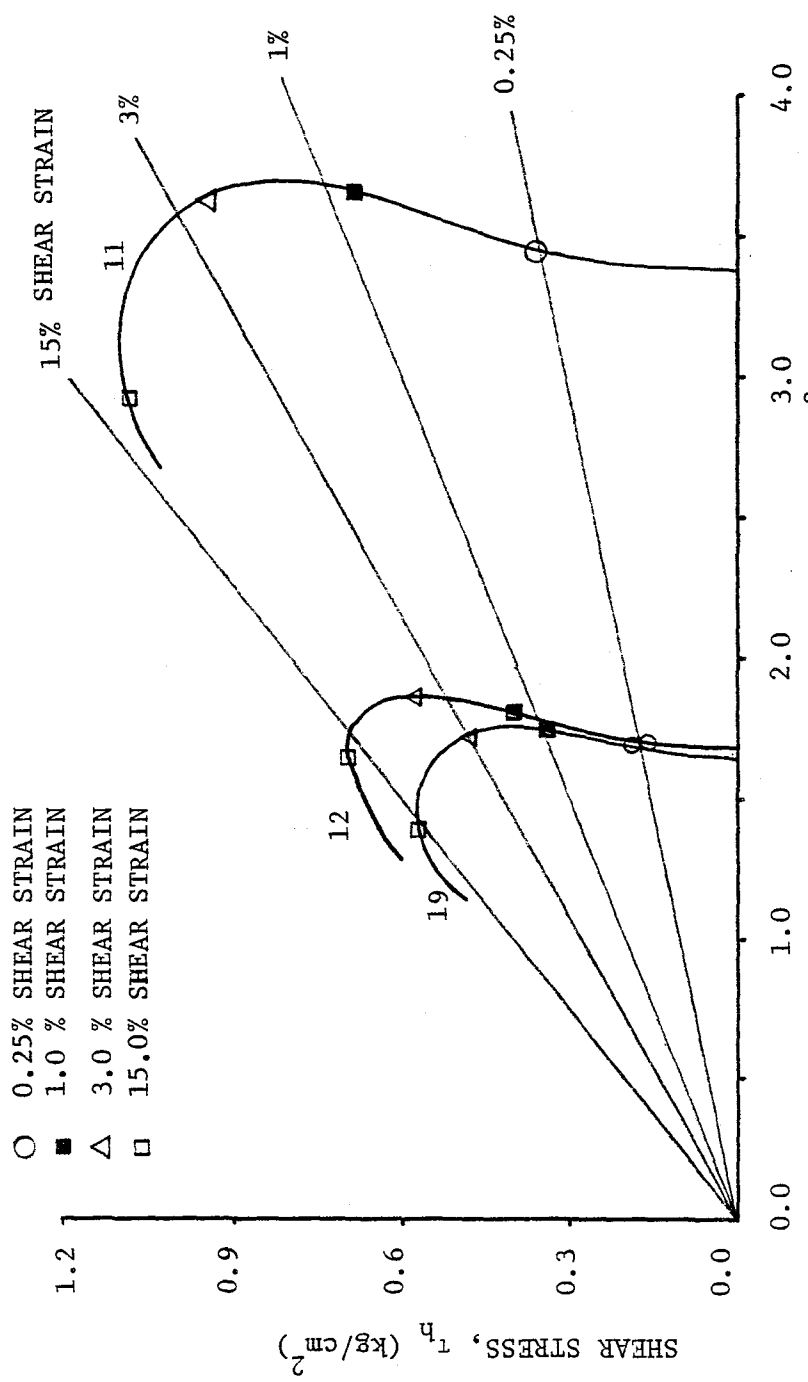

FIGURE 7.45. STRESS PATHS (τ_h VERSUS $\bar{\sigma}_v$) FOR STATIC TESTS - LIGHTLY OVERCONSOLIDATED CONCORD BLUE CLAY. STRAIN CONTOURS ARE ALSO SHOWN.

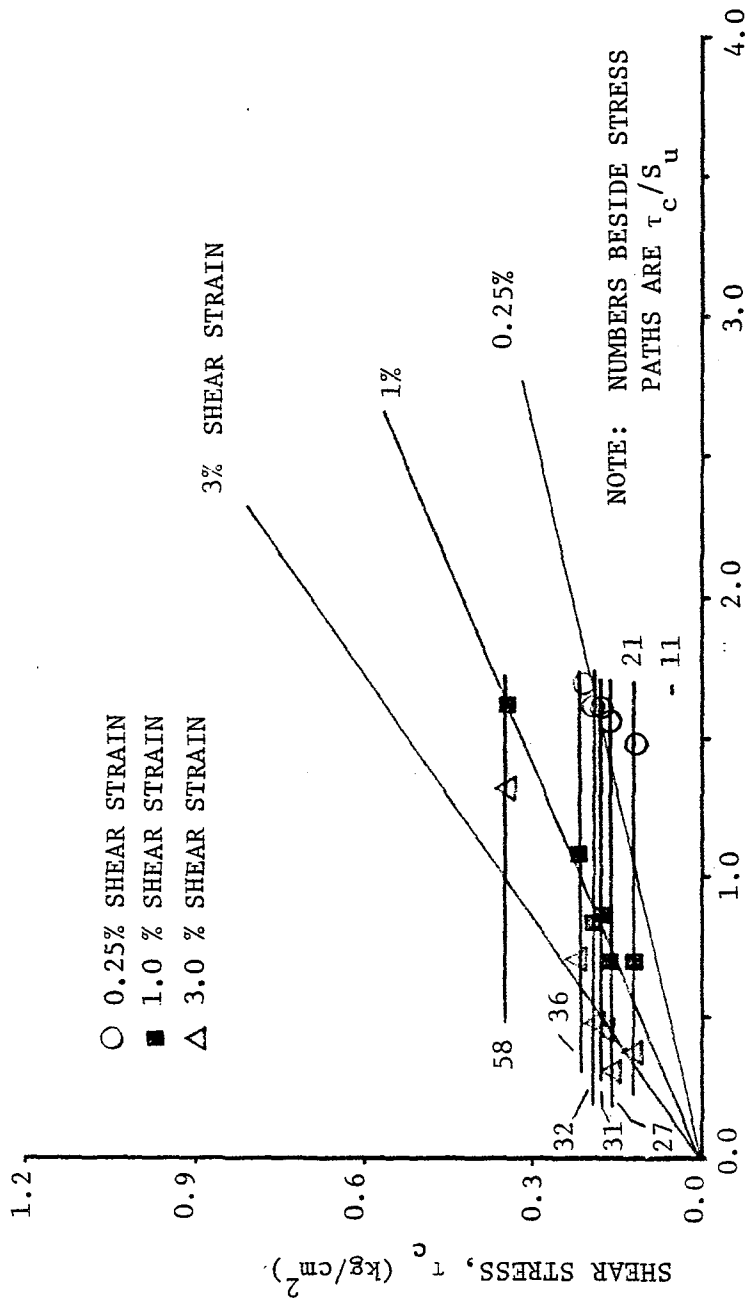

FIGURE 7.46. STRESS PATHS (τ_c VERSUS $\bar{\sigma}_v$) FOR CYCLIC LOADING TESTS - LIGHTLY OVERCONSOLIDATED CONCORD BLUE CLAY. STRAIN CONTOURS ARE ALSO SHOWN

The values of $(\phi)_c$ are consistently higher than the values of ϕ, especially at large shear strains. This trend was also found for the normally consolidated Concord Blue clay. For the static tests, the mobilized angle of internal friction, ϕ, is approximately the same for both the normally consolidated and lightly overconsolidated Concord Blue clay (at the same shear strains).

PART 8

DISCUSSION

An understanding of the behavior of fine grained soils subjected to cyclic loading has become important for the modern geotechnical engineer. The importance of laboratory testing and research on the cyclic loading behavior of soils was stressed at a recent workshop on "Research Needs and Priorities for Geotechnical Earthquake Engineering Applications" held at Austin, Texas (83).

A major portion of this research deals with the analysis of static and cyclic loading direct simple shear tests, using the additional information provided by lateral stress measurements. The lateral stresses were measured by means of calibrated wire reinforced rubber membranes. Prior to this study, the lateral stresses acting on direct simple shear samples have seldom been measured. For example, Roscoe, et al (87), using the Cambridge simple shear device, have measured the lateral stresses in sands during static shear. Youd (117) has used NGI calibrated membranes to measure lateral stresses in sand samples during cyclic loading.

The analysis of the static and cyclic loading tests in which lateral stresses were measured was based on the following assumptions:

1. The stress conditions existing in the central part of the sample are reasonably uniform and representative of the stresses imposed on the boundaries of the sample.
2. The shear stresses acting on the sides of an infinitesimal element of soil at the center of the sample are equal in magnitude to the applied horizontal shear stress.
3. A constant volume direct simple shear test is equivalent to an undrained direct simple shear test. The change in vertical stress necessary to maintain a constant sample volume during shear is equated to the excess pore pressure that would have developed in an undrained test.

The results and conclusions obtained from the tests with lateral stress measurements are dependent on the assumptions made about the state of stress within the soil sample. Since stress nonuniformities tend to increase with increasing shear strain (46), it will be assumed that the numerical results obtained are reasonably accurate for small shear strains (say, less than three percent). Only the general observed trends should be recognized for larger shear strains. From a practical viewpoint, a shear strain of three percent constitutes failure for most geotechnical engineering applications, and the behavior of soils at larger shear strains is relatively unimportant.

The calibrated wire reinforced rubber membrane provides a convenient method to determine, experimentally, the coefficient of lateral stress

at rest. For the Gulf of Alaska clay, the measured value of K_o agrees well with empirical values of K_o.

For the tests in which lateral stresses were measured, sufficient information is available to determine Mohr's circle of stress for a soil element at the center of the sample. On the basis of Mohr's circle analysis, various information was obtained about the state of stress within the sample during shear (for example, the magnitude and orientation of the principal stresses).

For direct simple shear tests, it is conventionally assumed that the horizontal plane of the sample is the plane of maximum obliquity, and the mobilized angle of internal friction, ϕ, is computed from Equation 7.9:

$$\phi = \tan^{-1} (\tau_h/\bar{\sigma}_v) \qquad 8.1$$

Alternatively, the mobilized angle of internal friction, ϕ_m, can be computed from $q - \bar{p}$ data:

$$\phi_m = \sin^{-1} (q/\bar{p}) \qquad 8.2$$

For the static tests performed on the Gulf of Alaska clay, it was found that ϕ_m is greater than ϕ, and at large shear strains (15%), the difference between the two is approximately 7°. It is of practical significance to determine how these two angles of internal friction compare with triaxial test results. However, there is insufficient data to make any definite conclusions.

Static and cyclic loading test data were plotted as stress paths (both τ versus $\overline{\sigma}_v$ and $q - \overline{p}$) in this report. Strain contours, approximated by straight lines passing through the origin, were determined for these stress paths. It is of practical significance to determine whether the strain contours for the static and the cyclic loading tests are the same. To facilitate this comparison, the strain contours were represented by the mobilized angle of internal friction, which is directly related to the inclination of the strain contour.

Therefore, the mobilized angle of internal friction was computed for both the static tests and the cyclic tests at several shear strain levels, and the results were compared. For the Gulf of Alaska clay, it was found that the strain contours for the static and cyclic tests were approximately the same, except at large shear strains. For Concord Blue clay, the discrepancy between the two is somewhat larger, especially at large shear strains.

The cyclic loading strength of soils is commonly expressed as the number of cycles to failure (specified by a cyclic shear strain). This relationship is summarized in Figure 8.1 for the Gulf of Alaska clay and Concord Blue clay (failure equals three percent shear strain). The critical level of repeated loading (93) can also be determined from

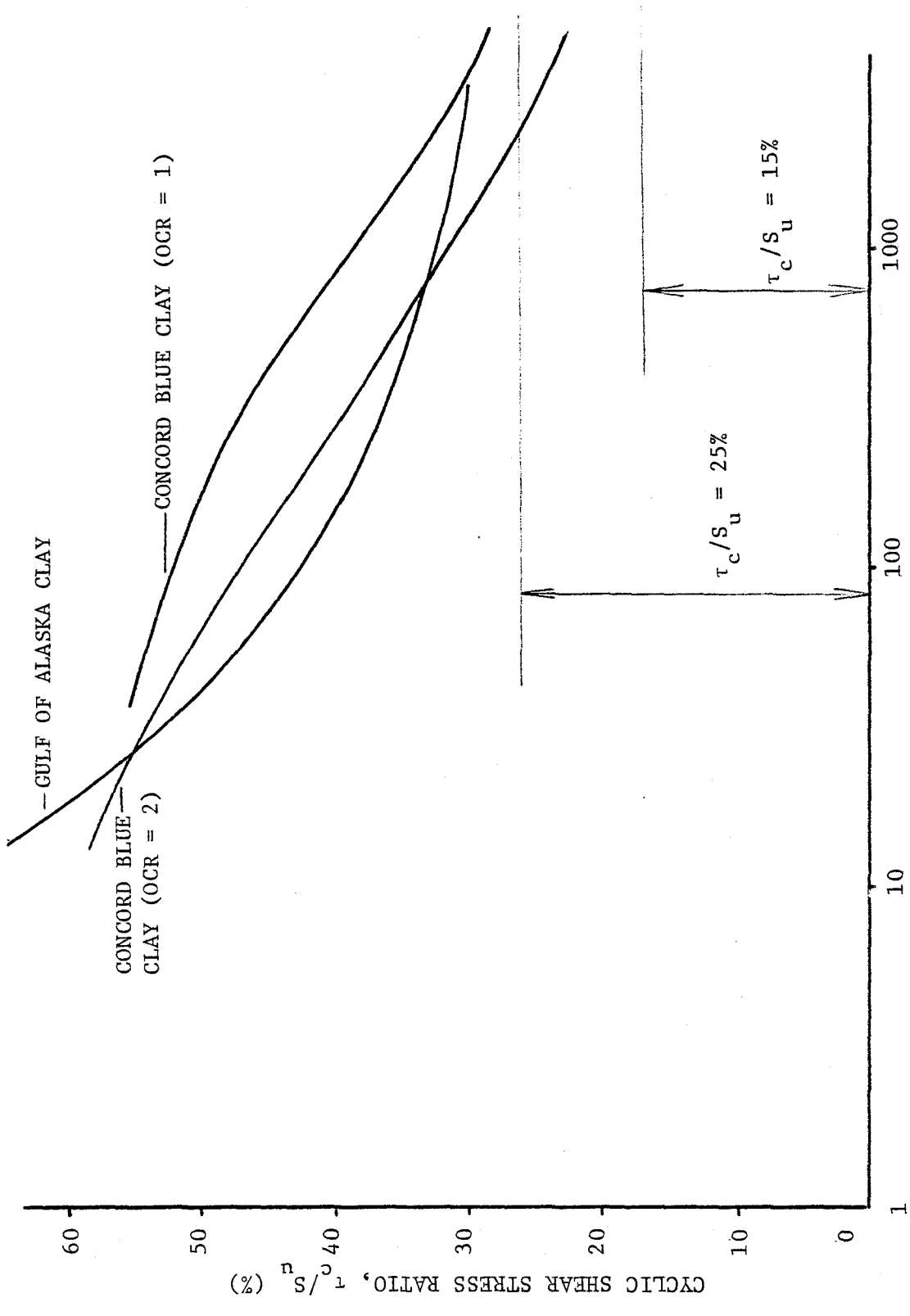

FIGURE 8.1. NUMBER OF CYCLES TO 3.0 PERCENT SHEAR STRAIN — SUMMARY PLOT

this figure, as shown. For both the Gulf of Alaska clay and the normally consolidated Concord Blue clay, the critical level of repeated loading is approximately 25 percent of the peak static undrained shear strength. For the lightly overconsolidated Concord Blue clay (OCR = 2), the critical level of repeated loading is approximately 15 percent.

Lee and Focht (67) summarized triaxial and direct simple shear cyclic loading strength data (τ_c/S_u versus number of cycles to failure) for a wide variety of clays. All data presented are for two-directional loading, with symmetric stress reversal. It can be inferred from this data that the critical level of repeated loading varies between approximately 10 and 50 percent. For cyclic loading without stress reversal, the critical level of repeated loading is typically larger, with values between 50 and 100 percent (13,64,93).

For the cyclic loading tests, it was observed that when the normalized pore pressure ($u/\bar{\sigma}_{vo}$) in the sample approaches a value of approximately 0.4, the rate of pore pressure generation (per cycle) accelerates, and failure occurs with further cyclic loading. As long as the normalized pore pressure is less than this critical value of 0.4, the rate of pore pressure generation tends to decrease with increasing number of loading cycles. Therefore, it appears that there is a fundamental difference in the behavior of the soil sample depending on whether the normalized pore pressure is greater or less than approximately 0.4.

In this report, the data for the cyclic loading tests were presented as a function of number of loading cycles, whereas the data for the static tests were presented as a function of shear strain. A better comparison can be made between the cyclic test data and the static test data if the data are compared at the same shear strain. Such a comparison is made for the Gulf of Alaska clay in Appendix B. In Tables B.1 through B.6, the test data are compared at 0.25, 0.50, 1.0, 2.0, 3.0, and 15.0 percent shear strain.

PART 9

SUMMARY AND CONCLUSIONS

This report presents the results of a series of consolidated constant volume (CCV) direct simple shear tests performed on two undisturbed clays: Concord Blue clay and a Gulf of Alaska clay. The Norwegian Geotechnical Institute direct simple shear device was used for all tests. Both static and cyclic tests were performed. Emphasis was placed on high strain level cyclic loading, such as that caused by earthquakes and storm waves.

Testing errors that are inherent to the NGI direct simple shear device were evaluated. It was found that two testing errors can have a significant effect on the test results:

1. False (vertical) deformation
2. Secondary consolidation or creep

Methods to correct for these errors are presented in Part 4. All tests were corrected for both false deformation and creep.

A series of nine tests were performed on undisturbed clay samples from the Copper River prodelta in the Gulf of Alaska. The Gulf of Alaska is in an area of intense seismic activity; storms with large waves are also common. Since petroleum related activities in the Gulf of Alaska region may stimulate major marine construction in this area, it is important to evaluate the static and cyclic loading behavior of these soils.

All test results for the Gulf of Alaska clay include lateral stress measurements that were taken during consolidation and shear. From the lateral stress measurements that were taken during consolidation, the coefficient of lateral stress at rest, K_o, was determined to be 0.54. The additional data provided by the lateral stress measurements that were taken during shear add to the knowledge of the stress conditions existing in the soil sample.

From the results of the static tests that were performed on the Gulf of Alaska clay, it was concluded that:

1. The pore pressure increases throughout each test; therefore, the vertical normal effective stress decreases during the test.

2. The horizontal normal effective stress remains approximately constant throughout each test, but the horizontal total stress increases.

3. The coefficient of lateral stress, $K = \bar{\sigma}_h/\bar{\sigma}_v$, increases throughout each test, and at large shear strains, K approaches a value of unity.

4. The principal stress ratio, $R = \bar{\sigma}_3/\bar{\sigma}_1$, decreases throughout each test.

5. At large shear strains, the horizontal plane of the sample is approximately the plane on which the maximum shear stress acts. Roscoe, et al (87), have found similar results for sands.

6. The horizontal plane of the sample is never the plane of maximum obliquity at any time during the test. Roscoe, et al (87), have found similar results for sands.

7. The mobilized angle of internal friction determined from Mohr's circle, $\phi_m = \sin^{-1}(q/\bar{p})$, is greater than the conventional mobilized friction angle, $\phi = \tan^{-1}(\tau_h/\bar{\sigma}_v)$. At large shear strains the difference between ϕ_m and ϕ is approximately 7°.

For the Gulf of Alaska clay, it was concluded from the cyclic loading test results that:

1. Cyclic shear strains increase gradually until failure is imminent, after which they increase very rapidly.

2. Cyclic loading failure does not occur if the cyclic shear stress is small. The critical level of repeated loading (93) is approximately 25 percent of the peak static undrained shear strength.

3. Both the vertical and the horizontal normal effective stresses decrease throughout each test.

4. The coefficient of lateral stress increases throughout each test, and it approaches a value of unity as the cyclic shear strain increases.

5. The principal stress ratio, R, decreases throughout each test.

6. At large shear strains, the horizontal plane of the sample is approximately the plane on which the maximum shear stress acts. The horizontal plane is never the plane of maximum obliquity at any time during the test.

7. The mobilized angle of internal friction for cyclic loading is virtually identical to the mobilized friction angle for the static tests, except at large shear strains. This implies that the strain contours determined from the static tests are identical to the strain contours determined from the cyclic tests.

The static and cyclic loading behavior of Concord Blue clay was also investigated. Both normally consolidated and lightly overconsolidated (OCR = 2) samples were tested. Lateral stress measurements were not taken for these tests. It was concluded that:

1. For the normally consolidated samples, the critical level of repeated loading is approximately 25 percent of the peak static undrained shear strength.

2. For the lightly overconsolidated samples, the critical level of repeated loading is approximately 15 percent of the peak static undrained shear strength.

3. The concept of non-failure equilibrium (112) is valid for a large number (6000) of loading cycles.

4. The mobilized angle of internal friction for cyclic loading is consistently higher than the mobilized friction angle for the static tests, especially at large shear strains. Because of this discrepancy, the strain contours for the static tests and the cyclic tests do not coincide.

PART 10

RECOMMENDATIONS FOR FURTHER STUDY

The measurement of lateral stresses acting on the NGI direct simple shear soil sample adds considerably to the knowledge of the stress conditions existing in the soil sample. However, it is not an easy task to measure the lateral stresses, largely because of the shortcomings of the calibrated reinforced rubber membranes.

It is of practical importance to eliminate the problems associated with the calibrated membranes, so that they can be regularly used on a routine basis.

If lateral stresses are measured, the angle of internal friction can be determined in two ways:

1. On the basis of the assumption that the horizontal plane is the plane of maximum obliquity
2. On the basis of Mohr's circle

From a practical viewpoint, it is important to determine how these two friction angles correlate with triaxial data. Further research is needed to answer this question.

The critical level of repeated loading is an important parameter determined from cyclic loading tests. From published data, it can be seen that the critical level of repeated loading varies over a wide range. It is of interest to find if there are any correlations between the critical level of repeated loading and soil parameters, such as plasticity

index, sensitivity, and void ratio. The relationship between the critical level of repeated loading and overconsolidation ratio should also be found.

The number of cycles to failure (specified by a cyclic shear strain) is also an important parameter determined from cyclic loading tests. The random nature of this parameter should be investigated. For example, the number of cycles to failure could be modeled by a Weibull probability distribution function, as is frequently done for fatigue studies of metals.

For the cyclic loading tests, it was observed that when the normalized pore pressure ($u/\bar{\sigma}_{vo}$) in the sample approaches a value of approximately 0.4, the rate of pore pressure generation (per cycle) accelerates, and failure occurs with further cyclic loading. This critical pore pressure may be a fundamental parameter in understanding the cyclic loading behavior of fine grained soils. Its significance should be investigated.

PART 11

REFERENCES

1. Alpan, I. (1967), "The Empirical Evaluation of the Coefficient K_o and K_{or}", Soil and Foundation, The Japanese Society of Soil Mech. and Found. Eng., Vol. 7, No. 1, pp. 31-40.

2. Andersen, K.H. (1976), "Behaviour of Clay Subjected to Undrained Cyclic Loading", Proc., International Conf. on the Behaviour of Off-Shore Structures, Norwegian Institute of Technology, Trondheim, Vol. 1, pp. 392-403.

3. Andersen, K.H. et al (1976), "Effect of Cyclic Loading on Clay Behaviour", Proc., Conf. on Design and Construction of Offshore Structures, London. Also published in: Norwegian Geotechnical Institute, Publication 113, Oslo, pp. 1-6.

4. Anderson, D.G. and Richart, F.E., Jr. (1976), "Effects of Straining on Shear Modulus of Clays", J. Geotechnical Eng. Div., ASCE, Vol. 102, No. GT9, pp. 975-987.

5. Anderson, D.G. and Woods, R.D. (1976), "Time-Dependent Increase in Shear Modulus of Clay", J. Geotechnical Eng. Div., ASCE, Vol. 102, No. GT5, pp. 525-537.

6. Arango, I. and Seed, H.B. (1974), "Seismic Stability and Deformation of Clay Slopes", J. Geotechnical Eng. Div., ASCE, Vol. 100, No. GT2, pp. 139-156.

7. Berre, T. (1979), Personal Communication, Norwegian Geotechnical Institute, Oslo.

8. Berre, T. (1978), Personal Communication, Norwegian Geotechnical Institute, Oslo.

9. Bishop, A.W. and Henkel, D.J. (1962), The Measurement of Soil Properties in the Triaxial Test, Edward Arnold Ltd., London.

10. Bjerrum, L. and Landva, A. (1966), "Direct Simple Shear Tests on a Norwegian Quick Clay", Geotechnique, Vol. 16, No. 1, pp. 1-20.

11. Brooker, E.W. and Ireland, H.O. (1965), "Earth Pressures at Rest Related to Stress History", Canadian Geotechnical Journal, Vol. 11, No. 1, pp. 1-15.

12. Brown, S.F., Andersen, K.H., and McElvaney, J. (1977), "The Effect of Drainage on Cyclic Loading of Clay", Proc., 9th ICSMFE, Tokyo, Vol. 2, pp. 195-200.

13. Brown, S.F., Lashine, A.K.F., and Hyde, A.F.L. (1975), "Repeated Load Triaxial Testing of a Silty Clay", Geotechnique, Vol. 25, No. 1, pp. 95-114.

14. Carlson, P.R. (1976), "Submarine Faults and Slides that Disrupt Surficial Sedimentary Units, Northern Gulf of Alaska", U.S. Geological Survey, Open File Report 76-294, Menlo Park, California.

15. Castro, G. (1975), "Liquefaction and Cyclic Mobility of Saturated Sands", J. Geotechnical Eng. Div., ASCE, Vol. 101, No. GT6, pp. 551-569.

16. Danielsen, E.F., Burt, W.V., and Rattray, M., Jr. (1957), "Intensity and Frequency of Severe Storms in the Gulf of Alaska", Transactions, American Geophysical Union, Vol. 38, No. 1, pp. 44-49.

17. De Alba, P., Seed, H.B., and Chan, C.K. (1976), "Sand Liquefaction in Large-Scale Simple Shear Tests", J. Geotechnical Eng. Div., ASCE, Vol. 102, No. GT9, pp. 909-927.

18. Duncan, J.M. and Dunlop, P. (1969), "Behavior of Soils in Simple Shear Tests", Proc., 7th ICSMFE, Mexico City, Vol. 1, pp. 101-109.

19. Egan, J.A. and Sangrey, D.A. (1978), "Critical State Model for Cyclic Load Pore Pressure", Proc., Earthquake Engineering and Soil Dynamics, ASCE Specialty Conf., Pasadena, Vol. 1, pp. 410-424.

20. Eide, O. (1974), "Marine Soil Mechanics - Applications to North Sea Offshore Structures", Proc., Offshore North Sea Technology Conf. and Exhibition, Stavanger. Also published in: Norwegian Geotechnical Institute, Publication 103, Oslo, pp. 1-20.

21. Esrig, M.I., Kirby, R.C., Bea, R.G., and Murphy, B.S. (1977), "Initial Development of a General Effective Stress Method for the Prediction of Axial Capacity for Driven Piles in Clay", Proc., 9th Offshore Technology Conf., Houston, pp. 495-506.

22. Esrig, M.I., Ladd, R.S., and Bea, R.G. (1975), "Material Properties of Submarine Mississippi Delta Sediments Under Simulated Wave Loadings", Proc., 7th Offshore Technology Conf., Houston, OTC 2188, pp. 399-411.

23. Ferritto, J.M. and Forrest, J.B. (1977), "Siting Structures in Seismic Liquefaction Areas", Proc., 9th ICSMFE, Toyko, Vol. 2, pp. 225-229.

24. Finn, W.D.L. (1972), "Soil Dynamics - Liquefaction of Sands", Proc., International Conf. on Microzonation, Seattle, Vol. 1, pp. 87-111.

25. Finn, W.D.L., Emery, J.J., and Gupta, Y.P. (1971), "Liquefaction of Large Samples of Saturated Sand on a Shaking Table", Proc. 1st Canadian Conf. on Earthquake Engineering, Vancouver, pp. 97-110.

26. Finn, W.D.L., Lee, K.W., and Martin, G.R. (1976), "An Effective Stress Model for Liquefaction", Liquefaction Problems in Geotechnical Engineering, ASCE National Convention, Philadelphia, pp. 169-198.

27. Finn, W.D.L., Pickering, D.J., and Bransby, P.L. (1971), "Sand Liquefaction in Triaxial and Simple Shear Tests", J. Soil Mech. and Found. Div., ASCE, Vol. 97, No. SM4, pp. 639-659.

28. Fischer, J.A., Koutsoftas, D.C., and Lu, T.D. (1976), "The Behaviour of Marine Soils under Cyclic Loading", Proc., International Conf. on the Behaviour of Off-Shore Structures, Norwegian Institute of Technology, Trondheim, Vol. 2, 407-417.

29. Foss, I., Dahlberg, R., and Kvalstad, T. (1978), "Foundation Design for Gravity Structures with Respect to Failure in Cyclic Loading", Proc., 10th Offshore Technology Conf., Houston, OTC 3114, pp. 535-545.

30. France, J.W. and Sangrey, D.A. (1977), "Effects of Drainage in Repeated Loading of Clays", J. Geotechnical Eng. Div., ASCE, Vol. 103, No. GT7, pp. 769-785.

31. Geonor (1968), "Description and Instruction for Use of Direct Simple-Shear Apparatus Model h-12", Geonor A/S, Oslo.

32. Gibson, R.E. (1958), "The Progress of Consolidation in a Clay Layer Increasing in Thickness with Time", Geotechnique, Vol. 8, No. 4, pp. 171-182.

33. Green, P.A. and Ferguson, P.A.S. (1971), "On Liquefaction Phenomena, by Professor A. Casagrande: Report of Lecture", Geotechnique, Vol. 21, No. 3, pp. 197-202.

34. Hamilton, E.L. (1971), "Elastic Properties of Marine Sediments", Journal of Geophysical Research, American Geophysical Union, Vol. 76, No. 2, pp. 579-604.

35. Hampton, M.A., et al (1978), "Quantitative Study of Slope Instability in the Gulf of Alaska", Proc., 10th Offshore Technology Conf., Houston, OTC 3314, pp. 2307-2318.

36. Hara, A. and Kiyota, Y. (1977), "Dynamic Shear Tests of Soils for Seismic Analyses", Proc., 9th ICSMFE, Toyko, Vol. 2, pp. 247-250.

37. Hardin, B.O. (1978), "The Nature of Stress-Strain Behavior for Soils", Proc., Earthquake Engineering and Soil Dynamics, ASCE Specialty Conf., Pasadena, Vol. 1, pp. 3-90.

38. Hardin, B.O. and Black, W.L. (1968), "Vibration Modulus of Normally Consolidated Clay", J. Soil Mech. and Found. Div., ASCE, Vol. 94, No. SM2, pp. 353-369.

39. Hardin, B.O. and Drnevich, V.P. (1972), "Shear Modulus and Damping in Soils: Measurement and Parameter Effects", J. Soil Mech. and Found. Div., ASCE, Vol. 98, No. SM6, pp. 603-624.

40. Hardin, B.O. and Drnevich, V.P. (1972), "Shear Modulus and Damping in Soils: Design Equations and Curves", J. Soil Mech. and Found. Div., ASCE, Vol. 98, No. SM7, 667-692.

41. Harr, M.E. (1977), Mechanics of Particulate Media, McGraw-Hill, Inc.

42. Herrmann, H.G. and Houston, W.N. (1976), "Response of Seafloor Soils to Combined Static and Cyclic Loading", Proc., 8th Offshore Technology Conf., Houston, OTC 2428, pp. 53-60.

43. Höeg, K. (1976), "Foundation Engineering for Fixed Offshore Structures", Proc., International Conf. on the Behaviour of Off-Shore Structures, Norwegian Institute of Technology, Trondheim, Vol. 1, pp. 39-69.

44. Holzer, T.L., Höeg, K., and Arulanandan, K. (1973), "Excess Pore Pressures During Undrainded Clay Creep", Canadian Geotechnical Journal, Vol. 10, No. 1, pp. 12-24.

45. Humphries, W.K. and Wahls, H.E. (1968), "Stress History Effects on Dynamic Modulus of Clay", J. Soil Mech. and Found. Div., ASCE, Vol. 94, No. SM2, pp. 371-389.

46. Hvorslev, M.J. and Kaufman, R.I. (1952), "Torsion Shear Apparatus and Testing Procedures", Waterways Experiment Station, Bulletin No. 38, Vicksburg.

47. Idriss, I.M., Dobry, R., Doyle, E.H., and Singh, R.D. (1976), "Behavior of Soft Clays Under Earthquake Loading Conditions", Proc., 8th Offshore Technology Conf., Houston, OTC 2671, pp. 605-616.

48. Idriss, I.M., Dobry, R., and Power, M.S. (1976), "Soil-Response Considerations in Seismic Design of Offshore Platforms", Journal of Petroleum Technology, March, pp. 244-252.

49. Ishibashi, I. and Sherif, M.A. (1974), "Soil Liquefaction by Torsional Simple Shear Device", J. Geotechnical Eng. Div., ASCE, Vol. 100, No. GT8, pp. 871-888.

50. Ishihara, K., Iwamoto, S., Yasuda, S., and Takatsu, H. (1977), "Liquefaction of Anisotropically Consolidated Sand", Proc., 9th ICSMFE, Tokyo, Vol. 2, pp. 261-264.

51. Kirby, R.C. and Wroth, C.P. (1977), "Application of Critical State Soil Mechanics to the Prediction of Axial Capacity for Driven Piles in Clay", Proc., 9th Offshore Technology Conf., Houston, pp. 483-494.

52. Kirkpatrick, W.M., Seals R.K., and Newman, F.B. (1974), "Stress Distributions in Triaxial Compression Samples", J. Geotechnical Eng. Div., ASCE, Vol. 100, No. GT2, pp. 190-196.

53. Kjellman, W. (1951), "Testing the Shear Strength of Clay in Sweden", Geotechnique, Vol. 2, No. 3, pp. 225-235.

54. Kovacs, W. D., Seed, H.B., and Idriss, I.M. (1971), "Studies of Seismic Response of Clay Banks", J. Soil Mech. and Found. Div., ASCE, Vol. 97, No. SM2, pp. 441-455.

55. Krizek, R.J. (1971), "Rheologic Behavior of Clay Soils Subjected to Dynamic Loads", Transactions, Society of Rheology, Vol. 15, No. 3, pp. 433-489.

56. Krizek, R.J., Ansal, A.M., and Bazant, Z.P. (1978), "Constitutive Equation for Cyclic Behavior of Cohesive Soils", Proc., Earthquake Engineering and Soil Dynamics, ASCE Specialty Conf., Pasadena, Vol. 1, pp. 557-568.

57. Kuribayashi, E. and Tatsuoka, F. (1975), "Brief Review of Liquefaction During Earthquakes in Japan", Soils and Foundations, The Japanese Society of Soil Mech. and Found. Eng., Vol. 15, No. 4, pp. 81-92.

58. Kvenvolden, K.A., Redden, G.D., and Carlson, P.R. (1977), "Hydrocarbon Gases in Sediments of Eastern Gulf of Alaska", American Association of Petroleum Geol. Bull., Vol. 61, p. 806.

59. Ladd, C.C. and Edgers, L. (1972), "Consolidated-Undrained Direct-Simple Shear Tests on Saturated Clays", Soils Publication No. 284, Dept. of Civil Engineering, Massachusetts Institute of Technology, Cambridge, Ma.

60. Ladd, C.C. and Foott, R. (1974), "New Design Procedure for Stability of Soft Clays", J. Geotechnical Eng. Div., ASCE, Vol. 100, No. GT7, pp. 763-786.

61. Lambe, T.W. and Whitman, R.V. (1969), Soil Mechanics, John Wiley and Sons, Inc.

62. Landva, A. (1964), "Equipment for Cutting and Mounting Undisturbed Specimens of Clay in Testing Devices", Norwegian Geotechnical Institute, Publication 56, Oslo, pp. 1-5.

63. Larew, H.G. and Leonards, G.A. (1962), "A Strength Criterion for Repeated Loads", Proc., Highway Research Board, Vol. 41, pp. 529-556.

64. Lashine, A.K.F. (1973), "Deformation Characteristics of a Silty Clay Under Repeated Loading", Proc., 8th ICSMFE, Moscow, Vol. 1.1, pp. 237-244.

65. Lee, K.L. (1976), "Fundamental Considerations for Cyclic Triaxial Tests on Saturated Sand", Proc., International Conf. on the Behaviour of Off-Shore Structures, Norwegian Institute of Technology, Trondheim, Vol. 1, pp. 355-373.

66. Lee, K.L. and Fitton, J.A. (1969), "Factors Affecting the Cyclic Loading Strength of Soil", Vibration Effects of Earthquakes on Soils and Foundations, ASTM, STP 450, pp. 71-95.

67. Lee, K.L. and Focht, J.A. (1976), "Strength of Clay Subjected to Cyclic Loading", Marine Geotechnology, Vol. 1, No. 3, pp. 165-185.

68. Lucks, A.S., Christian, J.T., Brandow, G.E., and Höeg, K. (1972), "Stress Conditions in NGI Simple Shear Test", J. Soil Mech. and Found. Div., ASCE, Vol. 98, No. SM1, pp. 155-160.

69. Mitchell, R.J. and King, R.D. (1977), "Cyclic Loading of an Ottawa Area Champlain Sea Clay", Canadian Geotechnical Journal, Vol. 14, No. 1, pp. 52-63.

70. Mitchell, R.J., Tsui, K.K., and Sangrey, D.A. (1973), "Failure of Submarine Slopes Under Wave Action", Proc., 13th International Conf. on Coastal Eng., Vol. 1.

71. Morgenstern, N.R. and Sangrey, D.A. (1978), "Methods of Stability Analysis", Landslides: Analysis and Control, Transportation Research Board, Washington, D.C., Chpt. 7.

72. Motherwell, J.T. and Wright, S.G. (1978), "Ocean Wave Load Effects on Soft Clay Behavior", Proc., Earthquake Engineering and Soil Dynamics, ASCE Specialty Conf., Pasadena, Vol. 2, pp. 620-635.

73. Norwegian Geotechnical Institute (1975), "Research Project, Repeated Loading on Clay: Summary and Interpretation of Test Results", Oslo.

74. Ogawa, S., Shibayama, T., and Yamaguchi, H. (1977), "Dynamic Strength of Saturated Cohesive Soil", Proc., 9th ICSMFE, Toyko, Vol. 2, pp. 317-320.

75. Park, T.K. and Silver, M.L. (1975), "Dynamic Triaxial and Simple Shear Behavior of Sand", J. Geotechnical Eng. Div., ASCE, Vol. 101, No. GT6, pp. 513-529.

76. Pender, M.J. (1977), "Modelling Soil Behavior under Cyclic Loading", Proc., 9th ICSMFE, Tokyo, Vol. 2, pp. 325-331.

77. Perloff, W.H. and Baron, W. (1976), Soil Mechanics-Principles and Applications, Ronald Press Co., New York.

78. Prevost, J.H. (1977), "Mathematical Modelling of Monotonic and Cyclic Undrained Clay Behaviour", International Journal for Numerical and Analytical Methods in Geomechanics", Vol. 1, pp. 195-216.

79. Prevost, J.H. and Höeg, K. (1976), "Reanalysis of Simple Shear Soil Testing", Canadian Geotechnical Journal, Vol. 13, No. 4, pp. 418-429.

80. Prevost, J.H. and Hughes, T.J.R. (1978), "Mathematical Modeling of Cyclic Soil Behavior", Proc., Earthquake Engineering and Soil Dynamics, ASCE Specialty Conf., Pasadena, Vol. 2, pp. 746-761.

81. Pyke, R., Seed, H.B., and Chan, C.K. (1975), "Settlement of Sands Under Multidirectional Shaking", J. Geotechnical Eng. Div., ASCE, Vol. 101, No. GT4, pp. 379-398.

82. Reimnitz, E. (1972), "Effects in the Cooper River Delta", The Great Alaskan Earthquake of 1964: Oceanography and Coastal Engineering, National Academy of Sciences, Washington, D.C., pp. 290-302.

83. "Research Needs and Priorities for Geotechnical Earthquake Engineering Applications" (1978), Report of Workshop, Univ. of Texas, Austin, prepared for the National Science Foundation.

84. Richart, F.E., Jr. (1975), "Some Effects of Dynamic Soil Properties on Soil-Structure Interaction", J. Geotechnical Eng. Div., ASCE, Vol. 101, No. GT12, pp. 1193-1240.

85. Richart, F.E., Jr., Hall, J.R., Jr., and Woods, R.D. (1970), Vibrations of Soils and Foundations, Prentice Hall, Inc.

86. Roscoe, K.H. (1953), "An Apparatus for the Application of Simple Shear to Soil Samples", Proc., 3rd ICSMFE, Zurich, Vol. 1, pp. 186-191.

87. Roscoe, K.H., Bassett, R.H., and Cole, E.R.L. (1967), "Principle Axes Observed During Simple Shear of a Sand", Proc., Geotechnical Conference, Oslo, Vol. 1, pp. 231-237.

88. Rowe, P.W., Craig, W.H., and Procter, D.C. (1976), "Model Studies of Offshore Gravity Structures Founded on Clay", Proc., International Conf. on the Behaviour of Off-Shore Structures, Norwegian Institute of Technology, Trondheim, Vol. 1, pp. 439-448.

89. Saada, A.S., Bianchini, G.F., and Shook, L.P. (1978), "The Dynamic Response of Anisotropic Clay", Proc., Earthquake Engineering and Soil Dynamics, ASCE Specialty Conf., Pasadena, Vol. 2, pp. 777-801.

90. Sangrey, D.A. (1977), "Marine Geotechnology - State of the Art", Marine Geotechnology, Vol. 2, pp. 45-80.

91. Sangrey, D.A. (1977), "Response of Offshore Piles to Cyclic Loading", Proc., 9th Offshore Technology Conf., Houston, OTC 2944, pp. 507-512.

92. Sangrey, D.A. (1971), "Changes in Strength of Soils Under Earthquake and Other Repeated Loading", Proc., 1st Canadian Conference on Earthquake Engineering, Vancouver, pp. 82-96.

93. Sangrey, D.A., Henkel, D.J., and Esrig, M.I. (1969), "The Effective Stress Response of a Saturated Clay Soil to Repeated Loading", Canadian Geotechnical Journal, Vol. 6, No. 3, pp. 241-252.

94. Sangrey, D.A., Pollard, W.S., and Egan, J.A. (1978), "Errors Associated with Rate of Undrained Cyclic Testing of Clay Soils", Dynamic Geotechnical Testing, ASTM, STP 654, pp. 280-294.

95. Seed, H.B. (1976), "Evaluation of Soil Liquefaction Effects on Level Ground During Earthquakes", Liquefaction Problems in Geotechnical Engineering, ASCE National Convention, Philadelphia, pp. 1-104.

96. Seed, H.B. (1968), "Landslides During Earthquakes Due to Soil Liquefaction", J. Soil Mech. and Found. Div., ASCE, Vol. 94, No. SM5, pp. 1053-1122.

97. Seed, H.B. and Chan, C.K. (1966), "Clay Strength Under Earthquake Loading Conditions", J. Soil Mech. and Found. Div., ASCE, Vol. 92, No. SM2, pp. 53-78.

98. Seed, H.B., Chan, C.K., and Monismith, C.L. (1955), "Effects of Repeated Laoding on the Strength and Deformation of Compacted Clay", Proc., Highway Research Board, Vol. 34, pp. 541-558.

99. Seed, H.B. and Idriss, I.M. (1971), "Simplified Procedure for Evaluating Soil Liquefaction Potential", J. Soil Mech. and Found. Div., ASCE, Vol. 97, No. SM9, pp. 1249-1273.

100. Seed, H.B. and Idriss, I.M. (1970), "Soil Moduli and Damping Factors for Dynamic Response Analyses", Earthquake Engineering Research Center, Report EERC 70-10, U. of California, Berkeley.

101. Shen, C.K., Herrmann, L.R., and Sadigh, K. (1978), "Analysis of Cyclic Simple Shear Test Data", Proc., Earthquake Engineering and Soil Dynamics, ASCE Specialty Conf., Pasadena, Vol. 2, pp. 864-874.

102. Sherif, M.A., Ishibashi, I., and Ling, S.C. (1977), "Dynamic Properties of a Marine Sediment", Proc., 9th ICSMFE, Tokyo, Vol. 2, pp. 387-391.

103. Silver, M.L., et al (1976), "Cyclic Triaxial Strength of Standard Test Sand", J. Geotechnical Eng. Div., ASCE, Vol. 102, No. GT5, pp. 511-523.

104. Skoglund, G.R., Marcuson, W.F., III, and Cunny, R.W. (1976), "Evaluation of Resonant Column Test Devices", J. Geotechnical Eng. Div., ASCE, Vol. 102, No. GT11, pp. 1147-1158.

105. Stevens, H.W. (1975), "The Response of Frozen Soils to Vibratory Loads", Technical Report 265, U.S. Army, CRREL, Hanover, N.H., June.

106. Taylor, D.W. (1952), "A Direct Shear Test with Drainage Control", Symposium on Direct Shear Testing of Soils, ASTM, STP 131, pp. 63-74.

107. Taylor, P.W. and Bacchus, D.R. (1969), "Dynamic Cyclic Strain Tests on a Clay", Proc., 7th ICSMFE, Mexico City, Vol. 1, pp. 401-409.

108. Theirs, G.R. and Seed, H.B. (1969), "Strength and Stress-Strain Characteristics of Clays Subjected to Seismic Loading Conditions", Vibration Effects of Earthquakes on Soils and Foundations, ASTM, STP 450, pp. 3-56.

109. Theirs, G.R. and Seed, H.B. (1968), "Cyclic Stress-Strain Characteristics of Clay", J. Soil Mech. and Found. Div., ASCE, Vol. 94, No. SM2, pp. 555-569.

110. Timoshenko, S.P. and Goodier, J.N. (1934), Theory of Elasticity, McGraw-Hill Book Company.

111. Valera, J.E. and Donovan, N.C. (1976), "Comparison of Methods for Liquefaction Evaluation", Liquefaction Problems in Geotechnical Engineering, ASCE National Convention, Philadelphia, pp. 359-388.

112. Vinson, T.S., Chaichanavong, T., and Czajkowski, R.L. (1978), "Behavior of Frozen Clay under Cyclic Axial Loading", J. Geotechnical Eng. Div., ASCE, Vol. 104, No. GT7, pp. 779-800.

113. Wilson, N.E. and Greenwood, J.R. (1974), "Pore Pressure and Strains After Repeated Loading of Saturated Clay", Canadian Geotechnical Journal, Vol. 11, pp. 269-277.

114. Woods, R.D. (1978), "Measurement of Dynamic Soil Properties", Proc., Earthquake Engineering and Soil Dynamics, ASCE Specialty Conf., Pasadena, Vol. 1, pp. 91-178.

115. Wright, D.K., Gilbert, P.A., and Saada, A.S. (1978), "Shear Devices for Determining Dynamic Soil Properties", Proc., Earthquake Engineering and Soil Dynamics, ASCE Specialty Conf., Pasadena, Vol. 2, pp. 1056-1075.

116. Yoshimi, Y. and Oh-Oka, H. (1973), "A Ring Torsion Apparatus for Simple Shear Tests", Proc., 8th ICSMFE, Moscow, Vol. 1.2, pp. 501-506.

117. Youd, T.L. and Craven, T.N. (1975), "Lateral Stress in Sands During Cyclic Loading", J. Geotechnical Eng. Div., ASCE, Vol. 101, No. GT2, pp. 217-221.

APPENDIX A

LIST OF SYMBOLS

A	Area of sample
DR	Dial gauge reading
FS	Factor of Safety
G	Shear Modulus (secant)
H	Height of soil slice
H_i	Initial height of sample
H_f	Final height of sample
K	Coefficient of lateral stress
K_o	Coefficient of lateral stress at rest
N	Number of cycles
N	Normal stress
OCR	Overconsolidation ratio
PI	Plasticity index
R	Principal stress ratio
S	Shear stress
S_t	Sensitivity
S_u	Undrained shear strength
U	Resultant of excess pore pressure on soil slice
W	Effective weight of soil slice
b	Width of soil slice
c	Cohesion
e	Void Ratio

LIST OF SYMBOLS

(CONTINUED)

f	Frequency
i	Slope angle
k	Membrane calibration factor
p	$(\sigma_1 + \sigma_3)/2$
q	$(\sigma_1 - \sigma_3)/2$
r	Microstrain reading
r_i	Initial microstrain reading
t	Time
u_f	Pore pressure at failure (static test)
u_N	Pore pressure at N cycles
w	Water content
γ	Shear Strain
γ'	Bouyant unit weight
γ_f	Shear strain at failure (static test)
γ_N	Shear strain at N cycles
Δu	Pore pressure in excess of hydrostatic
ε_v	Vertical strain
θ_f	Angle between the horizontal plane of the sample and the plane of maximum obliquity

LIST OF SYMBOLS

(CONTINUED)

θ_p Angle between the horizontal plane of the sample and the major principal plane

θ_q Angle between the horizontal plane of the sample and the plane of maximum shear stress

σ_1 Major principal stress

σ_3 Minor principal stress

σ_h Horizontal normal stress

σ_v Vertical normal stress

σ_{vo} Vertical consolidation stress

σ_{vm} Maximum preconsolidation stress

τ Shear stress

τ_c Cyclic shear stress

τ_h Horizontal shear stress

ϕ Angle of internal friction $= \tan^{-1}(\tau/\bar{\sigma}_v)$

ϕ_m Mobilized angle of internal friction $= \sin^{-1}(q/\bar{p})$

Note: A bar over a symbol (e.g., $\bar{\sigma}_v$) denotes an effective stress
A subscript c denotes cyclic loading

APPENDIX B

TEST DATA

In this report, the data for the cyclic loading tests were presented as a function of the number of loading cycles, whereas the data for the static tests were presented as a function of shear strain. A better comparison can be made between the cyclic test data and the static test data if the data are compared at the same shear strain. Such a comparison is made here for the Gulf of Alaska clay. In Tables B.1 through B.6, the test data are compared at shear strains of 0.25, 0.5, 1.0, 2.0, 3.0, and 15.0 percent.

TABLE B1

COMPARISON OF DATA AT 0.25 PERCENT SHEAR STRAIN (GULF OF ALASKA CLAY)

TEST	$\tau_h/\bar{\sigma}_{vo}$	$u/\bar{\sigma}_{vo}$	$\bar{\sigma}_v/\bar{\sigma}_{vo}$	$\bar{\sigma}_h/\bar{\sigma}_{vo}$	$\bar{\sigma}_h/\bar{\sigma}_v$	$\bar{p}$	q	$G/\bar{\sigma}_{vo}$	θ_p	θ_f	θ_q	ϕ_m	$\bar{\sigma}_3/\bar{\sigma}_1$	$\tau_h/\bar{\sigma}_v$
GOA1S	0.117	0.049	0.951	0.540	0.568	0.393	0.125	48.2	14.9	39.4	30.1	18.6	0.516	0.124
GOA2S	0.123	0.081	0.919	0.526	0.572	0.380	0.123	54.0	16.1	38.3	28.9	18.8	0.513	0.135
GOA3S	0.156	0.075	0.925	0.542	0.586	0.188	0.064	64.1	19.5	35.3	25.5	19.6	0.497	0.168
GOA4C	0.089	0.376	0.624	0.395	0.632	0.268	0.077	35.1	18.9	34.3	26.1	16.6	0.556	0.143
GOA5C	0.106	0.328	0.672	0.440	0.655	0.293	0.082	42.2	21.3	32.0	23.7	16.4	0.559	0.158
GOA6C	0.133	0.135	0.865	0.486	0.562	0.356	0.122	55.5	17.6	37.5	27.4	20.0	0.489	0.154
GOA7C	0.159	0.082	0.918	0.543	0.594	0.385	0.130	67.3	20.4	34.4	24.6	19.7	0.496	0.174
GOA8C	0.186	0.022	0.978	0.541	0.554	0.400	0.151	51.6	20.2	35.9	24.8	22.2	0.452	0.190
GOA9S	0.145	0.153	0.847	0.419	0.494	0.334	0.136	55.4	17.0	40.1	28.0	24.2	0.419	0.171

TABLE B2

COMPARISON OF DATA AT 0.50 PERCENT SHEAR STRAIN (GULF OF ALASKA CLAY)

TEST	$\tau_h/\bar{\sigma}_{vo}$	$u/\bar{\sigma}_{vo}$	$\bar{\sigma}_v/\bar{\sigma}_{vo}$	$\bar{\sigma}_h/\bar{\sigma}_{vo}$	$\bar{\sigma}_h/\bar{\sigma}_v$	$\bar{p}$	q	$G/\bar{\sigma}_{vo}$	θ_p	θ_f	θ_q	ϕ_m	$\bar{\sigma}_3/\bar{\sigma}_1$	$\tau_h/\bar{\sigma}_v$
GOA1S	0.157	0.110	0.890	0.526	0.591	0.373	0.127	31.7	20.4	34.5	24.6	19.8	0.492	0.177
GOA2S	0.163	0.128	0.872	0.505	0.579	0.363	0.130	33.2	20.9	34.5	24.1	20.9	0.475	0.188
GOA3S	0.196	0.118	0.882	0.534	0.606	0.182	0.067	41.3	24.1	31.7	20.9	21.7	0.459	0.222
GOA4C	0.089	0.524	0.477	0.319	0.668	0.210	0.063	17.8	24.3	29.6	20.8	17.5	0.539	0.187
GOA5C	0.106	0.492	0.508	0.364	0.717	0.230	0.068	21.1	28.0	26.6	17.0	17.1	0.545	0.209
GOA6C	0.133	0.335	0.665	0.373	0.561	0.274	0.104	26.6	21.1	35.0	23.9	22.3	0.449	0.200
GOA7C	0.159	0.147	0.720	0.516	0.716	0.325	0.100	32.3	28.7	25.2	16.3	17.9	0.531	0.222
GOA8C	0.186	0.154	0.846	0.462	0.547	0.345	0.141	38.5	22.1	35.0	23.0	24.2	0.419	0.221
GOA9S	0.186	0.170	0.830	0.413	0.498	0.327	0.147	39.2	20.9	37.5	24.1	26.8	0.379	0.224

TABLE B3

COMPARISON OF DATA AT 1.0 PERCENT SHEAR STRAIN (GULF OF ALASKA CLAY)

TEST	$\tau_h/\bar{\sigma}_{vo}$	$u/\bar{\sigma}_{vo}$	$\bar{\sigma}_v/\bar{\sigma}_{vo}$	$\bar{\sigma}_h/\bar{\sigma}_{vo}$	$\bar{\sigma}_h/\bar{\sigma}_v$	$\bar{p}$	q	$G/\bar{\sigma}_{vo}$	θ_p	θ_f	θ_q	ϕ_m	$\bar{\sigma}_3/\bar{\sigma}_1$	$\tau_h/\bar{\sigma}_v$
GOA1S	0.190	0.189	0.811	0.499	0.615	0.346	0.129	19.4	25.3	30.7	19.7	22.0	0.453	0.235
GOA2S	0.178	0.194	0.806	0.483	0.599	0.340	0.132	19.6	25.0	31.5	20.0	23.0	0.439	0.239
GOA3S	0.230	0.162	0.838	0.524	0.627	0.175	0.072	23.3	27.9	29.2	17.1	24.1	0.420	0.275
GOA4C	0.089	0.629	0.371	0.266	0.719	0.168	0.055	9.0	29.8	24.7	15.2	18.9	0.510	0.241
GOA5C	0.106	0.579	0.421	0.319	0.758	0.195	0.062	10.6	32.2	22.1	12.8	18.6	0.517	0.252
GOA6C	0.133	0.449	0.551	0.283	0.514	0.220	0.100	13.5	22.4	36.1	22.7	27.0	0.377	0.242
GOA7C	0.159	0.476	0.524	0.432	0.825	0.252	0.087	15.4	37.0	18.2	8.0	20.4	0.485	0.305
GOA8C	0.186	0.371	0.629	0.370	0.588	0.263	0.120	18.6	27.6	30.9	17.4	27.0	0.376	0.296
GOA9S	0.213	0.220	0.780	0.397	0.508	0.310	0.151	21.3	24.0	35.6	21.0	29.1	0.345	0.273

TABLE B4

COMPARISON OF DATA AT 2.0 PERCENT SHEAR STRAIN (GULF OF ALASKA CLAY)

TEST	$\tau_h/\bar{\sigma}_{vo}$	$u/\bar{\sigma}_{vo}$	$\bar{\sigma}_v/\bar{\sigma}_{vo}$	$\bar{\sigma}_h/\bar{\sigma}_{vo}$	$\bar{\sigma}_h/\bar{\sigma}_v$	$\bar{p}$	q	$G/\bar{\sigma}_{vo}$	θ_p	θ_f	θ_q	ϕ_m	$\bar{\sigma}_3/\bar{\sigma}_1$	$\tau_h/\bar{\sigma}_v$
GOA1S	0.209	0.246	0.753	0.481	0.638	0.325	0.131	10.5	28.4	28.5	16.6	23.8	0.424	0.277
GOA2S	0.214	0.301	0.699	0.448	0.641	0.303	0.131	10.8	29.8	28.0	15.2	25.7	0.395	0.307
GOA3S	0.264	0.235	0.765	0.500	0.654	0.163	0.076	13.4	31.7	27.2	13.3	27.9	0.363	0.346
GOA4C	0.089	0.693	0.307	0.237	0.770	0.143	0.051	4.5	34.2	21.2	10.8	20.7	0.478	0.291
GOA5C	0.106	0.678	0.322	0.268	0.831	0.156	0.058	5.4	37.8	18.1	7.2	21.8	0.458	0.330
GOA6C	0.133	0.558	0.442	0.224	0.506	0.176	0.091	6.8	25.3	35.3	19.7	31.2	0.318	0.301
GOA7C	0.159	0.588	0.412	0.407	0.990	0.215	0.084	8.2	44.6	11.9	0.2	23.0	0.439	0.388
GOA8C	0.186	0.499	0.501	0.355	0.710	0.226	0.105	9.5	34.3	24.6	10.7	27.9	0.363	0.372
GOA9S	0.236	0.285	0.715	0.373	0.521	0.286	0.154	10.9	27.0	34.2	18.0	32.4	0.302	0.330

TABLE B5

COMPARISON OF DATA AT 3.0 PERCENT SHEAR STRAIN (GULF OF ALASKA CLAY)

TEST	$\tau_h/\bar{\sigma}_{vo}$	$u/\bar{\sigma}_{vo}$	$\bar{\sigma}_v/\bar{\sigma}_{vo}$	$\bar{\sigma}_h/\bar{\sigma}_{vo}$	$\bar{\sigma}_h/\bar{\sigma}_v$	$\bar{p}$	q	$G/\bar{\sigma}_{vo}$	θ_p	θ_f	θ_q	ϕ_m	$\bar{\sigma}_3/\bar{\sigma}_1$	$\tau_h/\bar{\sigma}_v$
GOA1S	0.218	0.306	0.694	0.463	0.666	0.305	0.130	7.3	31.0	26.7	14.0	25.2	0.403	0.313
GOA2S	0.222	0.349	0.651	0.427	0.658	0.284	0.131	7.4	31.7	27.0	13.3	27.5	0.369	0.342
GOA3S	0.267	0.267	0.733	0.489	0.668	0.157	0.076	8.9	32.7	26.6	12.3	28.7	0.351	0.364
GOA4C	0.089	0.732	0.268	0.214	0.799	0.127	0.049	3.0	36.6	19.8	8.4	22.7	0.443	0.332
GOA5C	0.106	0.734	0.266	0.236	0.889	0.132	0.056	3.6	41.1	16.6	3.9	25.4	0.400	0.401
GOA6C	0.133	0.610	0.390	0.199	0.512	0.155	0.086	4.5	27.2	34.7	17.8	33.8	0.286	0.342
GOA7C	0.159	0.625	0.375	0.395	1.052	0.203	0.084	5.5	46.8	10.6	-1.8	24.7	0.412	0.426
GOA8C	0.186	0.548	0.452	0.348	0.774	0.211	0.102	6.5	37.3	22.2	7.7	28.9	0.348	0.413
GOA9S	0.247	0.321	0.679	0.359	0.528	0.273	0.155	8.2	28.5	33.7	16.5	34.5	0.277	0.363

TABLE B6

COMPARISON OF DATA AT 15.0 PERCENT SHEAR STRAIN (GULF OF ALASKA CLAY)

TEST	$\tau_h/\bar{\sigma}_{vo}$	$u/\bar{\sigma}_{vo}$	$\bar{\sigma}_v/\bar{\sigma}_{vo}$	$\bar{\sigma}_h/\bar{\sigma}_{vo}$	$\bar{\sigma}_h/\bar{\sigma}_v$	$\bar{p}$	q	$G/\bar{\sigma}_{vo}$	θ_p	θ_f	θ_q	ϕ_m	$\bar{\sigma}_3/\bar{\sigma}_1$	$\tau_h/\bar{\sigma}_v$
GOA1S	0.264	0.424	0.576	0.449	0.780	0.270	0.143	1.8	38.3	22.7	6.8	31.7	0.311	0.455
GOA2S	0.251	0.506	0.494	0.441	0.891	0.247	0.133	1.7	42.0	19.4	3.0	32.6	0.299	0.507
GOA3S	0.319	0.339	0.661	0.551	0.833	0.156	0.083	2.1	40.1	21.1	4.9	32.3	0.304	0.484
GOA4C	0.089	-	-	-	-	-	-	-	-	-	-	-	-	-
GOA5C	0.106	0.819	0.181	0.175	0.966	0.094	0.056	0.7	44.2	19.1	0.8	36.7	0.252	0.586
GOA6C	0.133	0.765	0.235	0.128	0.546	0.096	0.075	0.9	34.1	37.0	10.9	52.1	0.118	0.567
GOA7C	0.159	0.760	0.240	0.314	1.311	0.146	0.086	1.1	51.6	11.6	-6.6	36.3	0.256	0.666
GOA8C	0.186	0.716	0.284	0.240	0.838	0.138	0.101	1.2	41.9	29.7	3.1	39.9	0.179	0.655
GOA9S	0.298	0.444	0.556	0.359	0.646	0.241	0.166	2.0	35.9	30.8	9.1	43.4	0.185	0.537